

https://dspace.org/

Approaches to mix design and measurement of workability for self-compacting concrete.

Jooste, Josef Petrus

2007-02-28T12:42:00Z
http://hdl.handle.net/10539/2161

Downloaded from a DSpace repository. https://dspace.org/

APPROACHES TO MIX DESIGN AND MEASUREMENT OF WORKABILITY FOR SELF-COMPACTING CONCRETE

Josef Petrus Jooste

A dissertation submitted to the Faculty of Engineering and the Built Environment, University of the Witwatersrand, in fulfillment of the requirements of the degree of Master of Science in Engineering.

Johannesburg, 2006

DECLARATION

I declare that this dissertation is my own, unaided work. It is being submitted for the Degree of Master of Science in the University of the Witwatersrand, Johannesburg. It has not been submitted before for any degree or examination in any other University.



_____

(Signature of candidate)

28th day of August 2006

Abstract

Self-compacting concrete (SCC) is becoming a popular form of concrete usage in a range of applications throughout the world. This investigation considers the development of the technology and use of SCC. Importantly, the investigation aims to highlight the opportunities for using SCC in South Africa. A mixture design model is proposed and has been found to work well using local materials. The advantage of this model is the simplicity and the adaptability to any aggregate type. This method should be more acceptable to SCC producers who do not have special facilities and testing equipment

An overview concerning concrete rheology is included to explain the mechanisms used to describe the flow and deformation of both the concrete and mortar mixtures. Included is a comparison between concrete, mortar and paste rheology. The Tattersall Two Point Tester was used to measure the shear resistance at two shear deformation rates.

From the test results it was found that SCC can be made using South African materials and that it is possible to design a mixture with a lower cementitious content. The results from the Tattersall Two Point Tester gave additional information about the flowability of SCC.

ACKNOWLEDGEMENTS

I acknowledge, with gratitude, the assistance of the following persons and organisations who contributed to the completion of this project:

Prof Y Ballim, who supervised the project and offered enthusiastic support, gave innovative ideas, encouragement and advice during the execution of this research;

The Department of Civil Engineering Technology of the University of Johannesburg for the funding and support supplied. Dr G Fanourakis, Mr D Adegoke, Mr D Lange and Mr M Butler for their encouragement and support, the assistance from Mr N Alexander, Mr N Sfarnas, Mr T Mogopodi, Mr V Pino, Mr M Speelman and Mr S Mangaba in the laboratory;

The Cement and Concrete Institute for the donation of the Tattersall two point test apparatus and the use of their library facilities as well as for Mrs H Turner, Mrs A Martinek and Mrs G Legoale for their professional assistance;

All the people from industry for valuable information and support:

- Mr F Dinardo, Mrs S Badenhorst, Mr R Naidoo and Mr J Kellerman from Holchim for all the material and information.
- Mr E Kleinhans and Dr R Amtsbüchler from Lafarge for the information, material, and use of the ViscoCorder viscometer.
- Mr E Paton from PPC for the donation of cement.
- Mr E Correia, Mr A Marais, Mr P Flannigan and Mr H Woodman from Chryso for the information and material.
- Mrs M Rebolo from Advanced Laboratory Solutions for the calibration information.
- Dr R Kruger from Ash Resources for the fly ash and advice.
- Mr W Jerling, Mr G Evans and Mrs S Gouws from Grinaker-LTA for the advice and information.
- Mr T van Niekerk and Mr T Smith from Grace for the material, information and advice.
- Mr G Rossouw, Mr H Cronje and Mr A Botha from Murray and Roberts for the information.

All the people from educational institutions for valuable advice and information:

Prof P Banfill from Heriot-Watt University,

Dr P Domone from University College London,

Dr P Billberg from CBI,

Prof G van Zijl and Mr M Gazendam from Stellenbosch University

Last but not the least; I am grateful to my wife Miekie for her understanding and perseverance throughout the course of this project. I want to thank her especially for her patience, love, support and encouragement through tough times as well as good times. I would also like to extend this gratitude to my children.

Finally, I give all the glory to God, the Father, the Son and the Holy Spirit, from which all things come. He is my strength and without Him nothing is possible.

"Now in Him who is able to do immeasurably more than all we ask or imagine, according to His power that is at work within us, to Him be glory in the church and in Christ Jesus throughout all generations, for ever and ever! Amen." Eph.3:20-21

TABLE OF CONTENTS

CONTENTS		Page
DECLARATION		ii
ABSTRACT		iii
ACKNOWLEDGEMENTS		iv
CONTENTS		vii
LIST OF FIGURES		xi
LIST OF TABLES		xv
1	**INTRODUCTION**	**1**
1.1	Subject	1
1.2	Motivation	2
1.3	Objectives of this Investigation	3
1.4	Limitations	4
1.5	Methodology	5
1.6	Organisation of this Dissertation	6
2	**BACKGROUND AND LITERATURE REVIEW**	**8**
2.1	History of SCC	8
2.2	Properties of SCC	8
2.3	Benefits in using SCC	9
2.4	Disadvantages in using SCC	11
2.5	International applications	12
2.6	SCC in South Africa	14
2.6.1	The Nelson Mandela Bridge Project	15
2.6.2	Bridge 2235	17
2.6.3	Spiral Staircase	19
2.6.4	Other projects	22
2.7	Conclusions	23

3	**PRINCIPLES AND MEASUREMENT OF RHEOLOGY**	**24**
3.1	Introduction	24
3.2	Background on rheology	24
3.3	Concrete rheology	29
3.4	Mortar rheology	30
3.5	Paste rheology	31
3.6	Conclusion	34
4	**TEST METHODS AND MATERIALS**	**35**
4.1	Introduction	35
4.2	Test methods describing the fresh properties of SCC	36
4.2.1	The Tattersall Two Point Test	36
4.2.2	The Slump Flow Test	54
4.2.3	The J-Ring Test	55
4.2.4	The V-Funnel Test	60
4.2.5	The L-Box Test	61
4.2.6	Visual assessment Test	63
4.3	Test methods describing the fresh properties of the SCC mortar.	63
4.3.1	The Tattersall Two Point Test	64
4.3.2	The MC1 Rheolab rheometer	64
4.3.3	The mortar flow Test	67
4.3.4	The mini V-Funnel Test	69
4.4	Tests methods describing the rheology of mortar	70
4.4.1	The ViscoCorder	70
4.5	Workability retention	72
4.6	Testing the hardened properties of SCC	73
4.6.1	Compressive strength	73
4.7	Materials	73
4.7.1	Cement	73
4.7.2	Fly Ash	74

4.7.3	Condensed silica fume	76
4.7.4	Admixtures	76
4.7.5	Aggregates	77
4.8	Conclusion	82
5	**COMPARISON BETWEEN CONCRETE, MORTAR AND PASTE RHEOLOGY**	**83**
5.1	Introduction	83
5.2	Paste rheology measurements	83
5.3	Mortar rheology measurements	91
5.4	Concrete rheology measurements	95
5.5	Results of the paste, mortar and concrete rheology comparison	98
5.6	Conclusion	103
6	**MIXTURE DESIGN AND TEST RESULTS**	**104**
6.1	Introduction	104
6.2	Literature review	104
6.3	Proposed mixture design model	107
6.4	Laboratory Procedures	108
6.4.1	Mixture proportions	108
6.4.2	Mixing procedure	113
6.5	Results	113
6.5.1	Compressive strength	113
6.5.2	The fresh properties of SCC	115
6.5.3	The fresh properties of SCC mortar	120
6.5.4	Workability retention	124
6.5.5	Comparison between workability and rheological parameters	124
6.6	Conclusion	130

7 ALTERNATIVE MIXTURE DESIGN MODEL AND RESULTS 131

7.1 Introduction 131
7.2 Mixture design procedure 131
7.3 Laboratory Procedures 139
7.3.1 Mixture proportions 139
7.3.2 Mixing procedure 141
7.4 Results 141
7.4.1 Compressive strength 141
7.4.2 The fresh properties of the mixtures 142
7.4.3 Comparison between workability and rheological parameters 144
7.5 Conclusion 146

8 CONCLUSIONS AND RECOMMENDATIONS 148

8.1 Conclusions 148
8.2 Recommendations 151
8.3 Future research 152

REFERENCES 153

APPENDIX A CALIBRATION CALCULATIONS 159

APPENDIX B CALIBRATION MEASUREMENTS 165

APPENDIX C EXAMPLE TO CALCULATE YIELD STRESS AND PLASTIC VISCOSITY 169

LIST OF FIGURES

Figure		Page
2.1	The Nelson Mandela Bridge	15
2.2	Pumping and valve arrangement at the pylon base	16
2.3	Deck cross section	18
2.4	Bridge 2235	18
2.5	Spiral staircase	20
2.6	Repaired culvert in Cape Town	22
3.1	Hooke's law for a material in shear	25
3.2	Hookean solid in shear	25
3.3	Newton's law of viscous flow	26
3.4	Newtonian liquid: $\tau = \eta \dot{\gamma}$	27
3.5	Bingham model: $\tau = \tau_o + \mu \dot{\gamma}$	28
3.6	Nonlinear flow curves	29
4.1	Interrupted helical impeller for the Tattersall Two Point Tester	37
4.2	Tattersall Two Point Tester	38
4.3	Sample holder showing the filling mark	39
4.4	Side view of Torque calibration equipment	42
4.5	Front view of Torque calibration equipment	42
4.6	Pressure to Torque relationship	44
4.7	Arrhenius plot of *ln* η (in Pas) against the inverse of the absolute temperature (in 1/K)	45
4.8	T/N against η for the Tattersall Two Point Tester	47

4.9	Relation between ln $\dot{\gamma}$ and ln τ for the Tattersall Two Point Tester	52
4.10	The slump flow test	55
4.11	The J-Ring test	56
4.12	The J-Ring dimensions	58
4.13	Description of Step of blocking in the J-Ring test	59
4.14	V-Funnel	60
4.15	V-Funnel dimensions	60
4.16	L- Box	61
4.17	L-Box dimensions	62
4.18	Bob geometry	65
4.19	Six Blade Vane geometry	65
4.20	MC1 Rheolab rheometer	65
4.21	The mortar flow test	69
4.22	The mini V-Funnel	70
4.23	Cup and paddle dimensions for the ViscoCorder	71
4.24	ViscoCorder sand grading curve	78
4.25	Bothma filler sand grading curve	78
4.26	Andesite crusher sand grading curve	79
4.27	Granite crusher sand grading curve	79
4.28	Dolomite crusher sand grading curve	80
4.29	13 mm Dolomite grading curve	80
4.30	13 mm Andesite grading curve	81
4.31	13 mm Granite grading curve	81
5.1	Flow curve for paste mixture RN1P	86

5.2	Flow curve for paste mixture RN2P	86
5.3	Flow curve for paste mixture RN3P	87
5.4	Flow curve for paste mixture RN4P	87
5.5	Flow curve for paste mixture RN5P	88
5.6	Flow curve for paste mixture RN6P	88
5.7	Flow curve for paste mixture RN7P	89
5.8	Flow curve for paste mixture RN8P	89
5.9	Flow curve for paste mixture RN9P	90
5.10	Flow curve for paste mixture RN10P	90
5.11	Flow curve for paste mixture RN11P	91
5.12	Flow curves for mortar mixtures tested in the ViscoCorder	94
5.13	Plastic viscosity paste vs. plastic viscosity mortar	102
5.14	Yield stress paste vs. yield stress mortar	102
5.15	Plastic viscosity concrete vs. plastic viscosity mortar	102
5.16	Yield stress concrete vs. yield stress mortar	102
5.17	Plastic viscosity paste vs. plastic viscosity concrete	102
5.18	Yield stress paste vs. yield stress concrete	102
6.1	Relation between yield stress for concrete and mortar mixtures	123
6.2	Relation between plastic viscosity for concrete and mortar mixtures	123
6.3	Comparison between the slump flow and yield stress for the SCC mixtures tested	125
6.4	Comparison between the T50 and plastic viscosities for the SCC mixtures tested	126
6.5	Comparison between the V-Funnel times and plastic viscosities for the SCC mixtures tested	127

6.6	Comparison between the V-Funnel times and T50 for the SCC mixtures tested	127
6.7	Comparison between the V-Funnel times and slump flow for the SCC mixtures tested	128
6.8	Comparison between the T50 and slump flow for the SCC mixtures tested	129
7.1	Comparison between the slump flow and yield stress for the SCC mixtures tested	145
7.2	Comparison between the T50 and plastic viscosities for the SCC mixtures tested	145
A1	Arrhenius plot of *ln* η (in Pas) against the inverse of the absolute temperature (in 1/K)	160
A2	T/N against η for the ViscoCorder	161
A3	Relation between ln $\dot{\gamma}$ and ln τ for the ViscoCorder	163

LIST OF TABLES

Table		Page
2.1	Concrete mixture proportions for the Spiral staircase	20
3.1	Rheology of cement based materials	33
4.1	Example of the calculation for g, h, τ_o and μ from experimental data obtained from the Tattersall Two Point Tester	41
4.2	Torque calibration results	43
4.3	Viscosity measurements for Silicone di-methyl	45
4.4	Tattersall measurements and slope calculations for Silicone di-methyl	46
4.5	Variation of viscosity with temperature	47
4.6	Tattersall measurements and slope calculations for two aqueous solutions of hydroxyl ethyl cellulose	49
4.7	MC1 Rheolab rheometer measurements and slope calculations for 3% aqueous solutions of hydroxyl ethyl cellulose for the calibration of the Tattersall Two Point Tester	50
4.8	MC1 Rheolab rheometer measurements and slope calculations for 4% aqueous solutions of hydroxyl ethyl cellulose for the calibration of the Tattersall Two Point Tester	51
4.9	Power law parameters for hydroxy ethyl cellulose for calibration of the Tattersall Two Point Tester	52
4.10	Chemical analysis of CEM II 42.5 A-M	74
4.11	Chemical analysis of CEM I 42.5 N	74
4.12	Comparison of typical chemical composition for S.A. materials (%)	76
4.13	ViscoCorder sand grading	78
4.14	Bothma filler sand grading	78
4.15	Andesite crusher sand grading	79
4.16	Granite crusher sand grading	79
4.17	Dolomite crusher sand grading	80
4.18	13 mm Dolomite grading	80
4.19	13 mm Andesite grading	81

4.20	13 mm Granite grading	81
5.1	Paste mixture proportions	84
5.2	Summary of paste rheology results	85
5.3	Mortar mixture proportions for the mortar rheology measurements	92
5.4	ViscoCorder results for mortar mixtures	94
5.5	Concrete mixture proportions for concrete rheology measurements	96
5.6	Summary of concrete rheology results	98
5.7	Comparison between mortar rheology results for different test instruments	99
5.8	Paste, mortar and concrete rheology results	101
6.1	Concrete mixture proportions	108
6.2	Compressive strength results	114
6.3	Workability results for the mixture design investigation 1	116
6.4	EFNARC Specifications for SCC workability tests	118
6.5	SCC mortar, workability results	121
6.6	Mortar and concrete Tattersall rheology results	122
6.7	Workability retention results	124
7.1	Example of mixture design sheet	139
7.2	Concrete mixture proportions for alternative mixture design model	140
7.3	Compressive strength results for the alternative mixture design mixtures	142
7.4	Workability results for alternative mixture design model	143
A1	Viscosity measurements for Silicone di-methyl	159
A2	Variation of viscosity with temperature for the ViscoCorder	161
A3	Power law parameters for hydroxyl ethyl cellulose for calibration of the ViscoCorder	163
B1	ViscoCorder measurements and slope calculations for Silicone di-methyl	165
B2	ViscoCorder measurements and slope calculations for two aqueous solutions of hydroxyl ethyl cellulose	166

B3	MC1 Rheolab rheometer measurements and slope calculations for 1.92 % aqueous solutions of hydroxyl ethyl cellulose for the calibration of the ViscoCorder	167
B4	MC1 Rheolab rheometer measurements and slope calculations for 3.00 % aqueous solutions of hydroxyl ethyl cellulose for the calibration of the ViscoCorder	168
C1	Example of the calculation for g, h, τ_o and μ from experimental data obtained from the Tattersall Two Point Tester	170

CHAPTER 1
INTRODUCTION

1.1 Subject

Self-compacting concrete (SCC) is a specialized concrete designed to flow freely around obstacles, completely fill formwork and enclose all reinforcing bars without segregation or bleeding[1]. The three key properties of SCC are filling ability (highly fluid to ensure flow under self weight), passing ability (passing around obstacles without blocking) and resistance to segregation (no separation of phases during flow or at rest after placing). As the name indicates, this concrete type requires no external consolidation effort while still fulfilling all the requirements of conventional concrete.

The idea of a concrete that flows and compacts under self weight only, originated in Japan. Thereafter, the use of SCC spread through Asia into Europe and many parts of the world including South Africa. The development and application of SCC technology across the world is rapidly increasing, but in South Africa SCC is still in the infancy stage and much research is needed.

1.2 Motivation

This research project is warranted for the following reasons:

- The increasing need for a rheology based approach to concrete mixture design[2]. SCC is a very good example where superplasticisers are used to make concrete that can achieve full compaction without the need for mechanical vibration[3]. This is essential in heavily reinforced sections or where vibration is difficult.
- Unlike the well rounded European aggregates, South African aggregates are typically crushed, with less control over grading, and therefore water demand. Because SCC is so sensitive to the amount of water added, rheology measurements are required to determine a suitable mixture design method.
- The construction industry is experiencing a major upheaval at the moment, and the use of SCC will result in faster construction turnaround times as well as the manufacture of more complicated shapes.
- With the changes in local cement and extender specifications and the use of improved ground granulated blastfurnace slag (GGBS) and fly ash (FA) processing methods, the effect of the binder on the concrete rheology also needs to be fundamentally understood[2].
- The extensive use of cement replacement materials and chemical admixtures has led to the development of mixtures for special applications such as high performance concrete, which includes SCC. The research on the rheology of these concretes is therefore justified[3].
- Even if the materials used to produce SCC are expensive, the overall construction cost is reduced because of a reduction in construction time.

1.3 Objectives of this investigation

As a contribution to the development of SCC technology in South Africa, this investigation presents details of test programmes that were undertaken to measure the opportunities and potential for using local concrete-making materials to produce SCC. Unlike the well rounded European aggregates, South African aggregates are typically crushed, with less control over grading, and therefore water demand. Because SCC is so sensitive to the amount of water added, rheology measurements are required to determine a suitable mixture design method. The objective was to establish a model that can be used in the design and testing of SCC using South African materials under South African conditions. To achieve this objective, rheology was used to describe the flow and fresh properties of SCC in order to assist in the design of the optimum mixture.

This investigation also presents a brief review of the development of this technology as well as the basic principles and measurements of rheology. The Tattersall Two Point Test apparatus, ViscoCorder variable speed viscometer and Rheolab MC1 rheometer were used to measure the rheology of the three different phases. The principal operation of this equipment is explained to clarify the measuring process and interpretation of the results. Since the Tattersall Two Point Tester has never been used in South Africa, it was necessary to make sure that this test was reliable as well as repeatable. The Tattersall Two Point Test apparatus and ViscoCorder variable speed viscometer were also calibrated using fluids of known properties to convert the test results to fundamental units.

The results from the paste, mortar and concrete rheology tests were compared to determine the possible relation between these phases. This was required to determine the correlation between the rheology of the three different phases. Establishing such a correlation allowed a possible prediction of the concrete rheology based on mortar or paste rheology. Rheology test results were also compared to the empirical test results obtained from the slump flow, L-Box, J-Ring and V-funnel tests.

Various mixtures were used to determine the effect of fine and ultra fine fly ash (FA), ground granulated blastfurnace slag (GGBS), condensed silica fume (CSF) and different admixtures, on the workability of these mixtures. The workability retention of the different admixtures used was also investigated.

1.4 Limitations

This investigation concentrated on the rheology of SCC and did not address other engineering properties like shrinkage or creep. Only three different aggregates were used: dolomite from the Olifantsfontein quarry, andesite from the Eikenhoff quarry and granite from the Jukskei quarry. One filler sand was used in most of the mixtures. Ground granulated blastfurnace slag, condensed silica fume and fly ash were each restricted to a single source.

1.5 Methodology

A literature review was undertaken to gather information on the development and application of SCC across the world. In this search, information on mixture design and testing of SCC were obtained. A number of interviews with various people in the concrete industry were conducted to get information on SCC being used in South Africa.

Initially, tests were done to determine the relationship between the three different phases in SCC: the paste phase, the mortar phase and the concrete phase. In view of the fact that concrete rheology is concerned with particles suspended in a suspending medium, it can be expected that the concrete rheology is a function of the mortar rheology and the mortar rheology is a function of the paste rheology. To optimise the concrete rheology it is therefore important to optimise the paste and mortar rheology[1]. To determine the properties of fresh SCC made from South African materials, various mixtures were tested. Three different aggregate types were used to find the most suitable of these to be used for SCC. Experiments were also conducted using different superplasticisers and extenders.

The flowability and filling ability of the mixtures were measured using the slump flow, L-box, J-Ring and V-funnel tests. The passing ability and segregation resistance were assessed with the L-box, J-Ring and V-funnel tests. The Tattersall Two Point Test apparatus was used to determine the basic rheological parameters

of the concretes and mortars. To verify the rheology of the mortar as well as the paste, a Rheolab MC1 viscometer was used. This viscometer was also used in the calibration of the Tattersall Two Point Test apparatus. The mini slump cone was used to determine the slump flow of the mortar as well as the workability retention of the different admixtures used in this investigation. Cubes were made of each mixture to measure the compressive strength at 7 and 28 days.

1.6 Organisation of this Dissertation

In Chapter 2 an overview of SCC is given, elaborating on the history, properties, benefits, disadvantages and international applications. The South African experience of SCC is also addressed in this chapter and case studies are discussed. Chapter 3 discusses the principles and measurements of rheology.

All the test methods and equipment used are described in Chapter 4. This chapter includes an overview of the development and calibration of the Tattersall Two Point Tester. The calibration of the ViscoCorder, used for the mortar rheology measurements, is also included. A description of the material used in this investigation is discussed in this chapter. A comparison between concrete, mortar and paste rheology is given in Chapter 5. This includes the test results for the three different phases.

Chapter 6 reports on some of the mixture design methods used internationally. This chapter also investigates a design method for SCC previously used in South Africa. The test procedures used as well as the results of this investigation are also included.

An alternative model to design SCC using South African material is presented in Chapter 7. The test results for this model are included in this chapter.

The last chapter summarises the findings and conclusions of this investigation. Recommendations are given as well as options for future research.

CHAPTER 2

BACKGROUND AND LITERATURE REVIEW

2.1 History of SCC

SCC was first developed in 1988 by Okamura[4] at the Tokyo University and its use has gradually increased. From Japan the use of SCC spread through Asia and in 1993 it was also used in Europe. The First RILEM International Symposium on SCC was held in Stockholm, Sweden in 1999. Two years later the second symposium was held in Kochi, Japan and the third was held in 2003 in Reykjavik, Iceland. At this last symposium there were 108 contributions from 26 countries. In North America the use of SCC grew from an insignificant amount in the year 2000 to more than a million cubic meters in total at the end of 2002. Even though much research has been done across the world, SCC is still in its infancy stage and further research is required[5]. Unlike conventional concrete, which has been researched for many years, SCC is in existence for 18 years and all the questions have not been answered yet. In South Africa research was only done on the fresh properties of SCC and that is far from perfect.

2.2 Properties of SCC

SCC is a specialized concrete designed to flow freely around obstacles, completely fill formwork and enclose all reinforcing bars without segregation or bleeding. As the name indicates, this concrete type requires no external

consolidation effort while still fulfilling all the requirements of conventional concrete.

2.3 Benefits in using SCC

The most valuable benefit when using SCC is that no compaction of the fresh concrete is required. This leads to reduced energy requirement in the placing and finishing of the concrete. Because placing is quicker and easier, the construction time is reduced and workers can be used more effectively. This was evident in the construction of the anchorage of the Akashi-Kaikyo Bridge, where the use of SCC reduced the total construction time from 30 to 24 months. Another project where the use of SCC reduced the construction time from 22 to 18 months was the wall of the liquid natural gas tank for the Osaka Gas Company[(1)].

The high flowability of SCC makes alternative placing methods possible, like pumping the concrete continuously from the bottom of the structure. This method was used in the filling of the pylons of the Nelson Mandela Bridge.

The high flowability and elimination of the need for compaction make the use of special designs and shapes possible. With conventional concrete, designs were restricted to shapes where concrete could be placed manually and where compaction equipment could reach. The Science Centre in Wolfsburg,

Germany[6], the façade of the National Theater in The Hague[7] and the pylons of the Nelson Mandela bridge are examples where the use of conventional concrete would not have been possible. SCC lends itself to creative shapes and innovative construction systems. Designs with very congested reinforcing are also acceptable, since SCC can flow around these and external compaction is not required.

With the reduction of the noise levels (about 93 dB when compacting conventional concrete) the working environment is safer and the noise is reduced in built-up areas. When using SCC the noise level can be brought well below 80 dB. Intensities higher than 80 dB can cause deafness, stress and fatigue[7]. With lower noise, no ear protection is needed and communication on site is easier. Vibration above 0,25 m/s^2 causes pain and stiffness in limbs, back and neck[7]. A more serious ailment caused by continuously using the poker vibrator (vibration levels from 0,75 to 4 m/s^2) is known as "white fingers" which affects the blood circulation of the vibrator operator[6].

With well compacted concrete the possibility of air voids are reduced which increases the strength and density of the concrete. The bond between the concrete and the reinforcing steel is improved and there is a reduced chance of bleed water lenses beneath reinforcing and aggregate.

The off-shutter finish when using SCC is also very good. The chances of honeycombing and blow holes are very slim. The use of admixtures assures thorough mixing since all the cement particles are better dispersed throughout the mixture, resulting in a more homogeneous concrete. This was evident in the concrete finish achieved with the construction of Bridge 2235.

The properties of SCC are well suited to produce good quality precast elements reducing energy consumption in the production process. The energy required is not just the power to operate the plant, but also labour and equipment efficiency. Cycle time of the moulds is also shorter because the admixtures used in the mixture can accelerate the hydration process which accelerates strength development. There is also less wear and maintenance on the mixing equipment[8].

2.4 Disadvantages in using SCC

The biggest disadvantage in using SCC is the cost involved to make this type of concrete. The material cost is higher since admixtures must be used. The aggregate also needs to be a smaller size than that commonly used. The mixture requires a large percentage of fines and filler material to avoid segregation. SCC is also sensitive to variation in the aggregate and this needs to be well controlled for consistent quality and grading. The initial cost to set up the mixing plant can also be significant.

The material sensitivity of SCC means that strict quality control is necessary at the batching and mixing operation. The material used in the mixture needs to conform to a very narrow specification. This necessitate careful grading and washing of sand to control the fines content of the mixture. If the fines content of the sand is not controlled, the water demand and admixture content will be affected and the end product can not be predicted. This could lead to a mixture that either segregate or does not flow satisfactorily. Mixer operators must be well trained and always aware of the sensitivity of this product.

Furthermore, special formwork is required when using SCC. The formwork must be stronger to support the concrete at early ages since form pressure is higher than with conventional concrete. Formwork needs to be near watertight to prevent loss of fines from the concrete mixture.

2.5 International applications

One of the first big projects undertaken in Japan using SCC was the anchorage (83m long, 63m wide and approximately 45m high) of the Akashi-Kaikyo Bridge. This project is a very good example of where the use of SCC reduced the total construction time from 30 to 24 months. Another project where the use of SCC reduced the construction time from 22 to 18 months was the 0.8m thick wall of the liquid natural gas tank for the Osaka Gas Company[1]. More recent applications of SCC in Japan are lattice work (thin ribs), casting without a pump

(discharging concrete from the truck and allowing it to flow freely to fill the formwork) and tunnel linings. SCC is used in lattice work because conventional concrete cannot be vibrated in this manufacturing process. To prevent cold joints in tunnel linings, SCC is used because it limits bleeding or laitance at joints[4].

Sweden started to develop SCC in 1993 with a project where walls were cast using different materials as fillers in the mixture designs. In 1998 a bridge was constructed using SCC. This was the first bridge outside Japan where SCC was used for the whole structure[1]. Since then, SCC has been used in monolithic frame bridges, box tunnel monoliths, rock lining monoliths, tunnel entrances, headwalls, foundations and frame supports. The current use of SCC in Sweden's pre-cast and ready mix concrete industry is about 10% of the total concrete use[9].

The development of SCC is particularly favored in the precast concrete industry. Some precast concrete producers in the Netherlands only use SCC in the manufacture of their products[7]. Because of this extensive use of SCC, much experience has been gained and SCC is now used in pre-cast slabs, beams, walls, columns, arches and bridge elements. SCC has also been used in situ but only in special cases. The first major project was the façade of the National Theater in The Hague where only SCC could be used to fill the tiny ribs (8 mm deep). In some tunnel walls SCC was used because of congested reinforcement and the possibility of remote casting techniques. At the Rotterdam Zoo the heavily

reinforced walls of a large fish pond was done with SCC to ensure a homogeneous watertight structure. The design and shape of the bridge piers for the "South Tangent" traffic connection between Haarlem and Amsterdam was of such a nature that only SCC could be used. In this project 1800 m^3 of SCC was used. The most resent development in the Netherlands is self-compacting fiber reinforced concrete. Self-compacting fiber reinforced concrete is used to produce floor elements that are thinner and lighter[7].

Further examples of SCC applications are the steel form columns at the Toronto International Airport and the outrigger columns at Wall Centre in Vancouver (North America). A more interesting application was in the construction of houses in Houston where the exterior walls and slabs were cast monolithically out of SCC. The walls are textured and stained on the outside to resemble brick and have a polystyrene foam core for insulation. These houses are designed to withstand tornados and hurricane winds in excess of 218 km per hour[10].

2.6 SCC in South Africa

SCC is mainly utilized for specialized applications where the use of conventional concrete is very difficult and often impossible. The development of SCC is still in its infancy stage and its current use in South Africa is negligible.

The first project where SCC was used was the Nelson Mandela Bridge, which was constructed in 2002. The placement method used in this project, which entailed pumping from the bottom up, was also a first for South Africa. Furthermore, the height to which concrete was pumped seems to be a world record[11]. Other projects where SCC was used include a bridge deck (Bridge 2235) on the Bakwena Highway in 2002 and a spiral staircase at an office building in Pretoria a year later. In 2004 a number of relatively small projects were constructed using SCC.

2.6.1 The Nelson Mandela Bridge Project

This bridge (which is shown in Figure 2.1) is the largest cable-stayed bridge in South Africa connecting Braamfontein with Newtown, spanning the Braamfontein rail shunting yards. Newtown is the centre of the cultural precinct and the bridge provides access from the northern side of Johannesburg to this area.



Figure 2.1. The Nelson Mandela Bridge[11]

A serious challenge during this project was the placing of the concrete inside the hollow steel pylons. The pylons were constructed from 20 mm (southern pylons) and 40 mm (northern pylons) thick steel plate, rolled to produce 1.35 m diameter steel pipes which had to be filled with concrete to provide the required stiffness. The southern and northern pylons are respectively 31.1 m and 43.9 m high. This created difficulty with concrete lifting and placing, due the free fall limits, access constraints (due to operating railway lines) and stressing chambers at the top of the pylons[11]. In addition, mechanical vibration was impossible due to limited access. External vibration was inappropriate because of the large amount of energy needed to overcome the pylon inertia. To overcome this it was decided to pump SCC into the pylons from the bottom. The concrete was pumped through a special pipe and valve arrangement at the bottom of each pylon as shown in Figure 2.2[11].



Figure 2.2: Pumping and valve arrangement at the pylon base[11]

Each pylon was filled separately, taking 90 minutes to fill the first northern pylon and only 58 minutes for the second pylon[12]. The filling volume for the southern pylons is 34 m^3 and for the northern pylons 52 m^3. The pumping process couldn't be stopped at any stage and it was specified in the method statement that 60 % of the required concrete had to be on site and the balance dispatched and en route to site before the pumping process could commence[11].

The company policy of the concrete suppliers prohibited the disclosing of the mixture design of the SCC used in both the Mandela Bridge project and Bridge 2235. They did however reveal that the SCC used included a CEM II A-M (S) 42,5N (15 % fly ash, 30 % GGBS), no viscosity modifier and a superplasticizer. The aggregate used was 9.5 mm crushed andesite and andesite crusher sand in combination with a natural sand as a filler. A slump flow (see detail later in Chapter 4) of 650 mm was measured and the 28 day cube strength was 64 MPa[11].

2.6.2 Bridge 2235

Bridge 2235 forms part of an off ramp from the Bakwena highway. The Bakwena highway, which extends from Pretoria to Botswana, is part of the east-west link across the southern part of Africa. The bridge deck is a post-tensioned two-cell box girder type structure (Figure 2.3), unlike the conventional metal drum void formers used in similar bridges. To save time and labour costs, it was decided to

cast the deck of Bridge 2235 in one operation. Since compaction and placing was a problem in the reinforcing congested bottom slab, it was decided to use SCC.

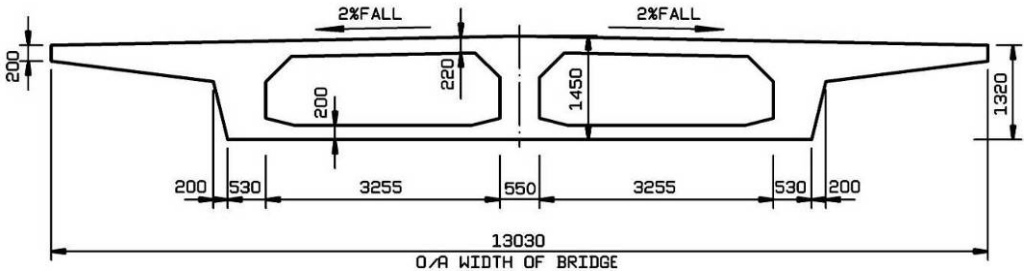


Figure 2.3: Deck cross section[13]

Before the deck was cast a representative fully reinforced replica of the bottom slab (4,2 m x 1,2 m x 0,2 m) with two upstand edge beams (0,4 m wide and 0,75 m high) was cast as a trial next to the bridge. The bottom part of this replica was fully shuttered to represent the bottom deck slab of the bridge.



Figure 2.4: Bridge 2235[13]

When the first trial was poured, the concrete showed signs of segregation and too much mortar. Adjustments to admixture/binder proportions were made and the trial was repeated the following day. The second attempt was successful and the concrete stayed in suspension and flowed from the one upstand through the bottom slab shutter filling both upstands to their full height[13]. The bridge deck was then cast successfully with very little trapped air voids visible. A 50 MPa SCC mixture with a slump flow of 600 mm was used to cast this bridge deck. Although this flow does not comply with the minimum of 650 mm specified in the EFNARC Specification[14], this mixture did not segregate and flowed successfully.

2.6.3 Spiral Staircase

In 2003, a spiral staircase at an office building in Pretoria was constructed using SCC. The position and geometry of this staircase made vibration impossible. It also had to be cast in one operation since no joints were allowed. At first, the formwork was not strong enough to withstand the concrete pressure and adjustments to the formwork were required. With the formwork problems solved, the construction of the staircase was successful and the appearance acceptable[15].



Figure 2.5 Spiral staircase

The mixture design for the SCC used in the staircase is given in Table 2.1.

Table 2.1: Concrete mixture proportions for the Spiral staircase[15]

Material	**kg/m³**
Cem II A-M 42.5	395 kg
GGBS	70 kg
Crusher Sand	750 kg
Filler Sand	290 kg
9.5mm Dolomite	750 kg
Water	195 ℓ
Super plasticizer B	4203 ml
Super plasticizer A	2335 ml
W:C	0.42

This mixture design differs from those of the preceding case studies in that two different superplasticizers were used. Trial mixtures indicated that the aggregate and cement varied too much for a sensitive superplasticizer. Superplasticizer B, which is the same as that used in the Nelson Mandela Bridge project, is a superplasticizer that is not too sensitive to over or under dosage. Unfortunately, this superplasticizer made the mixture very cohesive and superplasticizer A, which is much more sensitive to dosage, was included for flowability. The 9.5 mm crushed dolomite was used for its relatively good particle shape and the preference given to this particle size in SCC. It was found that the 13 mm aggregate from the same crusher was very flaky and did not yield the desired workability. A natural sand was used as a filler.

The actual slump flow as measured on the day of casting was 750 mm. The L-box, V-funnel and slump flow tests, in accordance with the EFNARC Specification[14], and the Tattersall Two Point Test were recently carried out using the same mixture proportions and materials. These results indicate that the mixture was cohesive yet flowable. According to the results obtained from the Tattersall Two Point Test, the yield stress and plastic viscosity is relatively low, confirming that this mixture is self compacting. The test methods used are discussed in Chapter 4.

2.6.4 Other projects

In 2004 a few small projects were completed using SCC. These include the following; At a mine close to Witbank, steel columns were encapsulated with concrete to strengthen them. Due to the size and position of these columns, mechanical vibration was difficult and it was decided to use SCC. The existing steel columns were boxed with timber shuttering and filled from the top with SCC. Even though the concrete fell through a height of four meters, no segregation occurred and the finish was acceptable[16]. The latest project where SCC was used was for the 100 mm thick walls for a safe vault. Due to the position of these walls vibration of the concrete was impossible[16].



Figure 2.6: Repaired culvert in Cape Town

SCC was also used on a project close to Cape Town for the repair of a culvert where the soffit had deteriorated to the extent that the reinforcing steel was exposed. To repair this, timber shuttering was placed below the soffit leaving

enough room for extra reinforcing steel and concrete. SCC was placed through openings drilled from the top.

Inspection openings were also provided at the other end of the slab to check if the space had been filled completely. The operation was completed quickly and successfully. The only problem that was encountered was that rain affected the mixture on one of the days and the superplasticizer dosage had to be adapted. An alternative to using SCC in this case was to build a detour and rebuild the culvert. With the use of SCC the problem was solved in a shorter time and more cost effectively[6].

2.7 Conclusions

SCC is primarily about workability, creating a very flowable mixture that requires no external compaction effort and does not segregate when placed. Various tests were developed to describe the workability of SCC, but the results of these tests are not very accurate and do not describe the properties of the mixture fully. Because of these shortcomings, rheology is used to describe the flow of SCC. To understand rheology and the significance to the flow properties of SCC, the next chapter gives a review on the fundamentals of rheology. This review includes the principles and measurements of concrete rheology as well as the methods used for the measurements.

CHAPTER 3

PRINCIPLES AND MEASUREMENT OF RHEOLOGY

3.1 Introduction

Since concrete is flowable in its fresh state, it is appropriate to use a rheological approach to describe its properties, especially SCC. To measure the rheology and interpret the results, a thorough understanding of rheology principles is required. This chapter explains the fundamental principles of rheology and the relevance to concrete, mortar and paste. The rheometer used to measure the rheology of concrete in this investigation was a Tattersall Two Point Tester. The ViscoCorder was used for the measuring of the mortar rheology. Much of the information in this section is drawn from Tattersall[17] and Tattersall and Banfill[18].

3.2 Background on rheology

Rheology is the science used to describe the flow and deformation of a material and uses fundamental engineering principles to describe and predict the movement between solids and liquids[19]. It is therefore used in materials where the flow properties are much more involved than in a simple fluid. Rheology is concerned with the relationships between stress, strain, rate of strain and time[17]. To understand the rheology of cementitious systems, an understanding of the simple relationships is necessary. The simplest model is described by Hook's law. This law states that in an ideal elastic material the deformation depends only on the load applied, which means that the strain is proportional to stress. This relationship is illustrated in Figure 3.1, where a regular prism is deformed by

equal but opposite forces applied tangentially to opposite faces. Area A is deformed by the shear stress, $\tau = F/A$ and the angle γ represents the deformation or shear strain. Shear stress is therefore proportional to shear strain as shown by Hooke's law (Equation 3.1),

$$\tau = n\,\gamma \tag{3.1}$$

n is the constant of proportionality, the shear modulus.

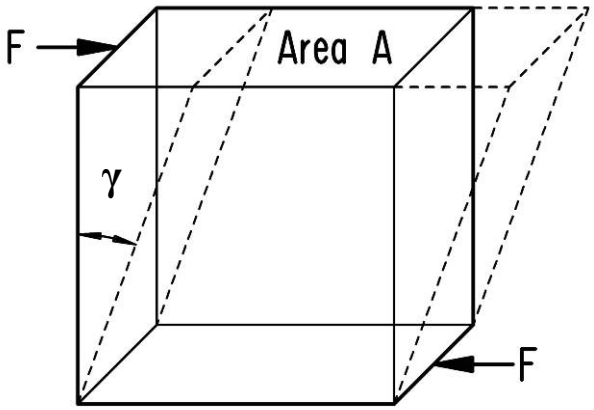


Figure 3.1 Hooke's law for a material in shear[17]

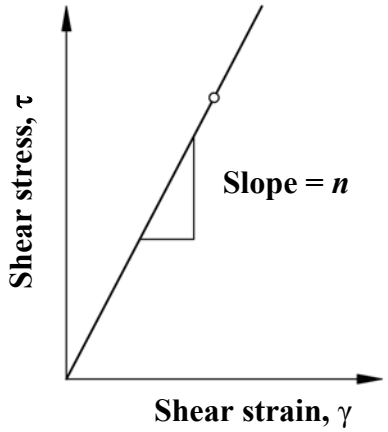


Figure 3.2 Hookean solid in shear[17]

Figure 3.2 shows the straight line relationship if τ is plotted as a function of γ with the slope equal to *n*. If a rectangular prism of a simple fluid could be made, the liquid would deform and keep deforming while the stress is applied. This deformation depends on the rate at which the stress is applied and is measured by the time differential of γ. For a simple liquid the time differential of γ is proportional to τ and the equation is:

$$\tau = \eta \frac{d\gamma}{dt} \tag{3.2}$$

This equation is similar to the Hooke's law except for the shear strain that is replaced by the shear stain rate and η is the constant of proportionality or the coefficient of viscosity. The liquid can be represented by thin laminae moving in laminar motion relative to and confined by the other as shown in Figure 3.3.

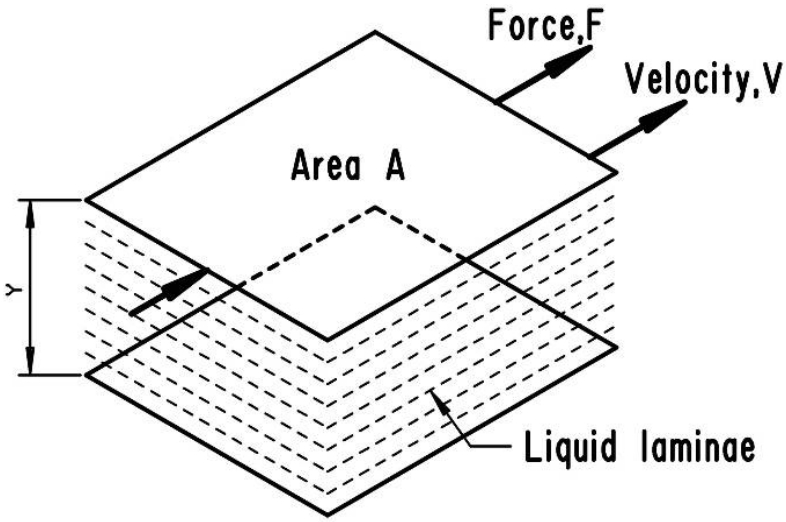


Figure 3.3 Newton's law of viscous flow[17]

This represents Newton's law of viscous flow where the shear stress is proportional to the velocity and inversely proportional to the distance between the planes (y):

$$\tau = \eta \frac{dv}{dy} \tag{3.3}$$

dv/dy is the velocity gradient which is the same as *dγ/dt* and Newton's law of viscous flow may be written as:

$$\tau = \eta \dot{\gamma} \tag{3.4}$$

For a Newtonian liquid in the laminar flow region, only one experimental point is needed since the straight line relationship between shear stress and shear rate will pass through the origin as shown in Figure 3.4. The reciprocal of the slope is equal to η, the coefficient of viscosity.

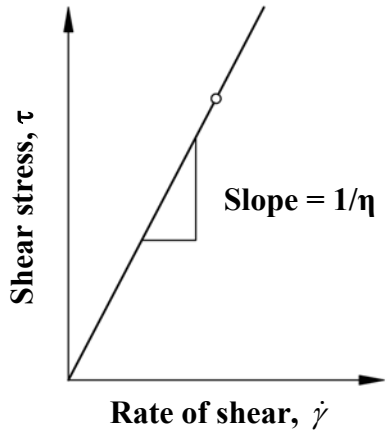


Figure 3.4 Newtonian liquid: $\tau = \eta\dot{\gamma}$ [17]

The Newtonian fluid is the simplest form to describe a fluid, but most substances (including concrete, mortar and cement paste) do not conform to this model. These fluids have a yield point (τ_o) that must be overcome before flow starts. To describe this flow, the shear resistance has to be measured at two shear deformation rates and then represented by a straight line not passing through the origin. The Bingham model, as shown in Figure 3.5, describes this method and the equation of this line is as follows:

$$\tau = \tau_o + \mu\dot{\gamma} \tag{3.5}$$

where τ is the shear stress, τ_o is the yield stress, μ is the plastic viscosity and $\dot{\gamma}$ is the shear strain rate[17].

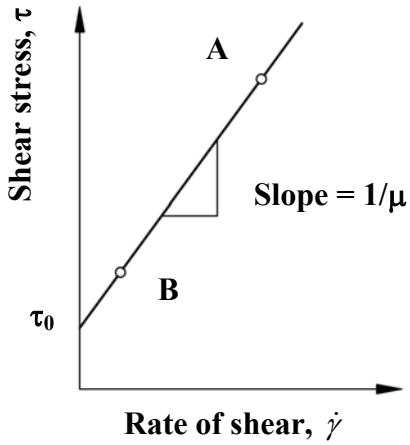


Figure 3.5 Bingham model: $\tau = \tau_o + \mu \dot{\gamma}$

A and **B** are the experimental points required to fix the line[17]

Even though the Bingham model can describe non-Newtonian fluids, it is still too simple for most substances used. The flow curves for these substances may not be linear, as shown in Figure 3.6. If the flow curve is concave towards the stress axis, it describes shear thickening because the shear stress increases more rapidly than the shear rate and the flow decreases rapidly at higher shear rates. Shear thinning on the other hand is caused when stress increases less rapidly than the shear rate, causing the flow to become easier with increasing stress. This flow curve is concave towards the shear rate axis and a typical example of this is a power-law fluid, represented by equation 3.6:

$$\tau = k \dot{\gamma}^{n} \tag{3.6}$$

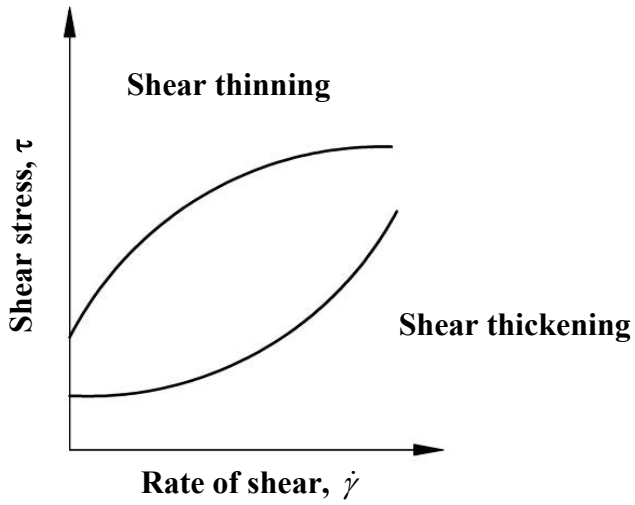


Figure 3.6 Nonlinear flow curves[17]

3.3 Concrete rheology

Since the flowability of concrete is so important, relevant tests are needed to describe this property. It is therefore appropriate to describe flowability through the concept of rheology. Rheology describes the flow of a material scientifically in terms of shear stress and shear rate. These two important parameters are measured simultaneously during one procedure. With a concrete that contains a large proportion of paste, like self-compacting concrete, the stability of the mixture is very important. Stability or resistance to segregation is influenced by five factors. The factors are: high yield value (counteracting sedimentation forces), high plastic viscosity (reducing the rate of sedimentation), thixotropy, lattice effect (smaller particles counter acting the sinking of larger particles) and the ability of the material migrating to the shearing zone[20]. Rheology is the only way to describe all these factors effectively.

Workability tests can be used, but then only one parameter of concrete behaviour is described. It is possible to develop SCC without the use of rheology, but then it is based on feeling which can not be quantified[20].

To measure the rheology of concrete, the two-point test, a dynamic test, was developed to measure shear resistance at two shear deformation rates. The yield stress (τ_o) and plastic viscosity (μ) can therefore be measured and used in the Bingham equation (Equation 3.5) to determine the shear resistance on the assumption that this model is applicable to concrete[18].

The rheology of concrete is best measured with the use of a rheometer. There are a number of rheometers available around the world with significantly different design and operation parameters. The five most commonly used rheometers were compared at the Laboratoire Central des Ponts et Chaussees (LCPC) facility in Nantes, France in 2000. The rheometers used in this comparison were the BML from Iceland, the BTRHEOM and CEMAGREF-IMG coaxial rheometer from France, the IBB from Canada and the Tattersall Two Point Tester from the UK. All these rheometers are designed to effectively describe the rheology of concrete[21].

3.4 Mortar rheology

Mortar rheology is mainly used to determine the optimum admixture dosage and the slump retention (this test method is described in the next chapter). The yield

stress of the mortar phase of SCC should typically be between 20 and 50 Pa and the plastic viscosity between 6 and 12 Pas[22]. The yield stress and plastic viscosity are measured with a rheometer and the fluidity is assessed with a small V-funnel and mini slump cone test. The equipment and procedures for these tests are described in Chapter 4. According to EFNARC[14], the spread when using the mini slump cone should be between 240 and 260 mm. V-funnel flow times should be between 7 and 11 seconds and the workability retention period about two hours[22].

According to Jin and Domone[23] mortar rheology can be used in the process of material selection and concrete proportioning, but different combinations of different materials will give different relationships and the statement is therefore not universally applicable.

3.5 Paste rheology

The biggest advantage in using paste rheology is to determine the cement and admixture compatibility. Superplasticizers are used in SCC to reduce the yield stress. The yield stress should be below 50 Pas and as close to zero as possible. This must be achieved with the lowest required dose to prevent segregation. To be compatible the superplasticizer should also enable the SCC mixture to remain self-compacting for at least 90 minutes in cold or warm temperature[1]. Apart from this there is no real benefit in using paste rheology, because of the

complexity of the properties and behaviour at the interface between aggregate and paste. This explains the difficulty in relating the results from paste tests to concrete made from the same paste. The interfacial paste, the paste closest to the aggregate, behaves differently and has different properties than the bulk paste that fills the space between the aggregate particles. Bulk cement paste consists of a two phase material, cement particles suspended in water. The paste develops its own microstructure and start to change from a liquid to a solid. If aggregate is added to the paste, the paste becomes the suspending medium for the aggregate and this changes the conditions under which the paste performs. This paste is referred to as the interfacial paste. To determine the properties of the interfacial paste it is difficult to simulate the effect during a rheological test. Because of these difficulties, very little research has been done to relate the properties of the bulk fresh paste to that of the fresh concrete[24].

Ferraris and Gaidis[25] used the gap between the plates of a parallel plate viscometer to simulate the space between aggregate particles when measuring the rheology of cement paste. This gap was not representative of the space between the aggregate particles because the particle interlock is part of the rheology and the flow in actual concrete is sensitive to the space between the particles. They also found that if the gap becomes smaller, the cement grains act as grit, reducing the flow. The flow of the concrete cannot be predicted by properties or the volume fraction of the paste alone. Struble, et al[26] states that hydration has a major effect on the flow of cement paste. During the hydration process, the yield

stress increases gradually until the end of the dormant period is reached and then the paste starts to lose its fluid properties. The yield stress and plastic viscosity increases further when aggregate is added to the paste.

According to Banfill[27] the rheology of paste is far more complex than that of concrete, because of structural breakdown in the paste. Structural breakdown occurs when a cement-based system is sheared. When the cement particles hydrate with water, a membrane forms around a group of particles. If this membrane is broken due to shear, more particles hydrate making the structure stronger. This process is irreversible and the links cannot reform when the structure comes to rest. The effect of this structural breakdown is masked or reduced in a concrete mixture. The aggregate present in the concrete changes the properties of the cement:water interface which governs the flow properties of the suspension. Table 3.1 shows the comparison between the rheological properties of cement based materials.

Table 3.1: Rheology of cement based materials:[27]

Material	**Cement paste, grout**	**Mortar**	**Flowing concrete**	**SCC**	**Concrete**
Yield stress (Pa)	10-100	80-400	400	10-50	500-2000
Plastic viscosity (Pas)	0.01-1	1-3	20	20-80	50-100
Structural breakdown	Significant	Slight	None	None	None

3.6 Conclusion

Although it is possible to develop SCC without the use of rheology, it is based on feeling which can not be quantified. Since SCC is more sensitive than conventional concrete, rheology is required to describe the three key properties. It is therefore recommended that rheology is used to evaluate the fresh properties of SCC. The next chapter describes the methods used to measure the rheology and workability of SCC. A description of the material used in the mixtures is also included.

CHAPTER 4

TEST METHODS AND MATERIALS

4.1 Introduction

To determine the appropriate self-compacting properties, e.g. good passing ability, filling ability and resistance to segregation, various test methods are used. The three key properties cannot be described adequately with one method and a combination of tests is required. In 2001 a European project, Testing SCC, was started to investigate and establish suitable test methods to assess the three key properties of SCC[28]. The test methods selected in the European project include the slump flow, the L-box, the V-funnel, the U-test, The Oriment, the 'static sieving' test and the J-Ring. Individually, these tests cannot assess all three properties and the resistance to segregation simultaneous and therefore rheology is required to describe the properties of SCC fully. The European project did not only focus on the test methods but also relate the results to fundamental rheological measurements. These rheological measurements will establish a scientific basis of the recommended properties[28].

The method used in this investigation to measure the rheology of concrete was the Tattersall Two Point Test. The rheology of mortar was measured by using the Tattersall Two Point Test, the ViscoCorder and the MC1 Rheolab rheometer. The MC1 Rheolab rheometer was also used to measure the rheology of paste. From the test methods selected in the European project, the slump flow, the L-box, the

V-funnel and the J-Ring were used to measure the workability of the concrete mixtures. The workability of the mortar mixtures were measured using the mortar flow test and the mini V-Funnel. These methods were used because of their stated suitability in other projects and, importantly, the availability of the equipment to perform these tests. All these methods are described in more detail below.

4.2 Test methods describing the fresh properties of SCC

4.2.1 The Tattersall Two Point Test

This test is used to measure shear resistance at two shear deformation rates. The yield stress (τ_o) and plastic viscosity (μ) can therefore be calculated from the speed and torque measurements and used in the Bingham equation (Equation 3.5) to determine the shear resistance of the concrete under investigation. Even though the Tattersall Two Point Tester has been used in more than twenty industrial and research laboratories and a number of construction sites around the world, there is no standard test procedure[29]. It is therefore necessary to explain the testing and calibration procedure as well as the calculation of the results.

The development of the Tattersall Two Point Tester

The only rheometer currently available in South Africa suitable to test concrete rheology is a Tattersall Two Point Tester which was donated for research purposes by the Cement and Concrete Institute of South Africa. For this reason

the Tattersall Two Point Tester was used in this investigation to measure and define the rheological properties of the concrete tested.

The Tattersall Two Point Tester originated because of impracticalities encountered with the original coaxial cylinders viscometers. The coaxial cylinders viscometers had to be very large to satisfy the requirements for measuring the rheology of a material like concrete. The requirements state that the gap between the two cylinders should be 10 times the size of the largest particle and the ratio of the outer to the inner cylinder radius less than 1,2[18], to ensure reliable measurements. Tattersall[18] initially used a Hobart food mixer to measure the electrical power input when mixing a standard quantity (25 kg) of concrete in the mixing bowl and also when empty. These measurements were taken at the three rotation speeds of the stirring hook. The difference between the two power inputs (P) is divided by the speed (N) to determine the torque (T). The torque was plotted against time and this gave a linear or near linear relationship. This concept was developed further and a bigger apparatus (Figure 4.2) with a special impeller (Figure 4.1) and reduction gearboxes was created to produce more effective results[18].



Figure 4.1: Interrupted helical impeller for the Tattersall Two Point Tester

The Tattersall Two Point Tester measures the pressure in a variable hydraulic transmission when turning an impeller in concrete at different speeds. Measurements at seven speeds are sufficient to calculate the intercept and reciprocal slope of the torque against speed relationship.

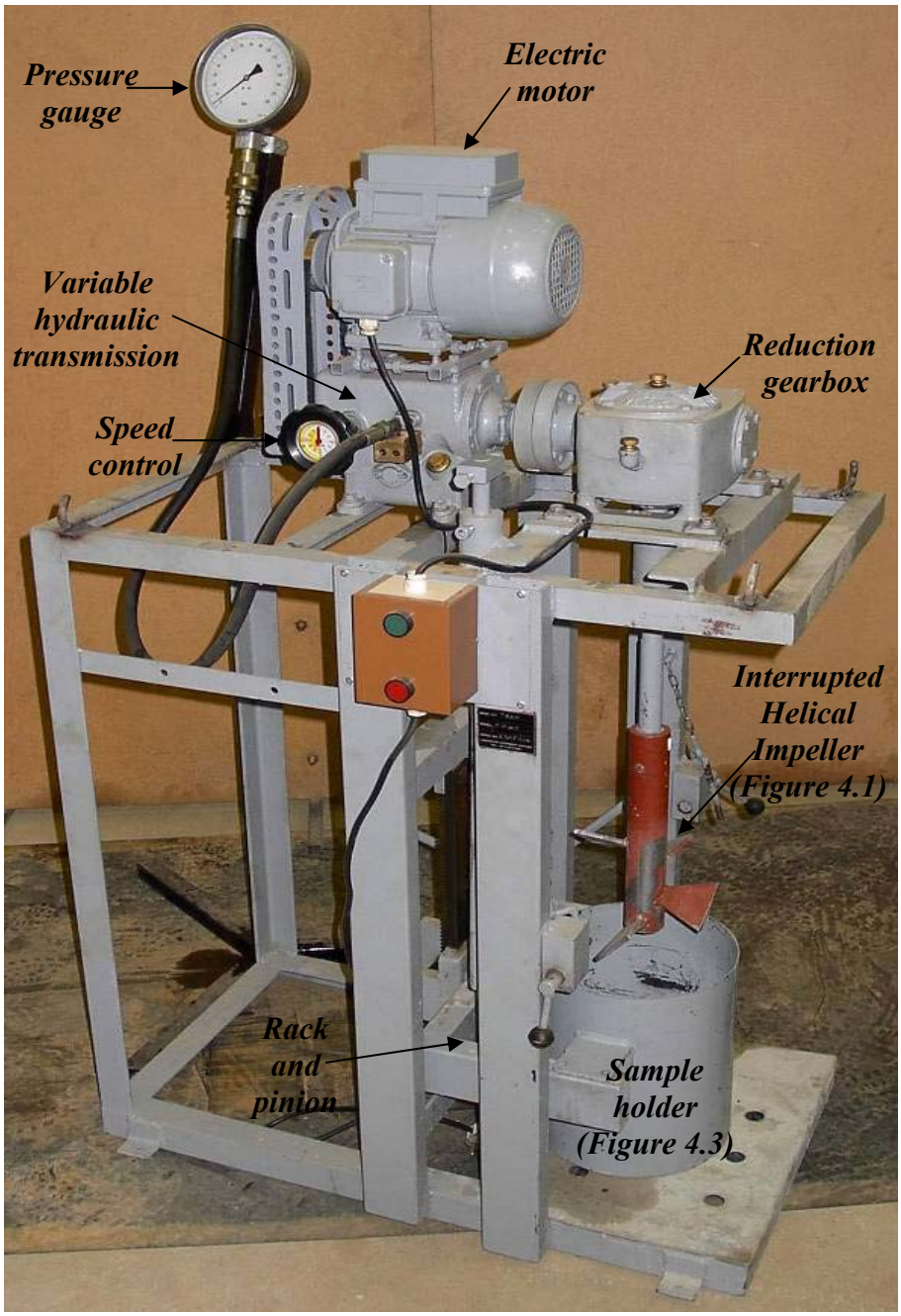


Figure 4.2: Tattersall Two Point Tester

Testing procedure: Before testing can be done, the apparatus must be set up to be level, the reduction gearbox and the hydraulic unit should be filled with the appropriate oil and the hydraulic unit should be free of entrapped air. The impeller is then allowed to turn freely for 60 minutes at the recommended speed of 3 rev/s to allow the oil in the drive unit to reach equilibrium temperature. After the warm up, the procedure for testing is as follows:[17]

- Raise the sample holder with the rack and pinion to the working position so that the clearance between the impeller and the bottom of the sample holder is 60 mm.



Figure 4.3: Sample holder showing the filling mark

- Fill the sample holder gradually with concrete to about 75 mm from the rim while the impeller rotates at approximately 0.7 rev/s.
- Increase the speed to 1.45 rev/s (speed setting 15) and allow the pressure to stabilise.

- Read the speed by tachometer.
- Read the pressure gauge and record the average position of the needle for the small oscillations. Ignore the large oscillations due to trapping of aggregate.
- Repeat procedures 4 and 5 at speeds of approximately 1.25, 1.05, 0.85, 0.65, 0.45, and 0.25 rev/s, (speed settings 13 to 3 in steps of 2).
- Lower the sample holder for the impeller to rotate freely and record the idling pressures at the same speeds used in the measurements on the concrete.

The results can either be plotted on a graph relating net pressure to speed and the intercept and reciprocal slope are then determined from this plot or by using the least squares method[17]. Since it has been shown that the flow properties of concrete conform to the Bingham model[17], the flow curves are taken as linear, the intercept on the torque axis and the reciprocal slope can also be calculated using the least squares method. The flow curve is represented by Equation 4.1:

$$T = g + hN \tag{4.1}$$

Where T is the torque at speed N, g is a measure of the yield value and h is a measure of plastic viscosity[17]. The values of g and h were calculated by multiplying the intercept and slope by the torque/pressure calibration constant.

Table 4.1 shows an example of a calculation for g, h, τ_o and μ from experimental data obtained from the Tattersall Two Point Tester.

Table 4.1: Example of the calculation for *g, h,* τ_o and μ from experimental data obtained from the Tattersall Two Point Tester.

TATTERSALL READINGS Calibration constant: 0.28 Nm/MPa							**RESULTS**					
N	**Pressure (MPa)**			**T**	**N^2**	**N x T**	**h**	**g**	**G**	**K**	**τ_o**	**μ**
(1/s)	**Total**	**Idling**	**Net**	**(Nm)**	**$(1/s)^2$**	**(Nm/s)**	**(Nms)**	**(Nm)**	**(m^3)**	**(no unit)**	**(Pa)**	**(Pas)**
1.45	2.40	1.30	1.1	0.31	2.10	0.45	**0.11**	**0.145**	**0.0082**	**0.6**	**11**	**13**
1.25	2.25	1.25	1	0.28	1.56	0.35						
1.05	2.10	1.21	0.89	0.25	1.10	0.26						
0.85	2.00	1.15	0.85	0.24	0.72	0.20						
0.65	1.85	1.10	0.75	0.21	0.42	0.14						
0.45	1.75	1.05	0.7	0.20	0.20	0.09						
0.25	1.65	1.02	0.63	0.18	0.06	0.04						

Calibration of the Tattersall Two Point Tester

Torque calibration.



Figure 4.4: Side view of Torque calibration equipment

To determine the torque/pressure calibration constant, an adjustable metal clamp with a copper sleeve, fixed so that the impeller drive shaft passes through it, was used. The desired level of frictional force was obtained by varying the tightness of the clamp bolts (Figure 4.5). A lever was attached to the clamp on the one side and a spring balance on the other side fixed to the frame to measure the retarding torque[18].

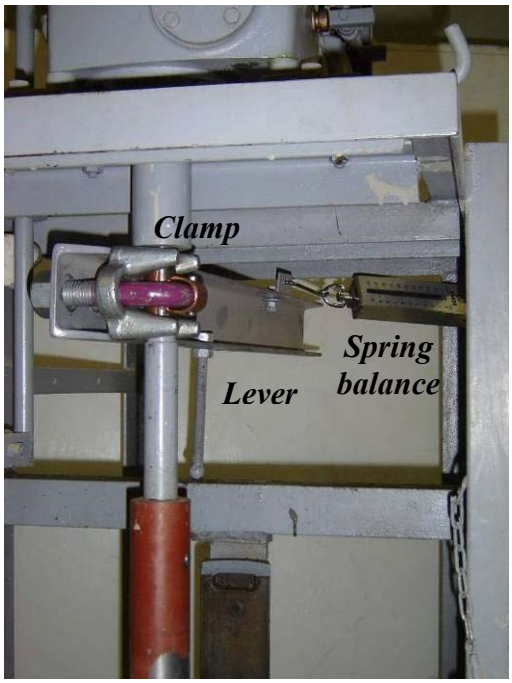


Figure 4.5: Front view of Torque calibration equipment

The spring balance gives a value of kilograms-force (kgf) which must be multiplied by 9.81 m/s^2 to give force in Newton. This force was multiplied by the lever arm (0.5 metres) to get torque in Nm (Newton metre). The torque calibration constant can then be used to calculate the Torque using Equation 4.2:

$$\text{Torque} = \text{constant} \times \text{pressure} \qquad (4.2)$$

Where torque is in Nm and pressure is in MPa[30].

The torque readings were plotted along the ***x*** axis and on the ***y*** axis the pressure readings. The slope of the line gave the constant needed (Figure 4.6). The least squares method (Table 4.2) was also used to determine the slope of this line. For this investigation the calibration constant is taken as 0.28 Nm/MPa.

Table 4.2: Torque calibration results

Force (N)	Torque (Nm)	Pressure (MPa)	(Torque)^2 (Nm)^2	Torque x Pressure (Nm MPa)	Slope (Nm/MPa)
13.50	6.75	2.50	45.56	16.88	**0.28**
27.50	13.75	4.50	189.06	61.88	
42.00	21	6.50	441.00	136.50	
55.75	27.88	8.50	777.02	236.94	
70.50	35.25	10.50	1242.56	370.13	
84.50	42.25	12.50	1785.06	528.13	

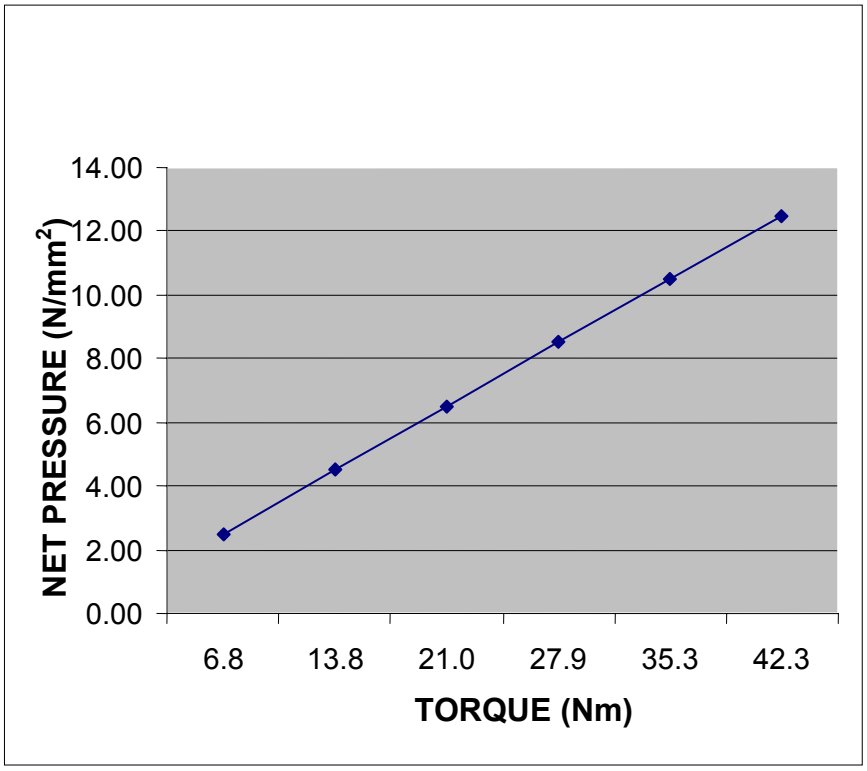


Figure 4.6: Pressure to Torque relationship

Calibration with fluids of known properties. The flow properties of concrete are represented by Equation 4.1. To relate *g* and *h* to the Bingham parameters, yield stress (τ_o) and plastic viscosity (μ) in fundamental units, the Tattersall Two Point Tester had to be calibrated. For the calibration, silicone di-methyl was used as a Newtonian fluid and an aqueous solution of hydroxy ethyl cellulose was used as the power law fluid[31].

To calibrate the Tattersall Two Point Tester the following method was used:[31]

Silicone di-methyl (Newtonian fluid) was tested in the MC1 Rheolab rheometer at five different temperatures as shown in Table 4.3. This information was then used to draw an Arrhenius plot (Figure 4.7) of *ln* η against the inverse of the absolute temperature ($1/T_a$) at which the silicone di-methyl was tested (the Celsius temperature is converted to absolute temperature by adding 273.2). An Arrhenius plot is used to show if the scatter of data points, determined experimentally, is small or large. If there is an Arrhenius relation the data points will be in a straight line[32].

Table 4.3: Viscosity measurements for Silicone di-methyl

Temp.(°C)	Ta (K)	1/Ta (1/K)	η (Pas)	*ln* η (Pas)
17	290.2	0.00345	21.33	3.06
26	299.2	0.00334	17.93	2.89
30	303.2	0.0033	16.62	2.81
36	309.2	0.00323	14.91	2.70
45	318.2	0.00314	12.89	2.56

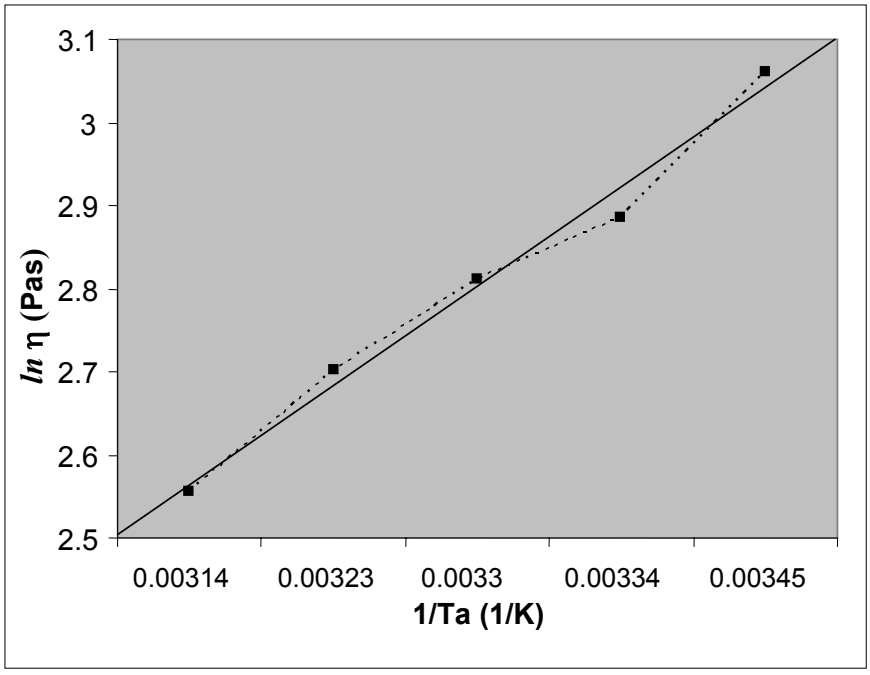


Figure 4.7: Arrhenius plot of *ln* η (in Pas) against the inverse of the absolute temperature (in 1/K)

The silicone di-methyl was also used in the Tattersall Two Point Tester to measure the torque at ten different speeds and three different temperatures. (Table 4.4 contains these results as well as the calculations for the slope of the T/N graph).

Table 4.4: Tattersall measurements and slope calculations for Silicone di-methyl

Temp	Speed (N)	Pressure (MPa)			Torque (T)	$(N)^2$	N x T	Slope
(ºC)	(1/s)	Total	Idling	Net	(Nm)	$(1/s)^2$	(Nm/s)	(Nms)
17.3	2.05	2.45	1.6	0.85	0.24	4.20	0.49	**0.12**
	1.85	2.3	1.55	0.75	0.21	3.42	0.39	
	1.65	2.15	1.48	0.67	0.19	2.72	0.31	
	1.45	2.05	1.45	0.6	0.17	2.10	0.24	
	1.25	1.9	1.38	0.52	0.15	1.56	0.18	
	1.05	1.72	1.3	0.42	0.12	1.10	0.12	
	0.85	1.55	1.25	0.3	0.08	0.72	0.07	
	0.65	1.4	1.17	0.23	0.06	0.42	0.04	
	0.43	1.25	1.1	0.15	0.04	0.18	0.02	
	0.25	1.15	1.03	0.12	0.03	0.06	0.01	
26	2.05	2.15	1.55	0.6	0.17	4.20	0.34	**0.09**
	1.85	2.05	1.5	0.55	0.15	3.42	0.28	
	1.65	1.95	1.42	0.53	0.15	2.72	0.24	
	1.45	1.85	1.38	0.47	0.13	2.10	0.19	
	1.25	1.72	1.32	0.4	0.11	1.56	0.14	
	1.05	1.6	1.28	0.32	0.09	1.10	0.09	
	0.85	1.45	1.2	0.25	0.07	0.72	0.06	
	0.65	1.35	1.15	0.2	0.06	0.42	0.04	
	0.43	1.22	1.1	0.12	0.03	0.18	0.01	
	0.25	1.12	1.05	0.07	0.02	0.06	0.00	
35	2.05	2.1	1.52	0.58	0.16	4.20	0.33	**0.07**
	1.85	1.98	1.48	0.5	0.14	3.42	0.26	
	1.65	1.85	1.42	0.43	0.12	2.72	0.20	
	1.45	1.75	1.38	0.37	0.10	2.10	0.15	
	1.25	1.65	1.32	0.33	0.09	1.56	0.12	
	1.05	1.55	1.25	0.3	0.08	1.10	0.09	
	0.85	1.43	1.2	0.23	0.06	0.72	0.05	
	0.65	1.33	1.13	0.2	0.06	0.42	0.04	
	0.43	1.2	1.07	0.13	0.04	0.18	0.02	
	0.25	1.12	1.02	0.1	0.03	0.06	0.01	

The viscosities (η) at the working temperatures used in the Tattersall Two Point Tester were found by interpolating and converting the values from Figure 4.7. These viscosities as well as the linear relationship between T and N at the three temperatures were then used to determine the apparatus constant (G) in Equation 4.3:

$$\frac{T}{N} = G\eta \tag{4.3}$$

Table 4.5 is a summary of these results.

Table 4.5: Variation of viscosity with temperature.

Temp (°C)	$1/T_a$ (1/K)	η (Pas)	Slope (Nms)
17.3	3.44×10^{-3}	21.33	0.12
26	3.34×10^{-3}	17.93	0.09
35	3.25×10^{-3}	15.18	0.07

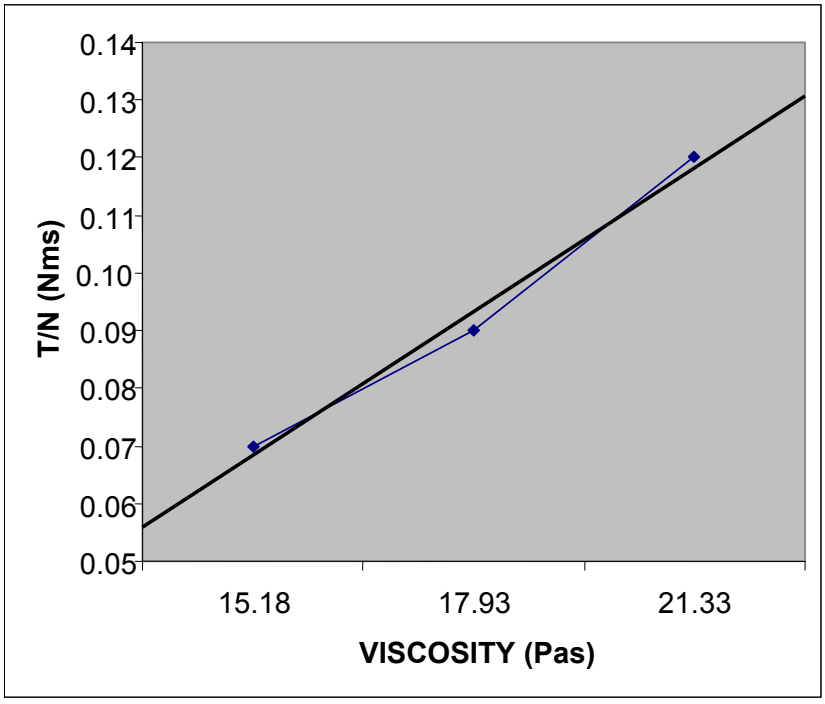


Figure 4.8: T/N against η for the Tattersall Two Point Tester

The value G = 0.0082 m^3 is the slope of the best straight line of the T/N against η relation[31], as shown in Figure 4.8. This value of G will be used in all the following calculations as well as the conversion of the g and h values obtained from the Tattersall Two Point Tester results.

To determine the value of K, constant of proportionality, two aqueous solutions of hydroxy ethyl cellulose (3 % and 4 %) were used. These were pseudo plastic fluids that obey the power law relation given in Equation 4.4:

$$\tau = k\dot{\gamma}^n \tag{4.4}$$

The torque values at ten different speeds were measured using these solutions in the Tattersall Two Point Tester. The results as shown in Table 4.6 were used to determine the relationship between *ln* Speed (*ln* N) and *ln* Torque (*ln* T). The slope of this line is equal to q (constant used in Equation 4.5) and from the intercept on the y-axis (ln p) the value of p is obtained in Equation 4.5:

$$\ln T = \ln p + q \ln N \tag{4.5}$$

Table 4.6: Tattersall measurements and slope calculations for two aqueous solutions of hydroxy ethyl cellulose (HEC)

	N (1/s)	Pressure (MPa)	T (Nm)	*ln* N (1/s)	*ln* T (Nm)	*(ln* N)^2 (1/s)^2	*ln* N x *ln* T (Nm/s)	Slope (q) (Nms)	*ln* p (Nm)	p (Nm)
3 % HEC	2.05	0.4	0.11	0.72	-2.19	0.52	-1.57	**0.31**	**-2.332**	**0.097**
	1.85	0.4	0.11	0.62	-2.19	0.38	-1.35			
	1.65	0.4	0.11	0.50	-2.19	0.25	-1.10			
	1.45	0.4	0.11	0.37	-2.19	0.14	-0.81			
	1.25	0.4	0.11	0.22	-2.19	0.05	-0.49			
	1.05	0.35	0.10	0.05	-2.32	0.00	-0.11			
	0.85	0.35	0.10	-0.16	-2.32	0.03	0.38			
	0.65	0.3	0.08	-0.43	-2.48	0.19	1.07			
	0.43	0.3	0.08	-0.84	-2.48	0.71	2.09			
	0.25	0.2	0.06	-1.39	-2.88	1.92	4.00			
4 % HEC	2.05	1.3	0.36	0.72	-1.01	0.52	-0.73	**0.17**	**-1.113**	**0.329**
	1.85	1.3	0.36	0.62	-1.01	0.38	-0.62			
	1.65	1.28	0.36	0.50	-1.03	0.25	-0.51			
	1.45	1.23	0.34	0.37	-1.07	0.14	-0.40			
	1.25	1.23	0.34	0.22	-1.07	0.05	-0.24			
	1.05	1.2	0.34	0.05	-1.09	0.00	-0.05			
	0.85	1.2	0.34	-0.16	-1.09	0.03	0.18			
	0.65	1.1	0.31	-0.43	-1.18	0.19	0.51			
	0.43	0.97	0.27	-0.84	-1.30	0.71	1.10			
	0.25	0.93	0.26	-1.39	-1.35	1.92	1.87			

The same aqueous solutions of hydroxy ethyl cellulose were used in the MC1 Rheolab rheometer to determine the relation between $ln\dot{\gamma}$ and $ln\ \tau$ at twenty different speeds (Table 4.7 and 4.8). Shear stress values are taken up to a speed of 2.2, readings at faster speeds show too much turbulence (the flow curve bends towards the speed axis)[33].

Table 4.7: MC1 Rheolab rheometer measurements and slope calculations for 3 % aqueous solutions of hydroxy ethyl cellulose for the calibration of the Tattersall Two Point Tester.

	Speed (1/s)	**τ (Pa)**	***ln* τ (Pa)**	$\dot{\gamma}$ **(1/s)**	$ln\ \dot{\gamma}$ **(1/s)**	$(ln\ \dot{\gamma})^2$ **$(1/s)^2$**	$ln\ \dot{\gamma}$ **x *ln* τ (Pa/s)**	**Slope s (1/Pas)**	***ln* r (1/s)**	**r (1/s)**
HEC 3 %	0.1032	187	5.23	1.5733	0.45	0.21	2.37	**0.362**	**4.5**	**89.74**
	0.112	193	5.26	1.708	0.54	0.29	2.82			
	0.1233	201	5.30	1.8808	0.63	0.40	3.35			
	0.1365	212	5.36	2.0816	0.73	0.54	3.93			
	0.1503	219	5.39	2.2926	0.83	0.69	4.47			
	0.1663	228	5.43	2.5366	0.93	0.87	5.05			
	0.1833	235	5.46	2.7958	1.03	1.06	5.61			
	0.205	245	5.50	3.1263	1.14	1.30	6.27			
	0.225	256	5.55	3.4313	1.23	1.52	6.84			
	0.25	265	5.58	3.8125	1.34	1.79	7.47			
	0.2767	274	5.61	4.2192	1.44	2.07	8.08			
	0.3067	283	5.65	4.6767	1.54	2.38	8.71			
	0.34	295	5.69	5.185	1.65	2.71	9.36			
	0.375	308	5.73	5.7188	1.74	3.04	9.99			
	0.415	317	5.76	6.3288	1.85	3.40	10.63			
	0.46	328	5.79	7.015	1.95	3.79	11.29			
	0.5083	341	5.83	7.7521	2.05	4.19	11.94			
	0.5617	348	5.85	8.5654	2.15	4.61	12.57			
	0.6217	362	5.89	9.4804	2.25	5.06	13.25			
	0.69	368	5.91	10.523	2.35	5.54	13.90			

Table 4.8: MC1 Rheolab rheometer measurements and slope calculations for 4 % aqueous solutions of hydroxy ethyl cellulose for the calibration of the Tattersall Two Point Tester.

	Speed (1/s)	τ (Pa)	*ln* τ (Pa)	$\dot{\gamma}$ (1/s)	*ln* $\dot{\gamma}$ (1/s)	$(ln\,\dot{\gamma})^2$ $(1/s)^2$	*ln* $\dot{\gamma}$ x *ln* τ (Pa/s)	Slope s (1/Pas)	*ln* r (1/s)	r (1/s)
HEC 4 %	0.205	31.4	3.45	6.068	1.80	3.25	6.21	**0.077**	**3.22**	**24.90**
	0.227	29.8	3.39	6.709	1.90	3.62	6.46			
	0.257	28.6	3.35	7.597	2.03	4.11	6.80			
	0.292	28.9	3.36	8.633	2.16	4.65	7.25			
	0.332	29.4	3.38	9.817	2.28	5.22	7.72			
	0.375	28.7	3.36	11.100	2.41	5.79	8.08			
	0.427	29.7	3.39	12.629	2.54	6.43	8.60			
	0.483	29.6	3.39	14.307	2.66	7.08	9.01			
	0.550	30.7	3.42	16.280	2.79	7.78	9.55			
	0.622	29.7	3.39	18.401	2.91	8.48	9.88			
	0.708	31	3.43	20.967	3.04	9.26	10.45			
	0.802	31.5	3.45	23.729	3.17	10.03	10.93			
	0.910	32.2	3.47	26.936	3.29	10.85	11.43			
	1.032	32.8	3.49	30.537	3.42	11.69	11.93			
	1.170	33.5	3.51	34.632	3.54	12.57	12.45			
	1.328	34.3	3.54	39.319	3.67	13.48	12.98			
	1.507	33.6	3.51	44.597	3.80	14.42	13.35			
	1.717	35.2	3.56	50.813	3.93	15.43	13.99			
	1.933	33.8	3.52	57.227	4.05	16.38	14.25			
	2.200	33.7	3.52	65.120	4.18	17.44	14.69			

From these values, linear regression is done to determine the relation between $ln\,\dot{\gamma}$ and *ln* τ. The slopes of these lines (linear), shown in figure 4.9, are equal to s (constant used in Equation 4.6) and from the intercept on the y-axis (*ln* r) the value of r is obtained in Equation 4.6:

$$ln\,\tau = ln\,r + s\,ln\,\dot{\gamma} \qquad (4.6)$$

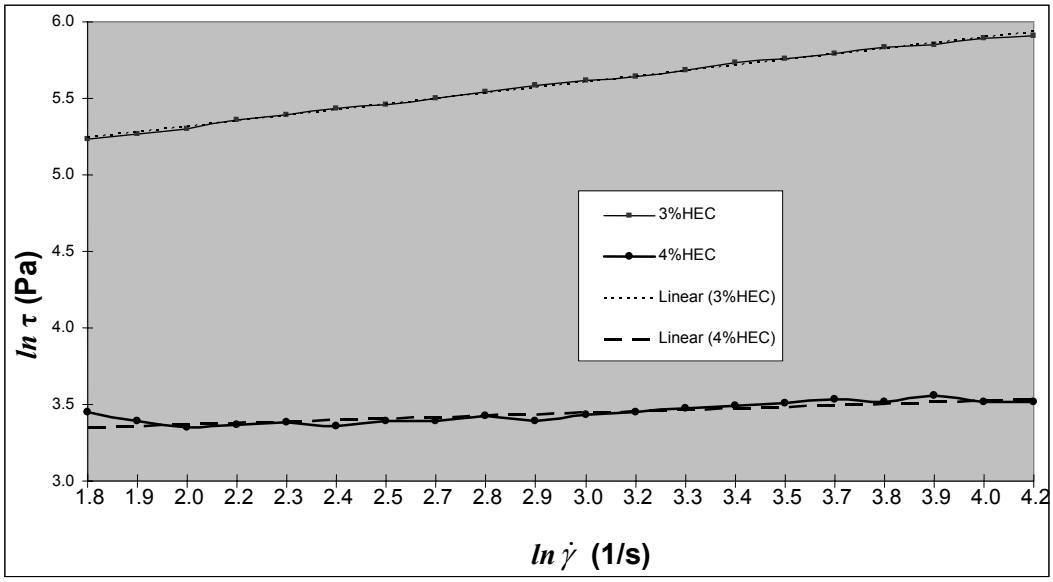


Figure 4.9: Relation between $ln\,\dot{\gamma}$ and $ln\,\tau$ for the Tattersall Two Point Tester.

Table 4.9 is a summary of these results.

Table 4.9: Power law parameters for hydroxy ethyl cellulose for the calibration of the Tattersall Two Point Tester.

	ln p	p	q	*ln* r	r	s
3 %	-2.332	0.097	0.31	4.5	89.74	0.362
4 %	-1.113	0.392	0.17	3.22	24.9	0.077

The degree of approximation is calculated for each solution using Equation 4.7 to determine if the relationship between shear rate and speed is linear.

$$\frac{q-1}{s-1} \tag{4.7}$$

For the 3 % hydroxy ethyl cellulose solution $\frac{q-1}{s-1} = 1.082$, which is close to one, indicating that the relationship between shear rate and speed is independent of the speed and is one of simple proportionality with a proportionality constant *K:*

$$K = \left(\frac{p}{rG}\right)^{\frac{1}{s-1}} (31) \tag{4.8}$$

$$K = 24.2$$

For the 4 % hydroxy ethyl cellulose solution $\frac{q-1}{s-1} = 0.9$, which is close to one, indicating that the relationship between shear rate and speed is independent of the speed and is one of simple proportionality with a proportionality constant *K:*

$$K = \left(\frac{p}{rG}\right)^{\frac{1}{s-1}} (31) \tag{4.8}$$

$$K = 0.6$$

The constant of proportionality converts the speed of rotation to a mean effective shear rate [34] and it is assumed that there was an average effective shear rate in the apparatus and this is given by Equation 4.9:[17]

$$\dot{\gamma}_{ave} = KN \tag{4.9}$$

The values of $G = 0.0082$ and $K = 0.6$ can be used to express the g and h values obtained from the Tattersall Two Point Tester in terms of τ_o and μ using the following equations:

$$\tau_o = (K/G)g \quad (4.10)$$

$$\mu = (1/G)h \quad (4.11)$$

Therefore:

$$\tau_o = 72.86 * g \quad (4.12)$$

$$\mu = 121.95 * h \quad (4.13)$$

4.2.2 The Slump Flow Test.

The slump flow test is used to evaluate the flowability, deformability and stability of SCC. Included in this test is the T50 value which describes the viscosity. A conventional slump cone is used in this test. The test is performed on a 900 mm x 900 mm base plate with a 500 mm ϕ circle drawn on the surface for the measurement of the T50 time.

Testing procedure: [29]

- Dampen the interior of the slump cone and the surface of the base plate.
- Make sure the base plate is flat and horizontal and place the cone in the centre of the 500 mm circle, on the base plate.

- While pressing the cone down firmly, fill the cone continuously with SCC to the top, without consolidating the concrete and level off.
- Remove the slump cone immediately and perpendicular to the base plate, starting the stopwatch as the lifting begins.
- Record the time the concrete takes to reach the 500 mm ϕ circle (T50).
- Measure the final diameter of the concrete as soon as it stops flowing. Assess the concrete for segregation and bleeding.

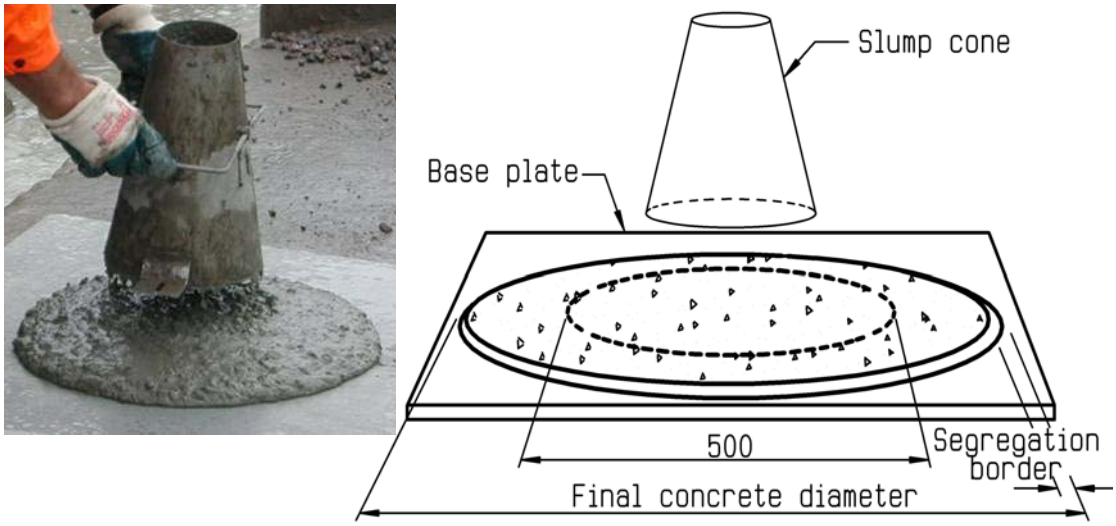


Figure 4.10: The Slump flow test[1]

4.2.3 The J-Ring test.

To assess the passing ability and segregation resistance of SCC the J-Ring test was used. Figure 4.11 shows the slump flow after the concrete has passed through the J-Ring. The J-Ring is a steel ring of section 25 mm x 30 mm, with 10 mm ϕ steel bars fixed to this ring. The internal diameter of this ring is 330 mm and spacing between the bars is 34 mm. This ring is used with the conventional slump

cone. In this investigation the cone was used in the inverted position to simplify the placing of the concrete in the cone.



Figure 4.11: The J-Ring test

Testing procedure:[29]

- Place the 900 mm x 900 mm base plate (as for slump flow test) on a level surface and wipe the surface with a damp cloth.
- Place the ring in the centre of the 500 mm ϕ circle on the base plate.
- Wipe the inside of the cone with a damp cloth and place it in the centre of the ring.
- While holding down the cone in the inverted position, fill the cone continuously with freshly mixed SCC to the top, without consolidating the concrete and level off.
- Lift the cone straight up in one continuous motion while someone else starts the stop watch as the lifting begins.

- Record the time the concrete takes to reach the 500 mm ϕ circle (T50).
- Measure the final diameter of the concrete as soon as it stops flowing.
- Place a straight bar on top of the ring and measure the distance from the bottom of this bar straight down to the centre of the slumped concrete. Record this reading as d_1.
- Measure the distances from the bottom of the bar straight down to the top of the slumped concrete at four positions (d_{a1}, d_{a2}, d_{a3} and d_{a4}) as shown in Figure 4.12, on the inside and outside of the ring. Record these values as $d_{a(1\text{ to }4)}$ and $d_{b(1\text{ to }4)}$ respectively.
- The values $h_1 = 125 - d_1$, $h_{a(1\text{ to }4)} = 125 - d_{a(1\text{ to }4)}$ and $h_{b(1\text{ to }4)} = 125 - d_{b(1\text{ to }4)}$, are then calculated.
- Calculate the four values $h_{m(1\text{ to }4)} = h_1 - h_{a(1\text{ to }4)}$ and the median value h_m of these values.
- Calculate the four values $h_{r(1\text{ to }4)} = h_{a(1\text{ to }4)} - h_{b(1\text{ to }4)}$ and the median value h_r of these values.
- Calculate St_J (step of blocking, shown in Figure 4.13) = $2(h_r - h_m)$.

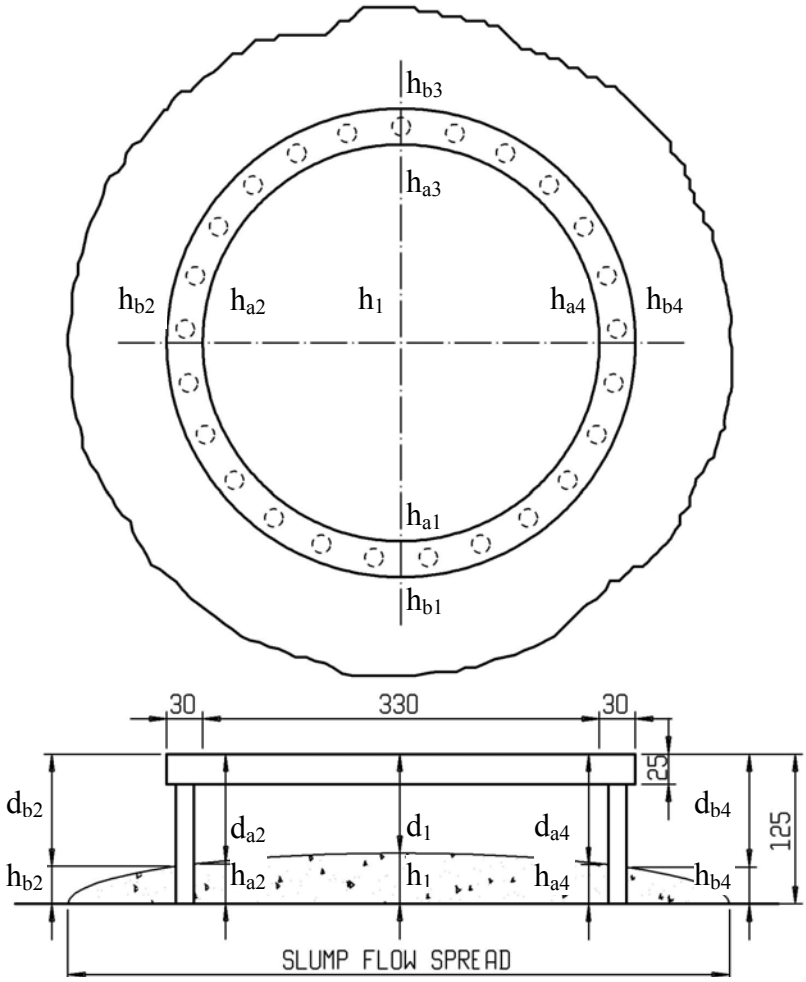


Figure 4.12: The J-Ring dimensions

Passing ability is satisfactory if the step of blocking (St_J) value is less than 15 mm and the SCC can be considered as not subject to blockage. A value of 10 mm indicates good passing ability[35]. The slump flow spread also gives an indication of the passing ability, the bigger the slump flow spread, the better the passing ability.

To determine the blocking index, Equation 4.14[35] is used:

$$\beta = \frac{V_{block}}{V_C} = \frac{\frac{\pi D^2}{4} st_J}{V_C} = \frac{\frac{\pi D^2}{4}}{V_C} st_J \qquad (4.14)$$

Where β blocking index

V_C whole concrete volume (volume of slump cone)

V_{block} blocked concrete volume

St_J step of blocking

D diameter of the idealized concrete shape

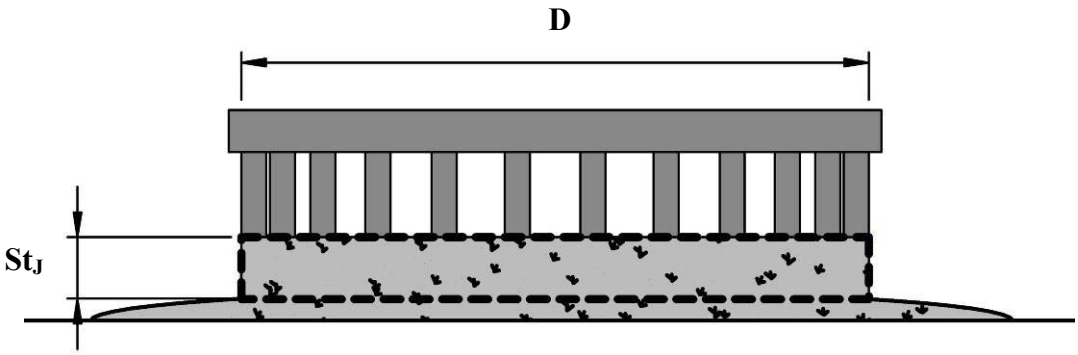


Figure 4.13: Description of Step of blocking in the J-Ring test

4.2.4 The V-Funnel Test.

This test is used to evaluate the passing ability and segregation resistance of SCC.



Figure 4.14: V-Funnel

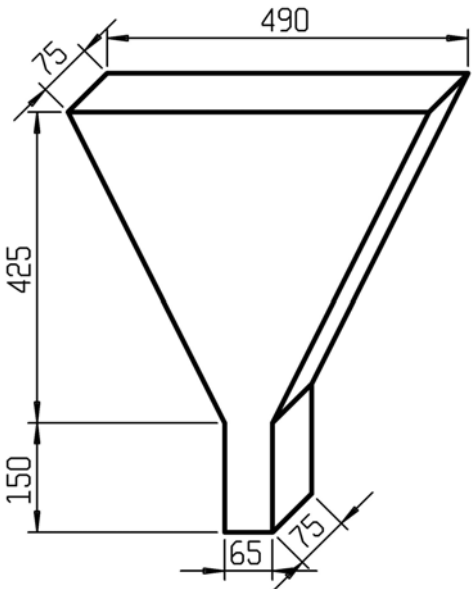


Figure 4.15: V-Funnel dimensions

Testing procedure: [29]

- Dampen the interior of the V-Funnel and place on a level surface with the gate closed and a container placed underneath the opening.
- Fill the V-Funnel continuously with SCC to the top, without consolidating the concrete.
- Wait one minute for the concrete to settle and observe for segregation and bleeding.
- Open the gate and start the stopwatch simultaneously.
- Record the time when the concrete has flowed out of the V-Funnel (flow time = t_0)
- If blocking occurs, it indicates instability of the SCC mixture.

- Repeat the test a few times with separate samples within 5 minutes of each other and take the average.

If there is segregation resistance, repeat the test procedure but wait 5 minutes before opening the gate. This flow time is recorded as t_5.

4.2.5 The L-Box test.

The L-Box test is based on the L-Flow test developed in Japan for underwater concrete. Peterson[29] developed the L-Box test to assess the through-flow ability and filling ability of SCC. The L-shaped box (as shown in Figure 4.16) is 700 mm long and 600 mm high with reinforcing bars placed in front of the gate.



Figure 4.16: L-Box

Testing procedure:

- Clean and dampen the interior of the L-Box and place on a level surface with the gate closed.
- Fill the vertical section of the L-Box continuously with SCC to the top, without consolidating the concrete.
- Wait one minute for the concrete to settle and observe for segregation and bleeding.
- Open the gate and start the stopwatch simultaneously, allowing the concrete to flow into the horizontal part.
- Measure the time it takes the concrete to reach the 200 mm (T_{20}) as well as the 400 mm (T_{40}) markings.
- Measure the H_1 and H_2 distances as soon as the concrete stops flowing.

The blocking ratio, H_2/H_1 should be between 0.8 and 1.0[14]

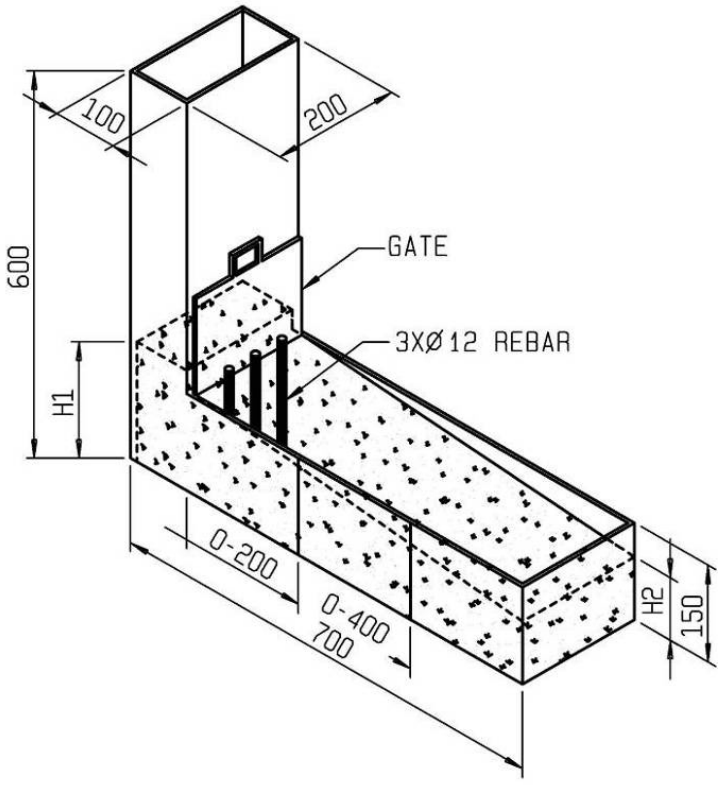


Figure 4.17: L-Box dimensions

4.2.6 Visual assessment test[29]

All the mixtures were assessed visually during mixing as well as before the standard tests, described above, were done. This test depends on the experience of the operator, but symptoms such as excessive bleeding and segregation can be picked up quickly. The standard tests usually confirm the results of the visual assessment. Visual assessment is done using a steel float passing through the freshly mixed concrete to assess the flow and to see how the concrete reacts when disturbed. The steel float is also used to determine the finish ability. Bleeding, cohesion, compact ability and segregation are continuously assessed while all the standard tests are performed. The cubes are also assessed for surface finish and denseness.

4.3 Test methods describing the fresh properties of the SCC mortar.

From recommendations by Jin and Domone[23] the mixture proportions for the mortar is similar to the concrete mixtures, excluding the stone content. A mixer similar to the Hobart as described in SABS EN-196-1[36] was used for the mixing.

The following workability tests were done to determine the correlation between the workability of the concrete and that of the mortar.

4.3.1. The Tattersall Two Point Test

The equipment and procedure is the same as for concrete.

4.3.2. The MC1 Rheolab rheometer.

This rheometer is used to measure the rheology of fluids. The MC1 was therefore used for the calibration of the Tattersall Two Point Tester and the ViscoCorder. It was also used for the measurement of the mortar and paste rheology. Two configurations were used in the measurements. A serrated bob in a Z3 DIN cup was used for the calibration of the Tattersall Two Point Tester as well as some of the cement paste mixtures. This configuration is shown in Figure 4.18 and Figure 4.20. For the measurement of the mortar and most of the cement paste mixtures a vane was used with the Z3 DIN cup, shown in Figure 4.19. Since the requirements state that the gap between the two cylinders should be 10 times the size of the largest particle, the bob could only be used to measure the cement paste. Both the bob and the vane were used to measure shear stress at different shear strain rates. This information was used to determine the yield stress and plastic viscosity of the paste or mortar mixtures. For the calibration of the Tattersall Two Point Tester and the ViscoCorder, the viscosity of the calibration fluid was measured with MC1 Rheolab rheometer.

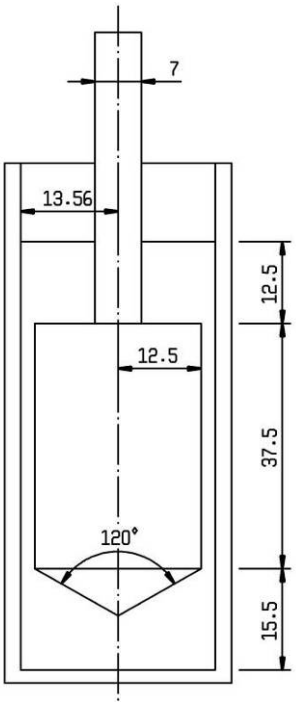


Figure 4.18: Bob geometry

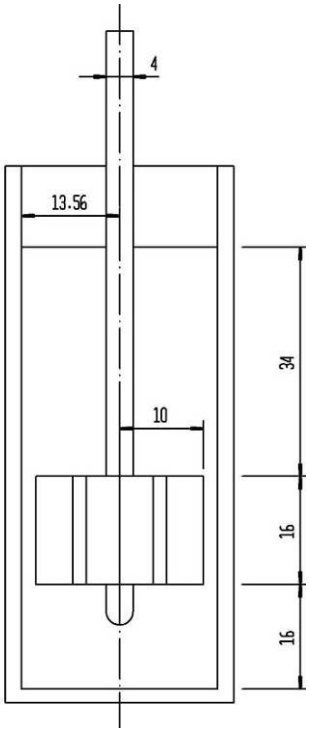


Figure 4.19: Six Blade Vane geometry

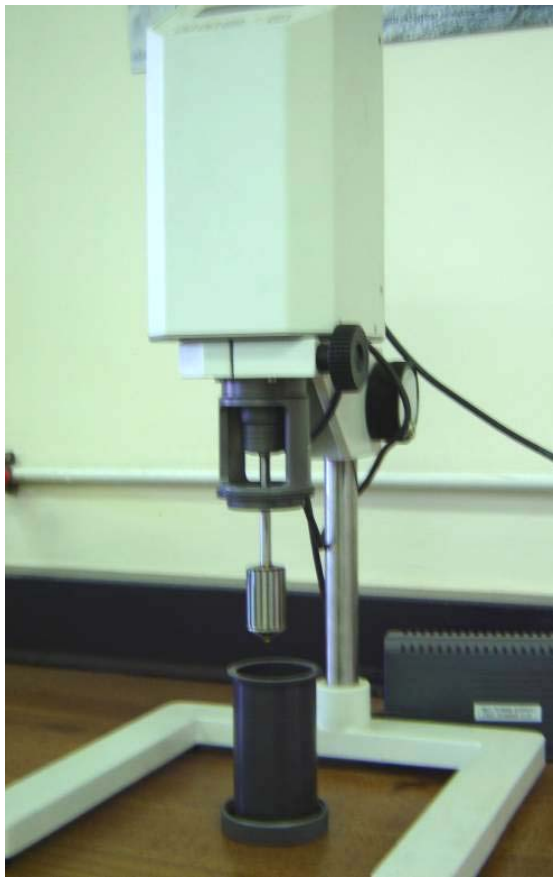


Figure 4.20: MC1 Rheolab rheometer

The testing procedure is fully automated and computerized. Specialized software (US 200 Paar Physica) drives the process and requires only the necessary inputs.

Testing procedure:

- Switch the rheometer on prior to starting up the computer.
- Start the computer, select the US 200 software and open a file.
- Select “File Assistant” for the appropriate procedure.
- Open “Workbook Assistant” and click “OK”.
- Select “Flow curve/CSR” and click “Finish” (CSR – Controlled shear rate).
- Enlarge the “Measurement 1: Flow curve/CSR” window.
- Double click on the “MC1+” icon and under “Measuring Systems” select either the bob or the vane.
- Select “Rotation γ, n” by double clicking.
- Under “Set variable” select “n speed” from the drop down menu and under “Unit” select “rpm”.
- Type in the desired rotational speed under “Initial” and click “OK”.
- Double click on “1”, the block showing the measurement point information.
- Under “Meas. Points” type in the desired number of data points.
- Type in the desired time duration per data point under “Meas. Points” in the “Duration” menu and click “OK”.
- Press the “OK” key on the rheometer.
- Select “Remote” using the arrow keys on the rheometer and press “OK”.
- Place the sample to be tested in the cup, filling it up to the ring inside the cup.

- Insert either the bob or vane into the rheometer and then the cup.
- Click the “Start” button in the “Measurement 1” window.
- Type in the desired “Data series name for the measurement” and the “Sample description”.
- Press “Enter” on the keyboard.
- Type in the “File name” keeping the *.mph* extension and a description of the test in “Remark”.
- Click “Save” to start the test.
- After completion of the test the data is presented in tabular form in “Table 1” and graphical form in “Diagram 1”.
- Click on “File” and select “Save” to type in the “File name”, keeping the *.ctx* extension.
- By clicking “Save” all the information will be saved in the US 200 software.
- The data can then be copied and pasted in a spreadsheet for analysis.

4.3.3 The mortar flow Test

The mortar flow test is similar to the slump flow test used for SCC. This test requires a cone as shown in Figure 4.21. The mortar is mixed in a Hobart, or similar, mixer before the test is performed.

Mortar mixing procedure is as follows:

- Pour the required amount of water in the mixing bowl, including the admixture if required, and then add the cement.
- Mix the cement paste for thirty seconds at speed 1 (140 rev/min).
- Stop the mixer after thirty seconds and add the sand.
- Mix for one minute and after stopping the mixer change to speed 2 (285 rev/min).
- Mix for a further one minute.

(The mixing procedure for paste is similar, except for adding the sand)

Testing procedure:

- Dampen the cone on the inside and place it on a smooth, level, watertight surface,
- Fill the cone with mortar from the mixer while pressing the cone down,
- Without compacting the mortar, scrape the top and lift the cone in one movement,
- Measure two perpendicular diameters of the flow and determine the deformability with Equation 4.15:

$$\Gamma_m = \frac{(d_1 \cdot d_2 - d_0^{\,2})}{d_0^2} \tag{4.15}$$

Where d_1 and d_2 are the two measured diameters and d_0 is the bottom diameter of the cone.

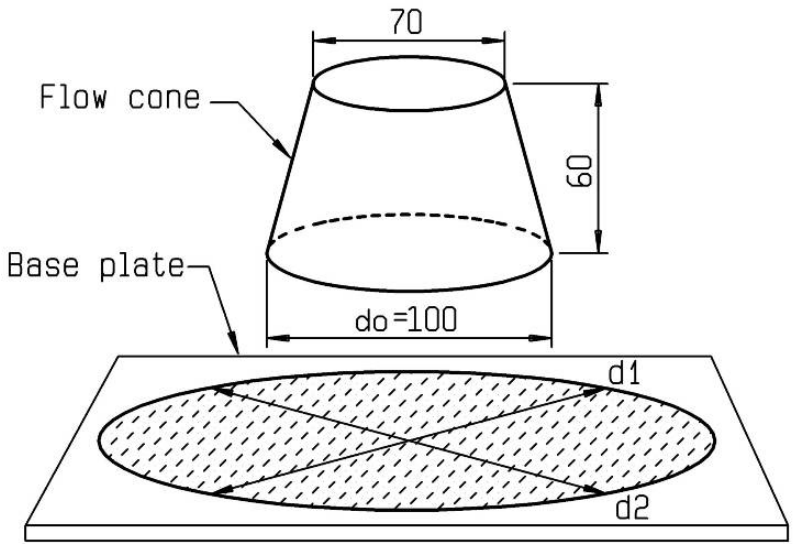


Figure 4.21: The mortar flow test.

Γ_m is the relative flow area and this describes the deformation capacity of the mortar. Larger Γ_m values indicate higher deformability and the recommended value is between 3 and 7[37].

4.3.4 The mini V-Funnel Test.

The procedure for this test is the same as for the V-funnel test and the dimensions of the mini V-funnel are shown in Figure 4.22. In this test the flow time t or the relative funnel speed R_m is used to describe the viscosity of the mortar. The smaller R_m values indicate higher viscosity. The recommended value of R_m is 1 for concrete to be classified as self compacting[38]. The relative flow time is calculated using Equation 4.16:

$$R_m = \frac{10}{\text{funnel time (sec)}} \tag{4.16}$$

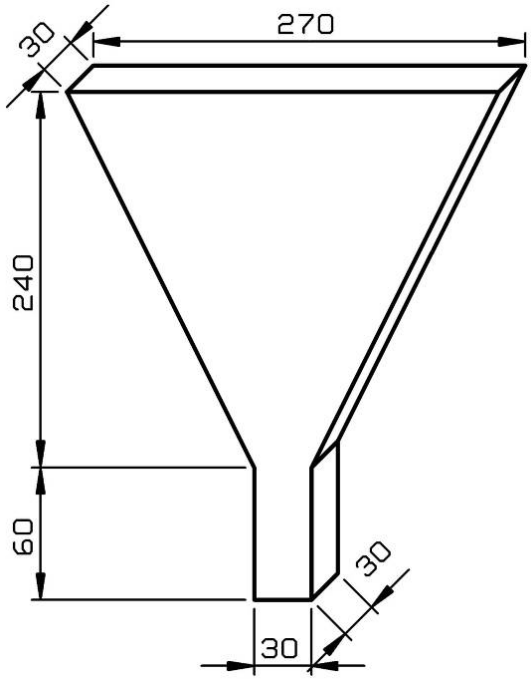


Figure 4.22: The mini V-funnel

4.4 Test method describing the rheology of mortar.

4.4.1 The ViscoCorder

The ViscoCorder is a variable speed viscometer developed for rheology testing in the food industry. The geometry of this viscometer is ideal for the testing of mortar, provided that the maximum particle size is less that one millimetre. For this reason silica sand conforming to the ViscoCorder sand grading was used in this investigation. The material to be tested is placed in a steel cup which is then fixed in position on the viscometer. This cup is then rotated at various speeds, controlled manually with a built-in tachometer. A stationary paddle inside the cup (Figure 4.23) measures the torque created by the rotating sample. The torque is then relayed through a spring to a pen which records the measurements on a chart that moves forward at a constant speed. A specified procedure is used for the

mixing and testing of the mortar sample[33]. The mixing procedure was set out earlier in this chapter.

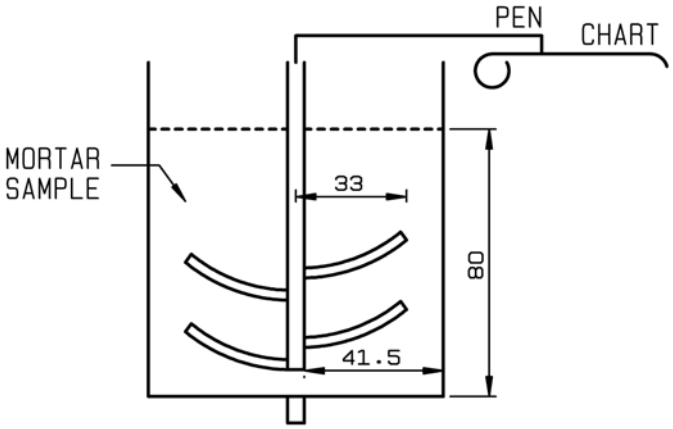


Figure 4.23: Cup and paddle dimensions for the ViscoCorder

Testing procedure:

- Remix the mortar by hand before filling the ViscoCorder cup up to the lower mark and start the ViscoCorder within one minute after completion of mixing.
- Start the testing at a speed of 50 rev/min and keep the speed constant for 10 seconds.
- Manually change the speed in increments of 50 up to a maximum of 250 rev/min and then down to 50 rev/min, keeping the speed constant for 10 seconds at each increment.
- The total test cycle time will be one and a half minutes.
- Torque measurements are then taken from the chart. A full-scale deflection (1000 chart units) is equal to a torque of 100 Nmm.

- A flow curve is then drawn of torque against speed from the values of torque obtained at each speed.
- From this plot the slope will give the *h* value and the intercept will give the *g* value in the Bingham equation ($T = hN + g$).
- The values *h* and *g* are then converted to fundamental units μ (plastic viscosity) and γ (yield stress) using the calibration constants G and K.

Calibration of the ViscoCorder

The calibration of the ViscoCorder is the same as for the Tattersall Two Point Tester, except for the torque calibration which is not required. Silicone di-methyl was used as a Newtonian fluid and the torque was measured at five different speeds (50, 100, 150, 200 and 250 rev/min.) and three different temperatures (30 ^{o}C, 36 ^{o}C and 45 ^{o}C)[33]. Two aqueous solutions of hydroxy ethyl cellulose was used as the power law fluids, both tested in the ViscoCorder at five different speeds (50, 100, 150, 200 and 250 rev/min.) and a temperature of 25 ^{o}C as well as in the MC1 Rheolab rheometer. The results and calculations are given in Appendix A and B.

4.5 Workability retention

The workability retention period for SCC depends on the application[39]. To determine this period the mortar mixtures were used. The mini slump flow test was done one minute after mixing and then repeated every 30 minutes until there

was a difference of 20 mm to the initial slump flow value. This time was recorded to the nearest half-hour.

4.6 Testing the hardened properties of SCC

4.6.1 Compressive strength

To check and compare the compressive strength of SCC mixtures used in this investigation, six cubes were made of each mixture. Standard 100 mm steel cube moulds, conforming to specifications described in SABS 860: 1994 [40], were used to make these cubes. The SCC was placed into the moulds, without any compaction, after all the workability tests were done.

After 24 hours the moulds were stripped and the cubes were put into the curing tank at a temperature of 22 ± 2 ºC[41]. After seven days, three of the cubes were weighed in a saturated, surface-dry condition and then crushed in a compression testing machine[42]. The average of the three results was taken as the seven day strength. The remaining three cubes were crushed at 28 days following the same procedure.

4.7 Materials

4.7.1 Cement

The cement type used for the first mixture design method and the rheology experiments was CEM II 42.5 A-M. This cement type, containing a combination

of extenders, is one of the most commonly used general purpose cements. The chemical analysis of the CEM II 42.5 A-M is given in Table 4.10.

Table 4.10: Chemical analysis of CEM II 42.5 A-M.

SiO_2	Al_2O_3	Fe_2O_3	Mn_2O_3	TiO_2	CaO	MgO	P_2O_5	SO_3	Cr_2O_3	K_2O	V_2O_5	LOI	Total
%	%	%	%	%	%	%	%	%	%	%	%	%	%
23.89	6.34	2.34	0.59	0.35	58.16	3.87	0.08	2.44	0.10	0.54	0.00	1.55	96.17

CEM I 42.5 N, containing no cement extenders, was used in the second mixture design method. This cement type was used because the mixture design method requires specified extender quantities. The chemical analysis of the CEM I 42.5 N is given in Table 4.11.

Table 4.11: Chemical analysis of CEM I 42.5 N.

SiO_2	Al_2O_3	Fe_2O_3	Mn_2O	TiO_2	CaO	MgO	P_2O_5	SO_3	Cl	K_2O	Na_2O	LOI	Total
%	%	%	%	%	%	%	%	%	%	%	%	%	%
20.5	3.6	2.42	0.51	0.24	64.9	2.1	0.02	2.07	0.01	0.33	0.12	2.50	99.4

4.7.2 Fly Ash

In South Africa the ash from the flue gasses of power stations burning pulverized coal is called fly ash. In many European countries it is known as pulverized fly ash. The fly ash is classified to conform to international standards such as BS 3892 part 1[(43)] and SABS 1491 part 2[(44)]. Fly ash is divided into four grades; coarse (reactive fine aggregate), medium (complying with EN 450 and particle size range from 120 micron to sub-micron), fine (mean particle size of 25 micron) and ultra fine (between 3.9 and 5.0 microns). The fine grade of fly ash is used in

the manufacture of concrete products and the ultra fine grade is suitable for SCC. The amounts of material for ultra fine fly ash with particle size greater than 15µm, 10µm and 5µm are usually less than 2%, 15%, and 55%, respectively[45]. Ultra fine fly ash is therefore a good fine filler between fine aggregate.

The inclusion of ultra fine fly ash in a mixture improves the workability and resistance to segregation and bleeding with a reduction in the superplasticizer and viscosity modifier content. The fly ash particles attach to the cement particles giving the cement particles a charge which break down the Van der Waals forces between the cement particles. This deflocculation of cement particles disperses the water through the mixture and improves the workability. Because fly ash is hydrophilic, it gives more free water entrainment which reduces segregation and bleeding. Cohesion is enhanced by the high number of inter particle contact points introduced by the small particle size of the ultra fine fly ash[46].

To manufacture cement requires a high energy input which makes cement expensive. The manufacturing of cement produces about 7 % of the total CO_2 emission[47]. If fly ash is used in the mixture, less cement is used and the CO_2 emission as well as the cost is reduced.

4.7.3 Condensed silica fume

Silica fume, from the production of elemental silicon or ferro-sillicon alloys, is a pozzolan with very small, spherical particles. The fume is condensed and used in concrete to accelerate the hydration process, making the paste denser and increasing the bond between the aggregate and the paste. In comparison with the surface area of a cement particle (300 m^2/kg), the surface area of a silica fume particle is 20 000 m^2/kg. Condensed silica fume can therefore be used in SCC instead of a viscosity modifier to make the mixture more cohesive and less prone to segregation.

Table 4.12: Comparison of typical chemical composition for S.A. materials(%)[46,48]

	CaO	SiO_2	Al_2O_3	Fe_2O_3	MgO
Portland Cement	63-68	19-24	4-7	1-4	0.5-3.5
GGBS	32-37	34-40	11-16	0.5	10-13
Fine Fly ash	4-8	45-50	25-30	3.5	2-4
Ultra fine Fly ash	4.4	53.5	34.3	3.6	1.0
Condensed Silica Fume	0.6	92	1.5	1.2	0.6

4.7.4 Admixtures

Two types of admixtures were used in this investigation. Superplasticisers were used to obtain the best flowability while viscosity modifiers were used to make the mixtures cohesive. Five different new-generation superplasticisers or water reducers, were used which were identified with letters from A to F. A and B were

polycarboxylates polymer (PCP) from the same supplier. Admixture A was a modified PCP high range water reducer with increased workability retention (longer than that of B). Superplasticiser C was a polycarboxylate ether from a different supplier. Admixture D was a synthetic carboxylate polyether, E was a modified synthetic carboxylated polymer and F a Polycarboxylate from another supplier.

4.7.5 Aggregates

The aggregates used in this investigation were from three different quarries. Crusher sand and 13 mm crushed stone from the Jukskei, Olifantsfontein and Eikenhof quarries were used. The sand used for the fine filler is known as Bothma filler sand as it is a naturally weathered material. A maximum stone size of 20 mm is recommended for use in SCC[14]. The 13 mm stone size was used to minimize segregation and blocking between reinforcing steel. This stone size is also more freely available than the 9.5 mm stone. Crusher sand is available and cheaper than natural river sand. Silica sand, specially graded to conform to the ViscoCorder sand requirement, was used in some mixtures to compare the coarse aggregate performance. This sand was used in the mortar mixtures. Gradings and grading curves of all aggregates used are given on the following pages.

Table 4.13: ViscoCorder sand grading

Particle Size (mm)	% Passing
9.5	100
4.75	100
2	100
1.18	100
0.6	64.6
0.3	43.1
0.15	13.8
0.075	1

FM = 1.8

Figure 4.24: ViscoCorder sand grading curve

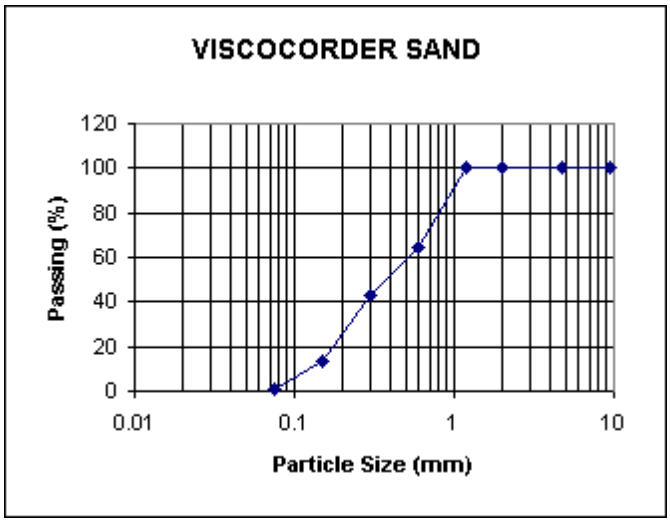


Table 4.14: Bothma filler sand grading

Particle Size (mm)	% Passing
9.5	100
4.75	99.8
2	95.2
1.18	91.8
0.6	86.8
0.425	78.8
0.3	62.3
0.15	16.8
0.075	7.7

FM = 1.7

Figure 4.25: Bothma filler sand grading curve

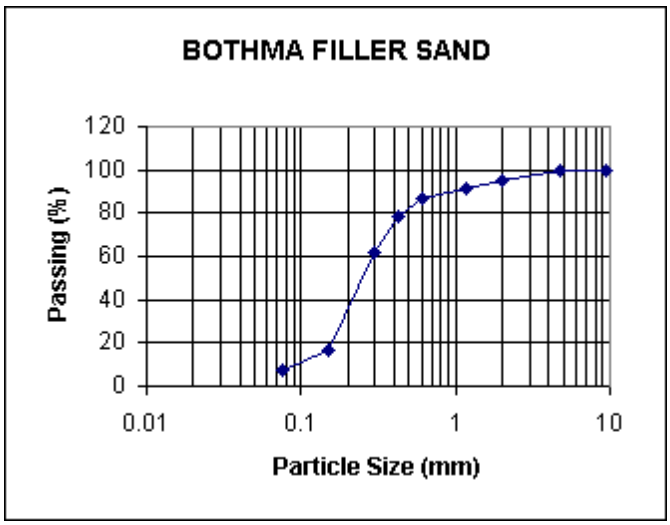


Table 4.15: Andesite crusher sand grading

Particle Size(mm)	% Passing
9.5	100
6.7	99.8
4.75	98.5
2.36	71.5
1.18	47.7
0.6	32.8
0.425	27.4
0.3	22.8
0.15	15.9
0.075	12.6

FM = 3.1

Figure 4.26: Andesite crusher sand grading curve

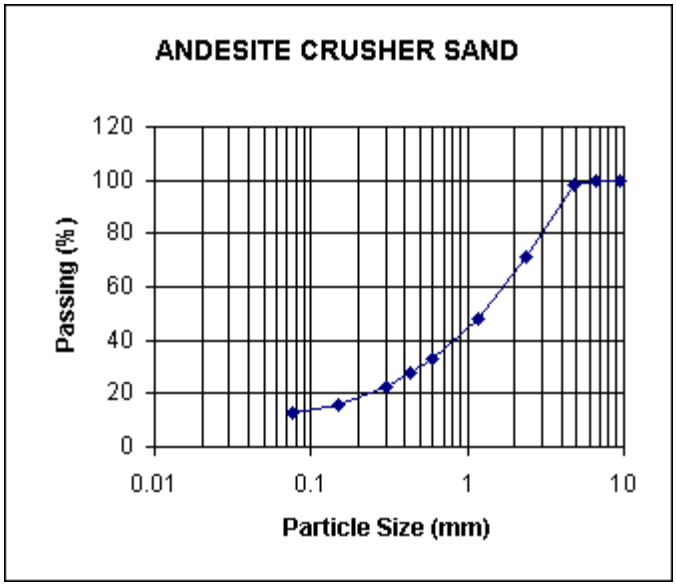


Table 4.16: Granite crusher sand grading

Particle Size (mm)	% Passing
6.7	100
4.75	98.8
2.36	75.7
1.18	54.8
0.6	37.8
0.425	30.7
0.3	24.5
0.15	15.1
0.075	10.6

FM = 2.9

Figure 4.27: Granite crusher sand grading curve

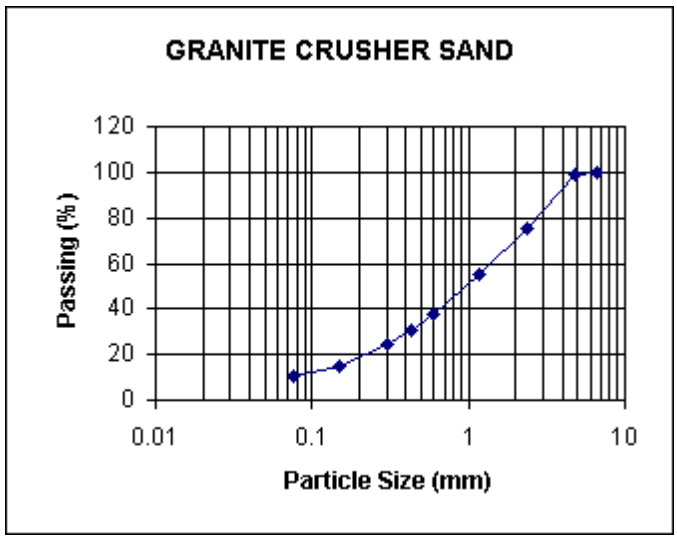
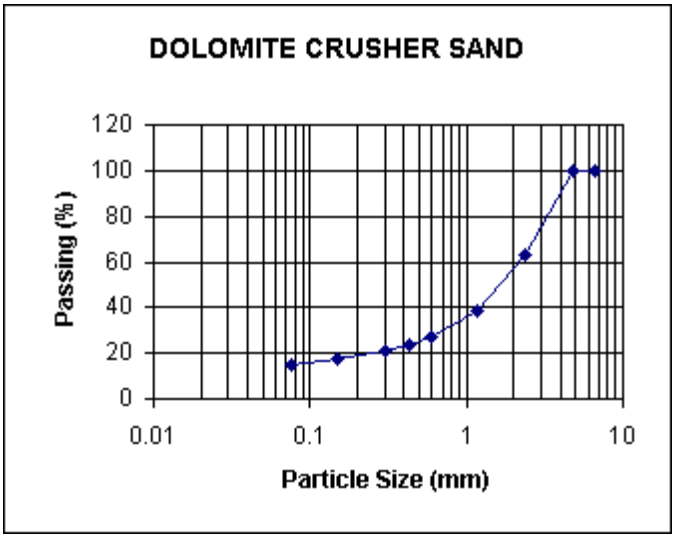


Table 4.17: Dolomite crusher sand grading

Particle Size (mm)	% Passing
6.7	100
4.75	99.7
2.36	62.7
1.18	38.2
0.6	27
0.425	23.6
0.3	20.9
0.15	17.1
0.075	14.9

Figure 4.28: Dolomite crusher sand grading curve



FM = 3.3

Table 4.18: 13 mm Dolomite grading

Particle Size (mm)	% Passing
19	100
13	83.1
9.5	30.2
6.7	3.3
4.75	0.4
3.35	0.3
2.36	0.3

Figure 4.29: 13 mm Dolomite grading curve

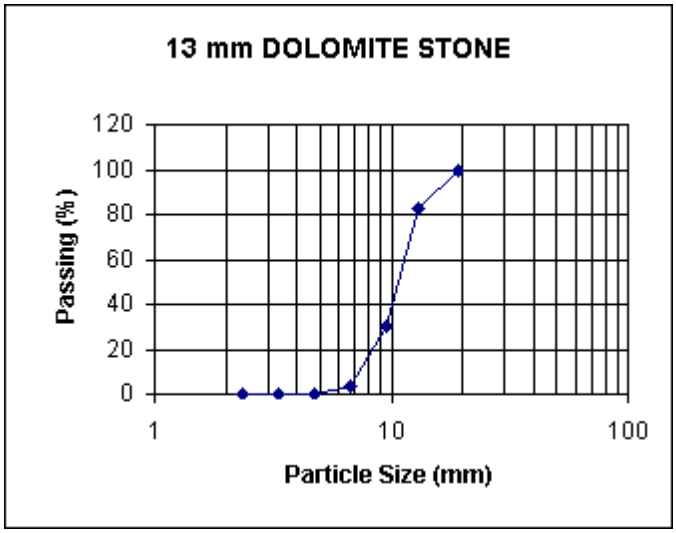


Table 4.19: 13 mm Andesite grading

Particle Size (mm)	% Passing
19	100
13	91.6
9.5	42.6
6.7	12.1
4.75	3.2
3.35	1.6
2.36	1.3

Figure 4.30: 13 mm Andesite grading curve

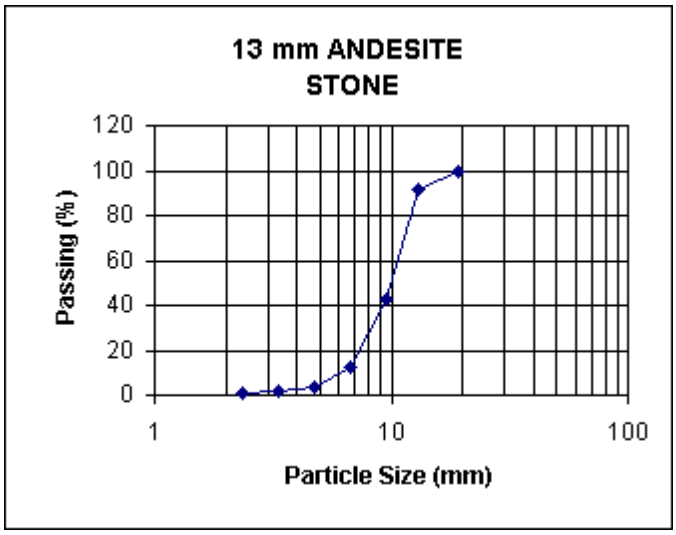
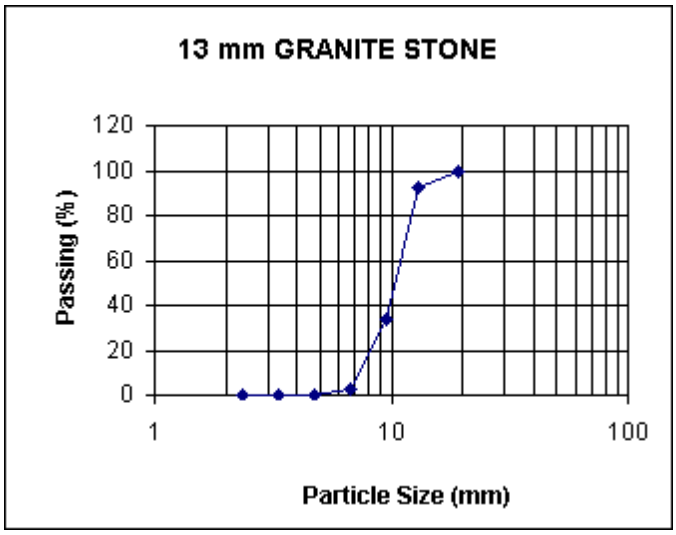


Table 4.20: 13 mm Granite grading

Particle Size (mm)	% Passing
19	100
13	92.6
9.5	34.1
6.7	2.8
4.75	0.4
3.35	0.2
2.36	0.2

Figure 4.31: 13 mm Granite grading curve



4.8 Conclusion

Various testing methods were developed to describe the workability and rheology of SCC. Most of these methods are laborious and need more than one operator. Except for the rheometer tests, all these tests assess only one or two of the three key properties (filling ability, passing ability and resistance to segregation) of SCC[28].

The following chapters describe different mixture design methods. The first of these chapters investigates the relation between concrete, mortar and paste rheology to assess whether mortar and paste rheology can be used to predict concrete rheology.

CHAPTER 5

COMPARISON BETWEEN CONCRETE, MORTAR AND PASTE RHEOLOGY

5.1 Introduction

The objective of the work reported in this chapter was to determine the relation between concrete, mortar and paste rheology. Since the properties of mortar and paste are dominant in SCC and the tests are much more convenient, it could be a convenient way to predict and quantify the properties of concrete. Testing mortar and paste requires smaller equipment, less space and less material. These tests do not require fully equipped concrete laboratories, especially when tests are done on site.

5.2 Paste rheology measurements

Three paste mixtures with different cement and extender contents and a water:cement ratio of 0,5 were tested. These three mixtures were also tested using a water:cement ratio of 0,65. All these mixtures were tested with and without superplasticizer A, giving a total of twelve mixtures. Initially a superplasticizer dosage of 0.85 % of the total cementitious content was used, but because of severe segregation the dosage was changed to 0.43 %. The mixture proportions for the paste mixtures are given in Table 5.1. For an adequate amount of paste to be tested, the cementitious content was taken as 450 kg/m^3 and the water content determined using the water: cement ratio.

Table 5.1: Paste mixture proportions

MIX RN1P		**MIX RN2P**	
Material	**kg/m³**	**Material**	**kg/m³**
Cem II AM 42.5	450	Cem II AM 42.5	450
Water	225	Water	225
Super plasticizer A	0	Super plasticizer A	2.322
W:C	0.5	W:C	0.5
MIX RN3P		**MIX RN4P**	
Material	**kg/m³**	**Material**	**kg/m³**
Cem II AM 42.5	450	Cem II AM 42.5	450
Water	293	Water	293
Super plasticizer A	0	Super plasticizer A	2.32
W:C	0.65	W:C	0.65
MIX RN5P		**MIX RN6P**	
Material	**kg/m³**	**Material**	**kg/m³**
Cem II AM 42.5	315	Cem II AM 42.5	315
Fly ash	135	Fly ash	135
Water	225	Water	225
Super plasticizer A	0	Super plasticizer A	2.322
W:C	0.5	W:C	0.5
MIX RN7P		**MIX RN8P**	
Material	**kg/m³**	**Material**	**kg/m³**
Cem II AM 42.5	315	Cem II AM 42.5	315
Fly ash	135	Fly ash	135
Water	293	Water	293
Super plasticizer A	0	Super plasticizer A	2.322
W:C	0.65	W:C	0.65
MIX RN9P		**MIX RN10P**	
Material	**kg/m³**	**Material**	**kg/m³**
Cem II AM 42.5	315	Cem II AM 42.5	315
Fly ash (Ultra Fine)	135	Fly ash (Ultra Fine)	135
Water	225	Water	225
Super plasticizer A	0	Super plasticizer A	2.322
W:C	0.5	W:C	0.5
MIX RN11P		**MIX RN12P**	
Material	**kg/m³**	**Material**	**kg/m³**
Cem II AM 42.5	315	Cem II AM 42.5	315
Fly ash (Ultra Fine)	135	Fly ash (Ultra Fine)	135
Water	293	Water	293
Super plasticizer A	0	Super plasticizer A	2.322
W:C	0.65	W:C	0.65

Results for the paste rheology, measured using the MC1 Rheolab rheometer, are summarised in Table 5.2.

Table 5.2: Summary of paste rheology results.

Mixture Number	τ_o (Pa)	μ (Pas)	
RN1P	3.23	0.01	
RN2P	4.30	0.03	
RN3P	7.42	0.01	
RN4P	19.47	0.05	
RN5P	47.81	0.09	
RN6P	7.22	0.01	
RN7P	-	-	Anomalous
RN8P	17.33	0.09	
RN9P	3.01	0.03	
RN10P	5.83	0.02	
RN11P	1.88	0.12	
RN12P	-	-	No results

Flow curves describing the rheology of each paste are shown in Figure 5.1 to Figure 5.11.

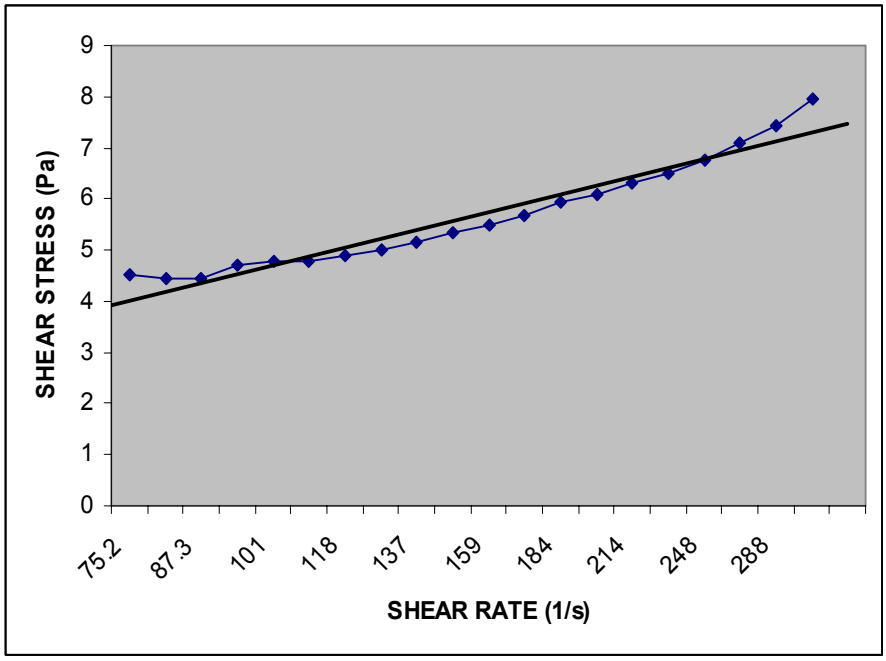


Figure 5.1: Flow curve for paste mixture RN1P

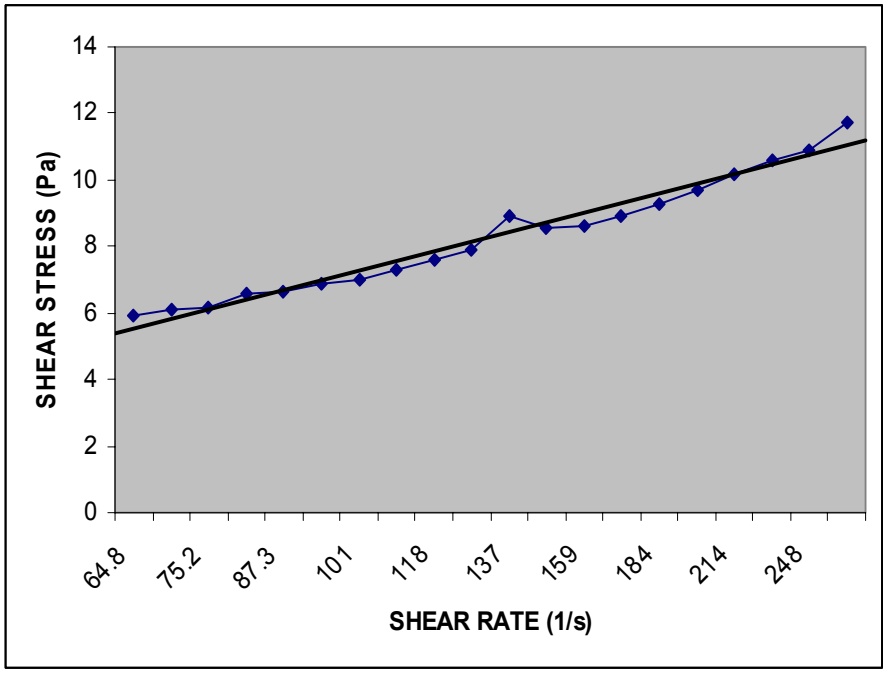


Figure 5.2: Flow curve for paste mixture RN2P

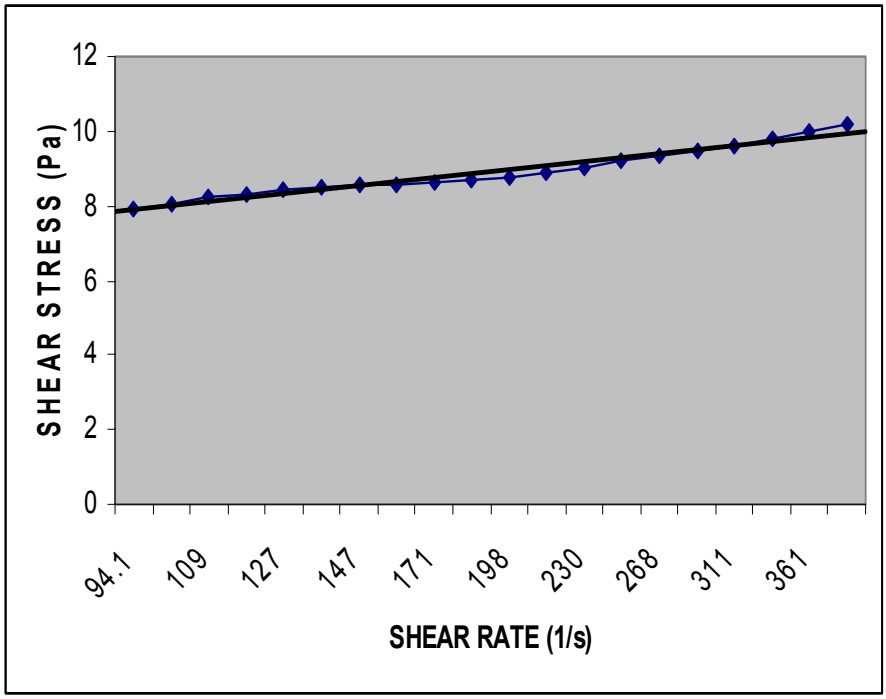


Figure 5.3: Flow curve for paste mixture RN3P

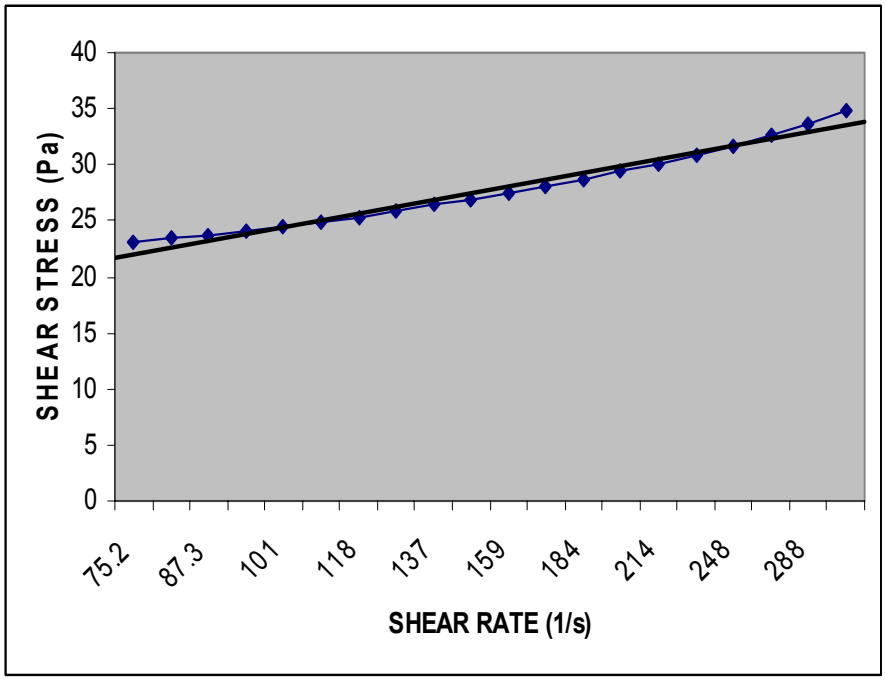


Figure 5.4: Flow curve for paste mixture RN4P

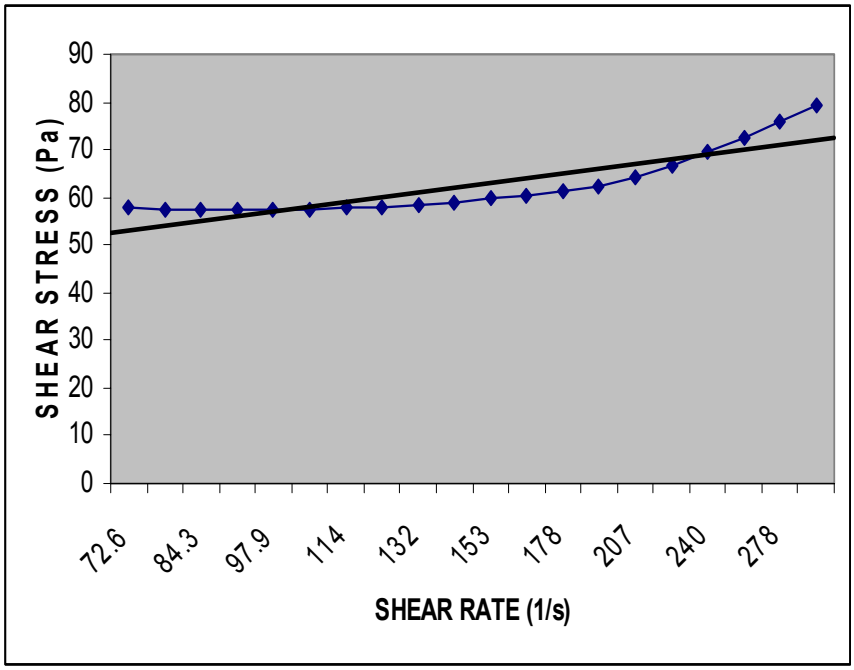


Figure 5.5: Flow curve for paste mixture RN5P

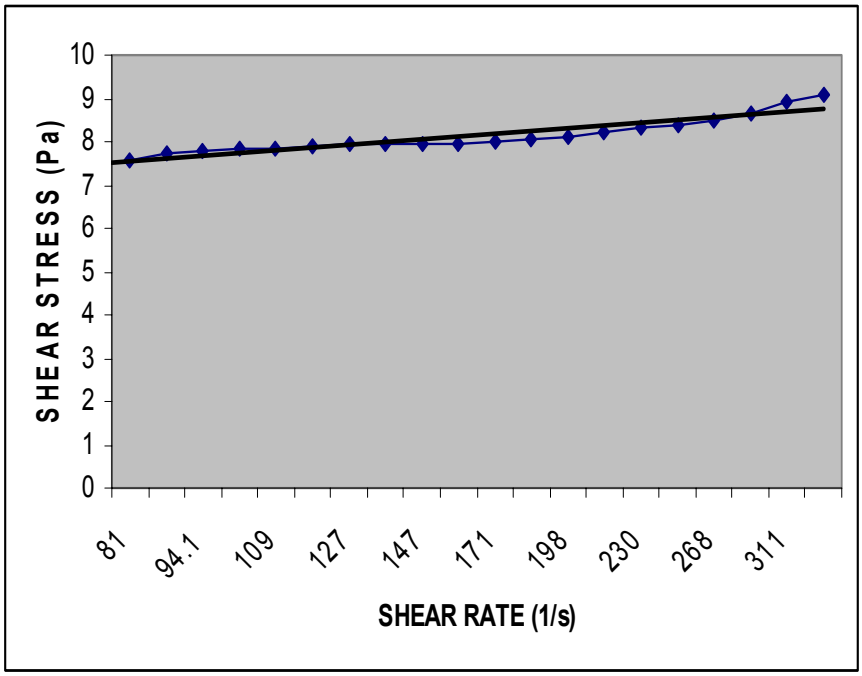


Figure 5.6: Flow curve for paste mixture RN6P

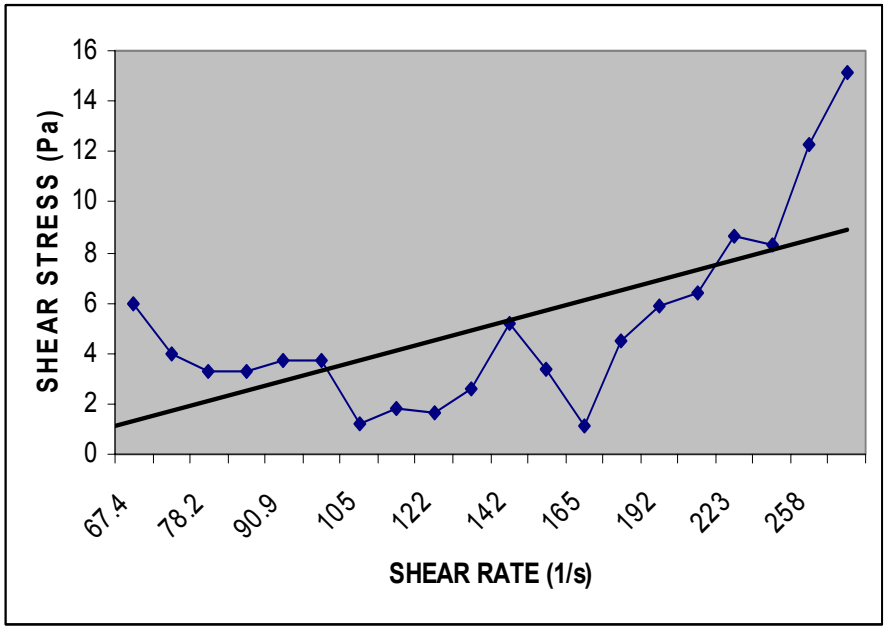


Figure 5.7: Flow curve for paste mixture RN7P

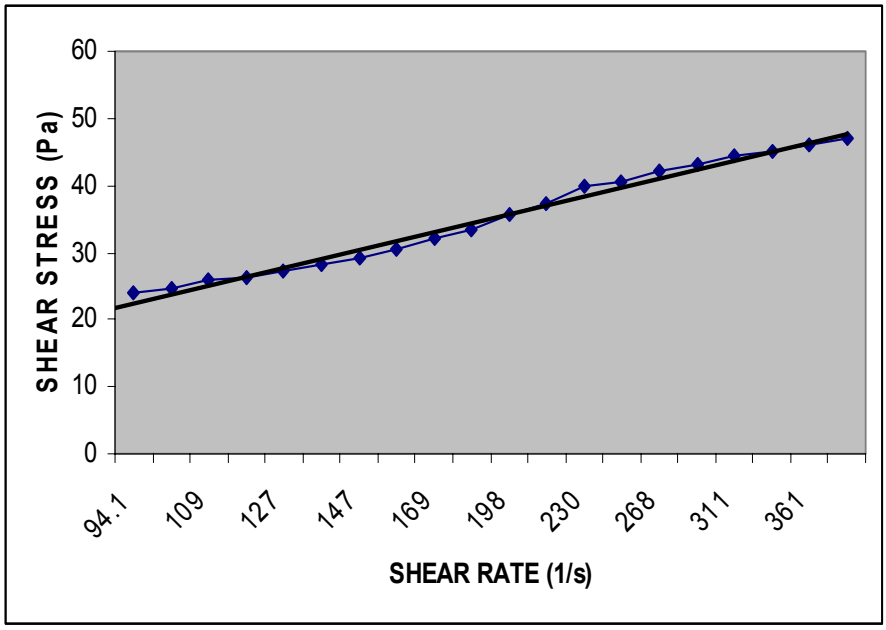


Figure 5.8: Flow curve for paste mixture RN8P

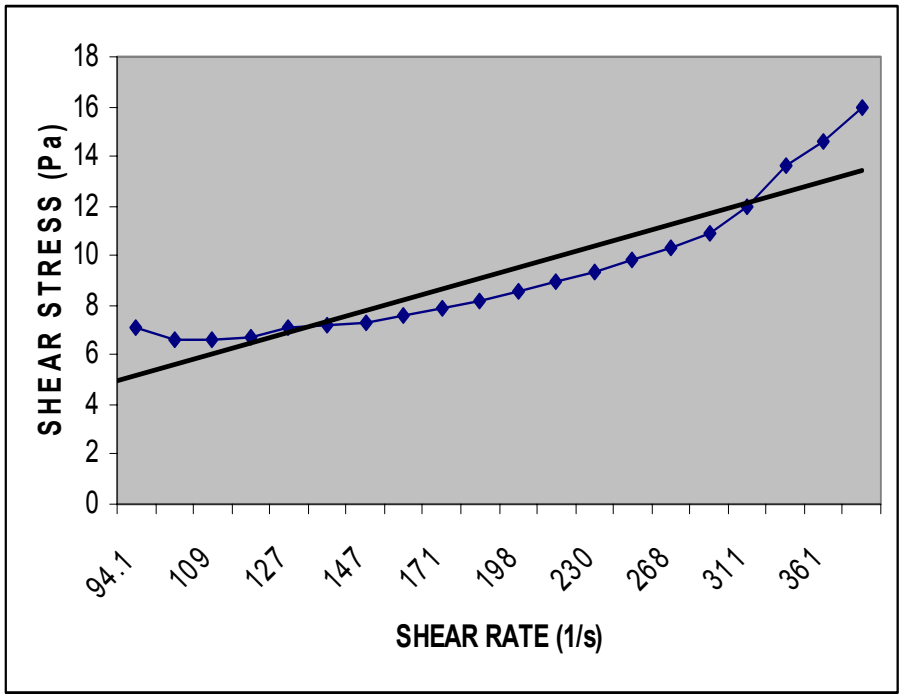


Figure 5.9: Flow curve for paste mixture RN9P

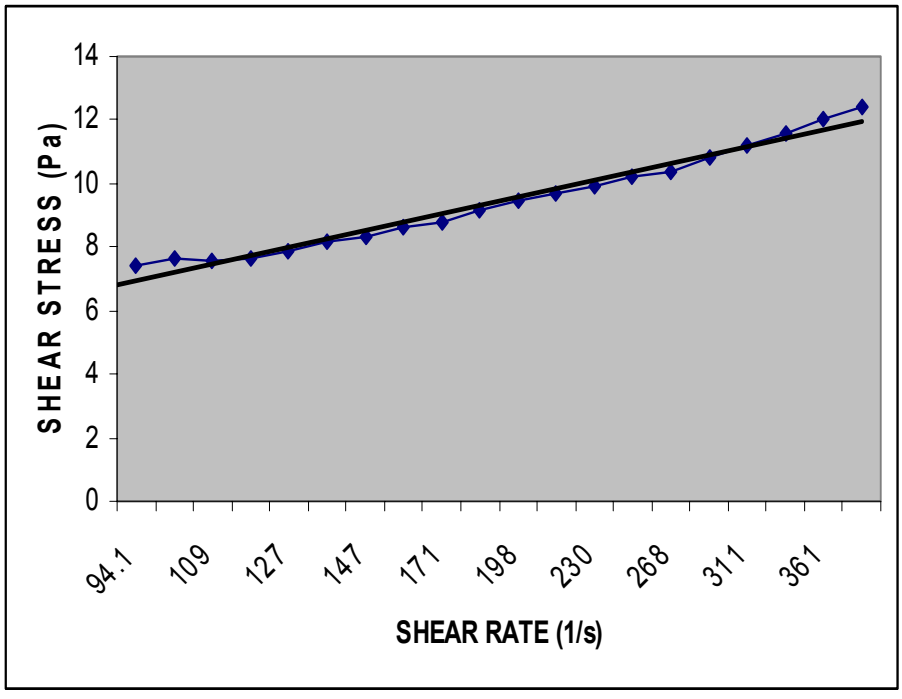


Figure 5.10: Flow curve for paste mixture RN10P

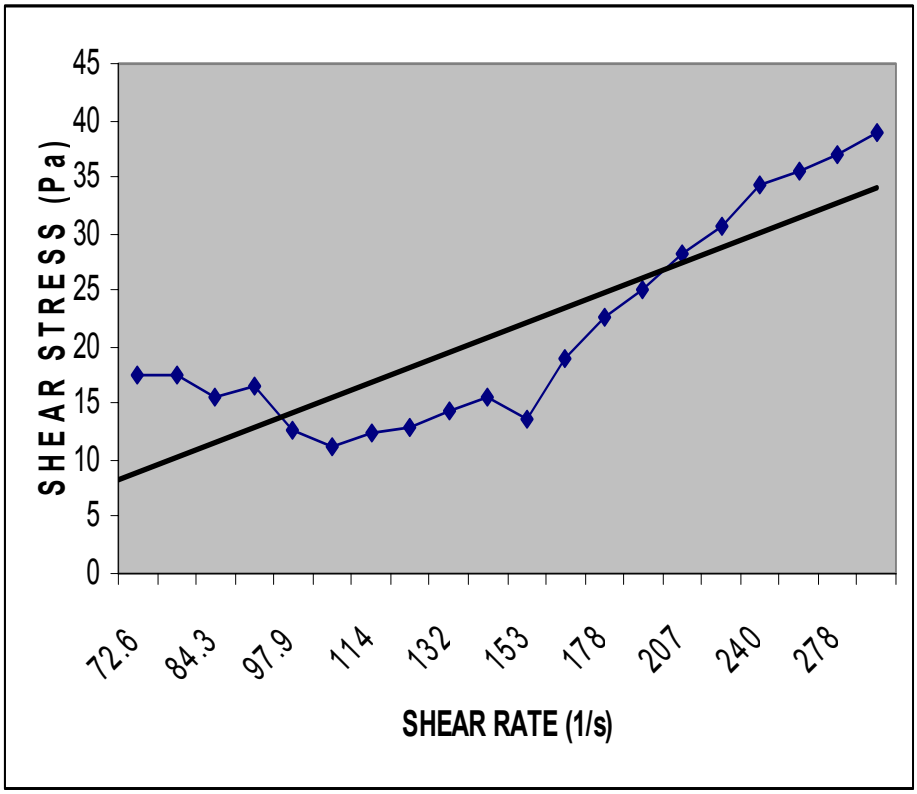


Figure 5.11: Flow curve for paste mixture RN11P

5.3 Mortar rheology measurements

The next phase was the design and measurement of the mortar rheology. Silica sand, specially graded to conform to the ViscoCorder specifications, was used in the mortar mixtures. Different ratios of sand:cement were tested and it was found that a ratio of 2:1 was best suited for most of the mixtures. This ratio of sand:cement was added to all the paste mixtures and tested to determine the mortar rheology. All the mixtures were tested in the ViscoCorder, some also in the Tattersall two point tester and some in the Rheolab MC1, using the six blade vane. The mixture proportions for the mortar mixtures are given in Table 5.3.

Table 5.3: Mortar mixture proportions for the mortar rheology measurements.

MIX RN1M		**MIX RN2M**	
Material	**kg/m³**	**Material**	**kg/m³**
Cem II AM 42.5	450	Cem II AM 42.5	450
Fly ash	0	Fly ash	0
Total Cement	450	Total Cement	450
ViscoCorder Sand	900	ViscoCorder Sand	900
Water	225	Water	225
Super plasticizer A	0	Super plasticizer A	2.322
W:C	0.5	W:C	0.5
MIX RN3M		**MIX RN4M**	
Material	**kg/m³**	**Material**	**kg/m³**
Cem II AM 42.5	450	Cem II AM 42.5	450
Fly ash	0	Fly ash	0
Total Cement	450	Total Cement	450
ViscoCorder Sand	900	ViscoCorder Sand	900
Water	293	Water	293
Super plasticizer A	0	Super plasticizer A	2.32
W:C	0.65	W:C	0.65
MIX RN5M		**MIX RN6M**	
Material	**kg/m³**	**Material**	**kg/m³**
Cem II AM 42.5	315	Cem II AM 42.5	315
Fly ash	135	Fly ash	135
Total Cement	450	Total Cement	450
ViscoCorder Sand	900	ViscoCorder Sand	900
Water	225	Water	225
Super plasticizer A	0	Super plasticizer A	2.322
W:C	0.5	W:C	0.5

Table 5.3: Mortar mixture proportions for the mortar rheology measurements. (Continued)

MIX RN7M		**MIX RN8M**	
Material	**kg/m³**	**Material**	**kg/m³**
Cem II AM 42.5	315	Cem II AM 42.5	315
Fly ash	135	Fly ash	135
Total Cement	450	Total Cement	450
ViscoCorder Sand	900	ViscoCorder Sand	900
Water	293	Water	293
Super plasticizer A	0	Super plasticizer A	2.322
W:C	0.65	W:C	0.65
MIX RN9M		**MIX RN10M**	
Material	**kg/m³**	**Material**	**kg/m³**
Cem II AM 42.5	315	Cem II AM 42.5	315
Fly ash (Ultra Fine)	135	Fly ash (Ultra Fine)	135
Total Cement	450	Total Cement	450
ViscoCorder Sand	900	ViscoCorder Sand	900
Water	225	Water	225
Super plasticizer A	0	Super plasticizer A	2.322
W:C	0.5	W:C	0.5
MIX RN11M		**MIX RN12M**	
Material	**kg/m³**	**Material**	**kg/m³**
Cem II AM 42.5	315	Cem II AM 42.5	315
Fly ash (Ultra Fine)	135	Fly ash (Ultra Fine)	135
Total Cement	450	Total Cement	450
ViscoCorder Sand	900	ViscoCorder Sand	900
Water	293	Water	293
Super plasticizer A	0	Super plasticizer A	2.322
W:C	0.65	W:C	0.65

Results for the mortar rheology, measured using the ViscoCorder, are given in Figure 5.12 and summarised in Table 5.4.

Table 5.4: ViscoCorder results for mortar mixtures.

Mixture Number	h (Nms)	g (Nm)	τ_o (Pa)	μ (Pas)
RN1M	-	-	-	-
RN2M	0.006	0.0135	72.59	7.048
RN3M	0.003	0.0112	60.21	3.299
RN4M	0.002	0.0027	14.52	2.849
RN5M	-	-	-	-
RN6M	0.006	0.0019	10.23	7.349
RN7M	0.003	0.0058	30.92	3.974
RN8M	0.002	0.0004	2.158	2.999
RN9M	0.008	0.0286	153.8	10.5
RN10M	0.004	0.0011	5.928	5.549
RN11M	0.003	0.0076	40.86	3.299
RN12M	0.002	0.0011	5.919	2.25

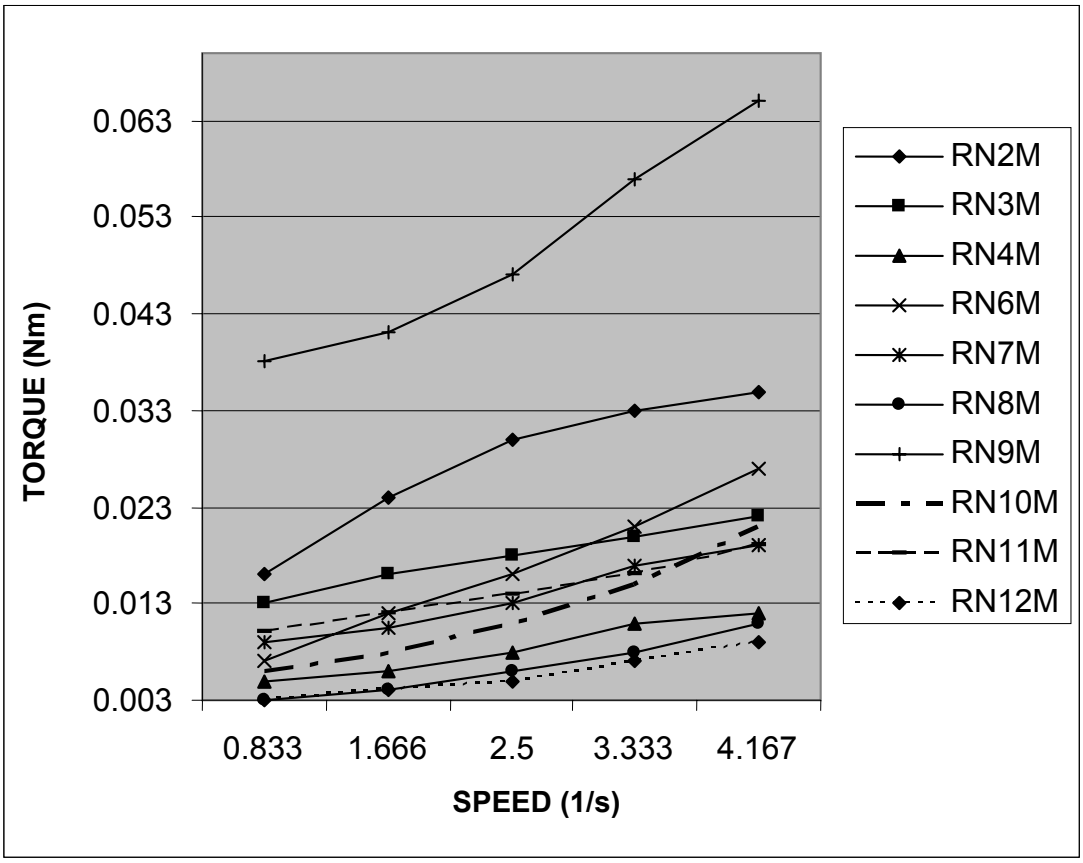


Figure 5.12: Flow curves for mortar mixtures tested in the ViscoCorder.

5.4 Concrete rheology measurements

The last phase in this comparison was the design and measurement of the concrete rheology. To ensure a reliable basis for comparison, the concrete mixtures contained the same ratios of sand:cement and water:cement as the mortar mixtures, as well as the same sand, graded according to the ViscoCorder specifications. The same coarse aggregate, 13 mm granite from the Jukskei quarry, was used in all the concrete mixtures. In the design of all the concrete mixtures, the coarse aggregate was added to the mortar mixture design until a calculated yield of 1000 litres was reached. This yield included 1 % air. Table 5.5 contains the material proportions for the concrete mixtures tested.

Table 5.5: Concrete mixture proportions for the concrete rheology measurements.

MIX 1RN		**MIX 2RN**	
Material	**kg/m³**	**Material**	**kg/m³**
Cem II AM 42.5	450	Cem II AM 42.5	450
Fly ash	0	Fly ash	0
Total Cement	450	Total Cement	450
ViscoCorder Sand	900	ViscoCorder Sand	900
13 mm Granite	758	13 mm Granite	758
Water	225	Water	225
Super plasticizer A	0	Super plasticizer A	2.322
W:C	0.5	W:C	0.5
MIX 3RN		**MIX 4RN**	
Material	**kg/m³**	**Material**	**kg/m³**
Cem II AM 42.5	450	Cem II AM 42.5	450
Fly ash	0	Fly ash	0
Total Cement	450	Total Cement	450
ViscoCorder Sand	900	ViscoCorder Sand	900
13 mm Granite	580	13 mm Granite	580
Water	293	Water	293
Super plasticizer A	0	Super plasticizer A	2.32
W:C	0.65	W:C	0.65
MIX 5RN		**MIX 6RN**	
Material	**kg/m³**	**Material**	**kg/m³**
Cem II AM 42.5	315	Cem II AM 42.5	315
Fly ash	135	Fly ash	135
Total Cement	450	Total Cement	450
ViscoCorder Sand	900	ViscoCorder Sand	900
13 mm Granite	730	13 mm Granite	725
Water	225	Water	225
Super plasticizer A	0	Super plasticizer A	2.322
W:C	0.5	W:C	0.5

Table 5.5: Concrete mixture proportions for the concrete rheology measurements. (Continued)

MIX 7RN		**MIX 8RN**	
Material	**kg/m³**	**Material**	**kg/m³**
Cem II AM 42.5	315	Cem II AM 42.5	315
Fly ash	135	Fly ash	135
Total Cement	450	Total Cement	450
ViscoCorder Sand	900	ViscoCorder Sand	900
13 mm Granite	550	13 mm Granite	550
Water	293	Water	293
Super plasticizer A	0	Super plasticizer A	2.322
W:C	0.65	W:C	0.65
MIX 9RN		**MIX 10RN**	
Material	**kg/m³**	**Material**	**kg/m³**
Cem II AM 42.5	315	Cem II AM 42.5	315
Fly ash (Ultra Fine)	135	Fly ash (Ultra Fine)	135
Total Cement	450	Total Cement	450
ViscoCorder Sand	900	ViscoCorder Sand	900
13 mm Granite	715	13 mm Granite	715
Water	225	Water	225
Super plasticizer A	0	Super plasticizer A	2.32
W:C	0.5	W:C	0.5
MIX 11RN		**MIX 12RN**	
Material	**kg/m³**	**Material**	**kg/m³**
Cem II AM 42.5	315	Cem II AM 42.5	315
Fly ash (Ultra Fine)	135	Fly ash (Ultra Fine)	135
Total Cement	450	Total Cement	450
ViscoCorder Sand	900	ViscoCorder Sand	900
13 mm Granite	533	13 mm Granite	533
Water	293	Water	293
Super plasticizer A	0	Super plasticizer A	2.322
W:C	0.65	W:C	0.65

The first mixture was too stiff to be tested and no results were obtained. Some of the mixtures were too fluid or segregated to the extent that rheology measurements were not possible. Results for the mixtures that could be tested are given in Table 5.6.

Table 5.6: Summary of Concrete rheology results.

Mixture Number	Tattersall Results				Slump flow	
	h (Nms)	g (Nm)	τ_o (Pa)	μ (Pas)	T50 (sec)	Final (mm)
MIX 2RN	0.10	0.25	17.92	12.74	4	200
MIX 3RN	0.03	0.06	4.72	3.25	4	530
MIX 5RN	0.08	0.56	40.84	9.46	4	85
MIX 6RN	0.07	0.04	2.82	8.46		635
MIX 7RN	0.12	0.11	7.72	14.75	4	630

5.5 Results of the paste, mortar and concrete rheology comparison

The first mixture tested was too dry and neither the mortar nor the concrete phases gave results. Mixture number two was tested in the MC1 Rheolab viscometer using the bob as well as the vane. The results obtained using the bob were more reliable than those obtained when using the vane. The mortar was also tested, but as with the paste, bleeding occurred. The concrete was tested successfully and a collapse slump of 200mm was measured.

With mixture number three the water:cement ratio was taken as 0.65. This caused segregation in all three phases, but tests were done and results obtained. The results obtained from the bob gave more reliable results than the vane when the paste was tested.

The concrete phase of mixture four segregated and bled too much to be tested. When the bob was used to test the paste, no results were obtained and the results from the vane test were used. Mortar results also indicated high fluidity caused by the segregation and bleeding.

Mixture 5 was very cohesive as indicated by the high yield stress values of both the paste and the concrete. The mortar mixture was too stiff to be tested in the ViscoCorder and no results were obtained. The better paste results were obtained using the bob. This mortar mixture was also tested in the Tattersall Two Point Tester, but no sensible results could be obtained.

The results from mixture six were the most acceptable. Mixture six was the only mortar mixture tested in the ViscoCorder, Tattersall Two Point Tester and MC1 Rheolab. The results are given in Table 5.7.

Table 5.7: Comparison between mortar rheology results for different test instruments.

Mixture Number	MC1 RHEOLAB		VISCOCORDER		TATTERSALL	
	τ_o (Pa)	μ (Pas)	τ_o (Pa)	μ (Pas)	τ_o (Pa)	μ (Pas)
RN6	178.84	1.55	10.23	7.35	2.82	8.46

From the results summarised in Table 5.7, it is obvious that the measurements between the different apparatus did not compare well. The Rheolab and the Tattersall rheometers, are not suited for testing mortar rheology. According to Banfill[49], the Tattersall Two Point Tester is not sensitive enough to measure very fluid materials. The Rheolab rheometer on the other hand cannot test suspensions containing particles larger than a tenth of the gap between the cup and the bob. When testing the mortar using the Rheolab rheometer, the flow curves obtained using the vane did not give a Bingham relationship which indicates that the vane is also not reliable.

Mixture seven was the last mixture that could be tested giving results, in all three phases. There were, however, big discrepancies between the results of the three different phases. The reason for this could be the segregation and bleeding that occurred in the mixture.

Mixtures eight to twelve were very fluid showing signs of severe segregation. Because of their high fluidity the concrete mixtures gave no significant results when tested in the Tattersall Two Point Tester.

The results of the comparison between the paste, mortar and concrete rheologies are summarized in Table 5.8.

Table 5.8: Paste, mortar and concrete rheology results

Mixture Number	Paste		Mortar		Concrete	
	τ_o (Pa)	μ (Pas)	τ_o (Pa)	μ (Pas)	τ_o (Pa)	μ (Pas)
RN1	3.23	0.01	-	-	-	-
RN2	4.30	0.03	72.59	7.05	17.92	12.74
RN3	7.42	0.01	60.21	3.30	4.72	3.25
RN4	19.47	0.05	14.52	2.85	-	-
RN5	47.81	0.09	-	-	40.84	9.46
RN6	7.22	0.01	10.23	7.35	2.82	8.46
RN7	-1.37	0.04	30.92	3.97	7.72	14.75
RN8	17.33	0.09	2.16	3.00	-	-
RN9	3.01	0.03	153.76	10.50	-	-
RN10	5.83	0.02	5.93	5.55	-	-
RN11	1.88	0.12	40.86	3.30	-	-
RN12	-	-	5.92	2.25	-	-

From these results no reliable comparison could be drawn.

To quantify the comparisons, graphs were used to determine if a relation exists between the three different phases. A comparison was made between the plastic viscosities of the paste and the mortar, Figure 5.13, the mortar and the concrete, Figure 5.15, and the concrete and paste, Figure 5.17. A comparison between the yield stresses of the paste and mortar, Figure 5.14, the mortar and the concrete, Figure 5.16, and the paste and the concrete, Figure 5.18, was also done.

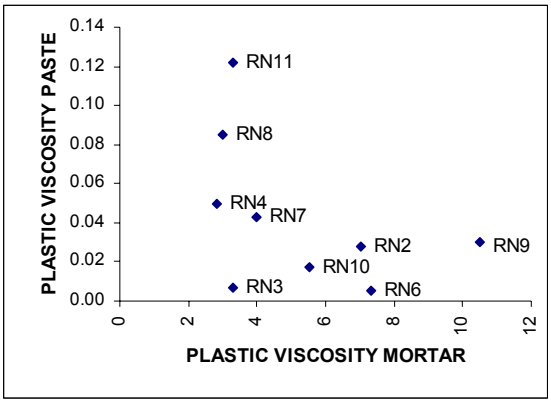


Figure 5.13: Plastic viscosity paste vs. plastic viscosity mortar

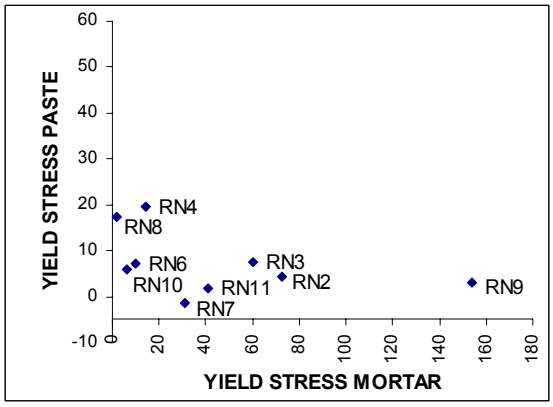


Figure 5.14: Yield stress paste vs. yield stress mortar

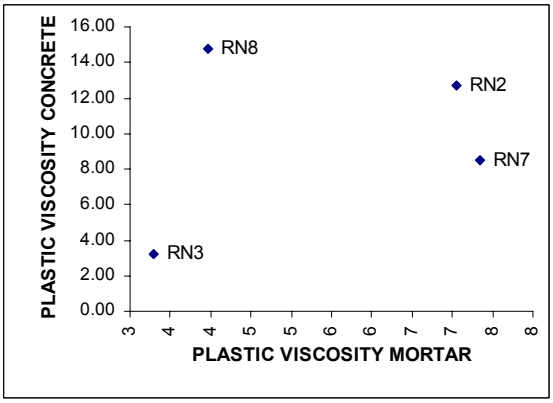


Figure 5.15: Plastic viscosity concrete vs. plastic viscosity mortar

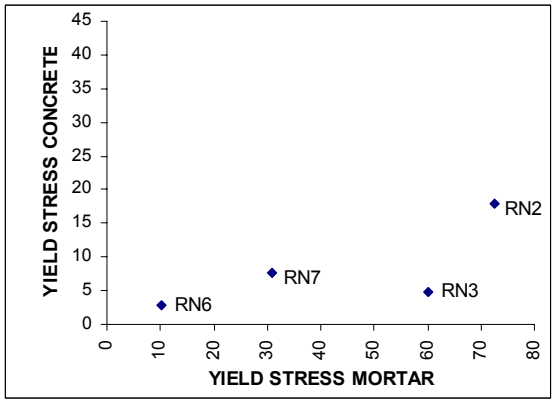


Figure 5.16: Yield stress concrete vs. yield stress mortar

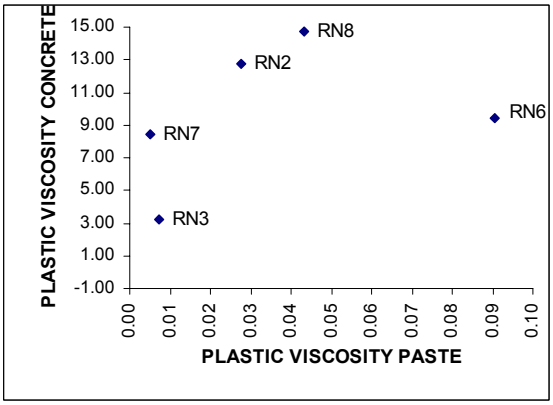


Figure 5.17: Plastic viscosity paste vs. plastic viscosity concrete

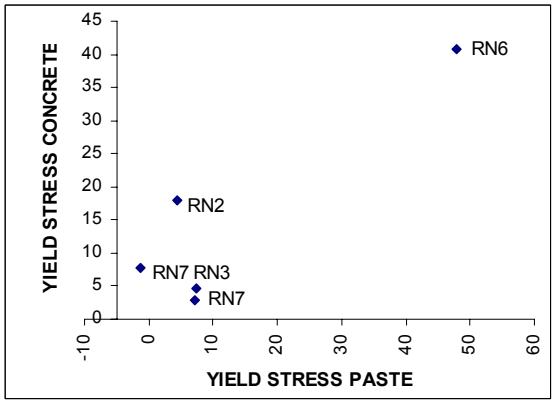


Figure 5.18: Yield stress paste vs. yield stress concrete

In none of these is a clear relationship evident, indicating that there is no noticeable relationship between any of the three phases. This could either mean that the influencing factors are not correctly accounted for in the rheology tests, or that the results are not reliable. It could also mean that the results from the three different apparatus are not comparable, as shown in Table 5.7. Ideally all three phases should be tested in the same apparatus, if such equipment is available.

5.6 Conclusion

All these results indicate that mortar and paste rheology, on their own, cannot be used to predict the rheology of a concrete mixture. A different approach to mixture design is clearly required. In the next chapter a review is given of different mixture designs used across the world. A mixture design method used in South Africa is included in this chapter. The results from mixtures done using this method are also included.

CHAPTER 6

MIXTURE DESIGN AND TEST RESULTS

6.1 Introduction

Mixture design is a very important part of SCC. In this chapter an overview is given of better known mixture design approaches used internationally. A proposed mixture design model is then discussed to establish a method for the design of SCC made from South African materials. The results of the workability and rheometry measurements are also included.

6.2 Literature review

Various mixture design methods have been developed throughout the world to design SCC mixtures. Unfortunately no universal SCC mixture design method can be produced, because of regional variability and availability of concrete materials. The main criterion for a SCC mixture is the self-compactability, i.e. good filling ability and passing ability without segregation or bleeding. SCC has to be well compacted and dense, without the need for external vibration.

The initial mixture design method used, when SCC was first developed, is known as the General Method. Okamura[4] suggested that the coarse aggregate content should be fixed at 50 % of the dry rodded weight of the mixture and the fine

aggregate content to be fixed at 50 % of the mortar volume. Mortar tests were used to determine the water:powder ratio (powder includes all particles in the concrete mixture less than 0.09 mm[38]) and the amount of superplasticizer. The General Method is a simple step by step method designed for Japanese materials. This method was developed at the University of Tokyo and gave good results for a general SCC mixture, but this mixture may not contain enough paste for adequate flowability when used with aggregate other than Japanese. Because this method is designed for Japanese materials the guideline given is a starting point and needs to be refined[38].

Many design methods have been derived from the General Method to make it adaptable to individual requirements and produce more efficient mixtures. These methods include those from Kochi University of Technology, University of Tokyo, Delft University and University College London[3].

The CBI method was developed in Sweden and consists of three stages. In the first stage the minimum paste volume is calculated according to the aggregate properties and water:cement ratio. The blocking criterion considers the minimum paste required to avoid coarse aggregate blocking between reinforcing steel. The second stage involves rheological measurements of the mortar part of the concrete and, in the final stage, the fresh and hardened properties of the concrete is verified. In Sweden the design for a SCC mixture starts with the structural

requirements for each project (strength and the environment) and then special consideration is given to the aggregate used in the mixture. Empirical formulae are used to determine if blocking will occur with the aggregate to be used. This approach takes into consideration the specific aggregate type to be used and the minimum paste required to cover this aggregate ensuring an adequate inter-particle distance to prevent blocking[1].

Domone[3] undertook a study on all these methods and concluded that there is a wide range of mixture proportions that can be used to produce SCC. The key factors, expressed in volumetric terms are as follows:

- 30-34 % of the concrete volume to be coarse aggregate.
- 0.25-0.5 as the water to powder ratio and mixtures with values at the upper end of this range require a viscosity modifier to enhance the viscosity.
- 155-175 ℓ/m^3 water if no viscosity modifier is used and up to 200 ℓ/m^3 with a viscosity modifier.
- 34-40 % of the concrete volume to be paste.
- 40-50 % of the mortar volume to be fine aggregate.

These volumes can be expressed as approximate proportions by weight as follows:

coarse aggregate	750 - 920 kg/m^3
fine aggregate	710 - 900 kg/m^3
powder	450 - 600 kg/m^3
water	150 - 200 kg/m^3

6.3 Proposed mixture design model

The mixture design method used for this investigation was adapted from a mixture design used for conventional concrete. The aim was to design an adaptable mixture with a specific water to binder ratio and target strength. In the development of these mixtures, three different aggregate types from the Gauteng area were used to determine the most suitable type as well as the best blend of these aggregates. To achieve the required flowability with no segregation, superplasticizers and high-range water-reducing admixtures were used at an appropriate dosage in relation to the mixture design. The dosage was determined using the manufacturers guidelines as a starting point and the by assessing the mixture visually. After mixing was stopped, the flowability and resistance to segregation was assessed using a steel float. This mixture design method is largely based on experience and difficult to quantify. A mixture was put together, mixed and tested using the slump flow test. The slump flow result and behaviour of the mixture was then assessed visually to determine if more or less admixture was required.

To determine the flowability and filling ability of the mixtures, the slump flow, L-box and V-funnel tests were used. The passing ability and segregation resistance were assessed with the L-box and V-funnel tests. Each mixture was tested in the Tattersall Two Point Tester to determine the rheological properties. The same mixtures were used for the workability tests and the results were compared with

the rheology test results. To evaluate the compressive strength of the different mixtures, cubes were made, cured and crushed.

6.4 Laboratory Procedures

6.4.1 Mixture proportions

As stated earlier, this mixture design method was adapted from a mixture design used for conventional concrete. The proportions of aggregates used were from experience and trial mixtures. Many trial mixtures were tested and the final mixture proportions used in this part of the investigation are given in Table 6.1. These mixtures were used to compare the use of the three different aggregate types, Granite, Andesite and Dolomite, as well as the influence of admixtures and extenders. The mixtures are identified as follows, the first letter indicates the aggregate type (Andesite (A), Granite (G) and Dolomite (D)), and the number indicates the mixture series. The last letter indicates the superplasticizer type.

Table 6.1: Concrete mixture proportions

MIXTURE A1A		**MIXTURE G1A**	
Material	**kg/m³**	**Material**	**kg/m³**
Cem II AM 42.5	196	Cem II AM 42.5	204
Fly ash (Fine)	84	Fly ash (Fine)	87
Andesite Crusher	804	Granite Crusher	698
Bothma Filler sand	400	Bothma Filler sand	372
13 mm Andesite	810	13 mm Granite	810
Water	183	Water	190
Super plasticizer(A)	5.275	Super plasticizer(A)	5.238
Viscosity modifier	0.08	Viscosity modifier	0.04
W:C	0.65	W:C	0.65

Table 6.1: Concrete mixture proportions (continued)

MIXTURE D1A		MIXTURE A2A	
Material	**kg/m³**	**Material**	**kg/m³**
Cem II AM 42.5	183	Cem II AM 42.5	196
Fly ash (Fine)	79	Fly ash (Fine)	138
Dolomite Crusher	823	Andesite Crusher	804
Bothma Filler sand	409	Bothma Filler sand	400
13 mm Dolomite	835	13 mm Andesite	810
Water	171	Water	183
Super plasticizer(A)	3.38	Super plasticizer(A)	6.293
Viscosity modifier	0.04	Viscosity modifier	0.03
W:C	0.65	W:C	0.55
MIXTURE G2A		**MIXTURE D2A**	
Material	**kg/m³**	**Material**	**kg/m³**
Cem II AM 42.5	204	Cem II AM 42.5	183
Fly ash (Fine)	143	Fly ash (Fine)	130
Granite Crusher	698	Dolomite Crusher	823
Bothma Filler sand	372	Bothma Filler sand	354
13 mm Granite	810	13 mm Dolomite	835
Water	190	Water	171
Super plasticizer(A)	6.246	Super plasticizer(A)	3.756
Viscosity modifier	0.03	Viscosity modifier	0.02
W:C	0.55	W:C	0.55
MIXTURE A3A		**MIXTURE G3A**	
Material	**kg/m³**	**Material**	**kg/m³**
Cem II AM 42.5	196	Cem II AM 42.5	204
Fly ash (Ultra Fine)	84	Fly ash (Ultra Fine)	87
Andesite Crusher	804	Granite Crusher	698
Bothma Filler sand	400	Bothma Filler sand	372
13 mm Andesite	810	13 mm Granite	810
Water	183	Water	190
Super plasticizer(A)	3.84	Super plasticizer(A)	3.492
Viscosity modifier	0.03	Viscosity modifier	0
W:C	0.65	W:C	0.65

Table 6.1: Concrete mixture proportions (continued)

MIXTURE D3A		MIXTURE A4A	
Material	**kg/m³**	**Material**	**kg/m³**
Cem II AM 42.5	183	Cem II AM 42.5	256
Fly ash (Ultra Fine)	79	Fly ash (Fine)	110
Dolomite Crusher	823	Andesite Crusher	762
Bothma Filler sand	409	Bothma Filler sand	360
13 mm Dolomite	835	13 mm Andesite	810
Water	171	Water	183
Super plasticizer(A)	2.58	Super plasticizer(A)	3.876
Viscosity modifier	0	Viscosity modifier	0
W:C	0.65	W:C	0.5
MIXTURE G4A		**MIXTURE D4A**	
Material	**kg/m³**	**Material**	**kg/m³**
Cem II AM 42.5	266	Cem II AM 42.5	240
Fly ash (Fine)	114	Fly ash (Fine)	102
Granite Crusher	644	Dolomite Crusher	777
Bothma Filler sand	346	Bothma Filler sand	383
13 mm Granite	810	13 mm Dolomite	830
Water	190	Water	171
Super plasticizer(A)	3.65	Super plasticizer(A)	3.53
Viscosity modifier	0.023	Viscosity modifier	0.03
W:C	0.5	W:C	0.5
MIXTURE D5B		**MIXTURE D5C**	
Material	**kg/m³**	**Material**	**kg/m³**
Cem II AM 42.5	240	Cem II AM 42.5	240
Fly ash (Fine)	102	Fly ash (Fine)	102
Dolomite Crusher	777	Dolomite Crusher	777
Bothma Filler sand	383	Bothma Filler sand	383
13 mm Dolomite	830	13 mm Dolomite	830
Water	171	Water	171
Super plasticizer(B)	4.9	Super plasticizer(C)	3
Viscosity modifier	0.03	Viscosity modifier	0.03
W:C	0.5	W:C	0.5

Table 6.1: Concrete mixture proportions (continued)

MIXTURE D5D		MIXTURE D5E	
Material	**kg/m³**	**Material**	**kg/m³**
Cem II AM 42.5	240	Cem II AM 42.5	240
Fly ash (Fine)	102	Fly ash (Fine)	102
Dolomite Crusher	777	Dolomite Crusher	777
Bothma Filler sand	383	Bothma Filler sand	383
13 mm Dolomite	830	13 mm Dolomite	830
Water	171	Water	171
Super plasticizer(D)	2.25	Super plasticizer(D)	3.55
Viscosity modifier	0.02	Viscosity modifier	0.02
W:C	0.5	W:C	0.5
MIXTURE D5F		**MIXTURE D6A**	
Material	**kg/m³**	**Material**	**kg/m³**
Cem II AM 42.5	240	Cem II AM 42.5	240
Fly ash (Fine)	102	Fly ash (Fine) (20%)	68
		CSF (10%)	34
Dolomite Crusher	777	Dolomite Crusher	777
Bothma Filler sand	383	Bothma Filler sand	383
13 mm Dolomite	830	13 mm Dolomite	830
Water	171	Water	171
Super plasticizer(F)	3.53	Super plasticizer(A)	3.53
Viscosity modifier	0.03	Viscosity modifier	0.03
W:C	0.5	W:C	0.5

Before the workability testing was done, the water demand for each of the selected crusher sands was determined by doing trial mixtures. The water demand was determined using mixtures with similar slump. Using this information the first set of mixtures was designed with the three different aggregate types but the same target strength of 30 MPa and a water:cement ratio of 0,65. The water:cement ratio was taken from strength curves from the cement supplier. A few trial mixtures were done with a 70/30 cement:fly ash content and the different aggregates to determine an appropriate admixture dosage for each type. The second set of mixtures was the same as the first set except for a 60/40 cement:fly

ash content and a water:cement ratio of 0,55. This set was assessed to see the effect of the increased fly ash content on the workability. To assess the effect of the ultra fine fly ash on the workability of SCC, the third set of mixtures was designed and tested. Workability and compressive strength tests were done for each mixture.

From the compressive strength results (Table 6.2) of the mixtures A1A – D3A, it was clear that the cementitious content was too low or the water:cement ratio was too high and the target strength of 30 MPa was not reached. To reach the target strength initially decided on, the binder content was increased and the water:cement ratio reduced to 0,5. The fine aggregate proportions and admixture dosages were adapted accordingly. This was the fourth set of mixtures tested.

From the workability results (Table 6.3) of these mixtures, the aggregate that gave the best workability results was selected to be used in the successive set of mixtures. In this case mixture D4A was chosen, because it showed the best visual performance and required less superplasticizer. A set of mixtures was then designed to determine the workability retentions of the different admixtures. This last set (set five), which also included D4A, had the same ingredients and mixture proportions as the previous set except for the admixture type. The aim was to achieve similar flow characteristics and workability retention for the mixtures in this set. To achieve similar flow the admixture dosage was adapted and recorded.

The last mixture (D6A) was similar to D4A, except for the extender types. The extender content was made up of 20 % fly ash and 10 % condensed silica fume.

6.4.2 Mixing procedure

Twenty litre mixtures were prepared and mixed in an 80 litre pan mixer of all the mixtures shown in Table 6.1. The dry ingredients were mixed before the water was added. After mixing for approximately one minute the superplasticizer was added and the mixture assessed visually. The viscosity modifier was added if the mixture needed improved cohesion and then mixed for a further two minutes. The slump flow test was carried out after mixing stopped. After the slump flow test, the concrete was returned to the mixer and mixed for a minute before the V-funnel test was performed. The concrete was returned to the mixer again and mixed for another minute before the L-box test was done. The concrete was then transferred to the Tattersall Two Point Tester's bucket and the rheology test was done.

6.5 Results

6.5.1 Compressive strength

The main aim of this investigation was not to comment on the strength of SCC or to compare the strengths of the different mixtures used. Since a lower binder content and lower water:cement ratio was used it became apparent that the strengths are very important and form part of the results. The density of the

concrete cubes indicated to what extend the mixture was self compacting. Good workability results are also meaningless if the target strengths are not met.

The strength results are very inconsistent which might indicate inconsistency in materials used or errors in mixture preparation or poor compaction.

Table 6.2: Compressive strength results

		Compressive Strength Results					
		7 Days			28 Days		
Mixture No.	**Date**	**Density (kg/m^3)**	**Individual (MPa)**	**Average (MPa)**	**Density (kg/m^3)**	**Individual (MPa)**	**Average (MPa)**
		2474	18.1		2514	22.3	
A1A	07 Sep	2475	9.5	12.0	2444	21.9	23.1
	2004	2460	8.3		2486	25.1	
		2173	5		2144	11.5	
G1A	07 Sep	2127	5.1	5.2	2148	14.2	13.0
	2004	2173	5.6		2128	13.2	
			10.6		2446	22.3	
D1A	16 Aug		8.9	10.1	2430	22.7	22.6
	2004		10.9		2448	22.8	
					2516	33.6	
A2A	17 Jun	2514	14.5	14.5	2514	33.1	33.1
	2004				2511	32.6	
					2280	36.7	
G2A	17 Jun	2330	17.6	17.6	2320	39	37.8
	2004				2330	37.8	
					2448	26.6	
D2A	10 Jun	2454	12	12	2484	28.4	27.8
	2004				2480	28.4	
		2404	7.2		2415	18.3	
A3A	17 Sep	2358	7	6.9	2414	19	17.9
	2004	2344	6.4		2348	16.5	
		2351	9		2524	35.4	
G3A	08 Sep	2387	8.9	8.9	2500	32.2	33.0
	2004	2328	8.7		2468	31.5	
		2494	13.9		2334	22.5	
D3A	08 Sep	2536	15	14.6	2328	24.6	23.7
	2004	2495	14.8		2361	24.1	

Table 6.2: Compressive strength results (contitued)

		Compressive Strength Results					
		7 Days			28 Days		
Mixture No.	Date	Density (kg/m^3)	Individual (MPa)	Average (MPa)	Density (kg/m^3)	Individual (MPa)	Average (MPa)
		2478	17		2473	38.9	
A4A	22 Sep	2524	17.4	17.4	2491	39.6	39.4
	2004	2504	17.7		2504	39.8	
		2381	16.9		2383	36.5	
G4A	21 Sep	2375	16.4	16.4	2343	34.9	35.6
	2004	2330	16		2354	35.5	
		2424	11.6		2292	23.9	
D4A	10 Sep	2401	10.8	10.7	2319	25	23.3
	2004	2276	9.6		2350	20.9	
		2337	17		2316	34	
D5B	28 Sep	2318	18.8	18.3	2392	35.9	34.8
	2004	2338	19		2325	34.5	
		2353	13.8		2393	26	
D5C	05 Oct	2379	15.3	14.4	2398	26.4	27.0
	2004	2352	14.1		2400	28.5	
		2487	20.3		2489	39.5	
D5D	05 Oct	2438	19.6	20.9	2515	39.8	40.6
	2004	2549	22.7		2511	42.6	
		2490	17.6		2473	34.4	
D5E	05 Oct	2502	18.1	17.5	2488	36.7	36.3
	2004	2413	16.8		2496	37.8	
		2403	15.6		2440	35.1	
D5F	12 Oct	2419	16.1	15.8	2377	35.4	35.7
	2004	2399	15.6		2463	36.6	
		2509	32.4			60.1	
D6A	19 Oct	2500	33.6	33.0		60.6	60.3
	2004	2459	32.9			60.3	

6.5.2 The fresh properties of SCC

Table 6.3 presents the test results obtained using the four test methods used.

Table 6.3: Workability results for the mixture design investigation 1

Mixture Number	Tattersall Results		Slump flow		V-Funnel		L-Box					Observations and Comments
	τ_o (Pa)	μ (Pas)	T50 (sec)	Final (mm)	Flow time (sec)	Speed (m/s)	T20 (sec)	T40 (sec)	H1 (mm)	H2 (mm)	H2/H1	
A1A	15	31	3	580	6	0.34	1	4	200	80	0.40	Blocking occurred in L-box. Needs more superplasticizer
G1A	8.4	15	1	680	4	0.51	0.5	1.5	120	60	0.50	Blocking occurred in L-box. Needs more viscosity modifier
D1A	11	24	3	570	5	0.41	1	2	130	50	0.38	Blocking occurred in L-box. Too much viscosity modifier was used
A2A	11	39	5	620	11	0.19	1	3	120	70	0.58	No segregation was visible
G2A	1.5	59	3	715	25	0.08	1	4	90	80	0.89	Showed signs of segregation and bleeding. V-Funnel test was done last, therefore bad results
D2A	8	37	4	610	6	0.34	1	2	120	70	0.58	Visual assessment indicated that this was a good mixture
A3A	8.1	11	2	590	4	0.51	0.5	1	180	0	0.00	Blocking occurred in L-box. Cube surface finish also bad
G3A	12	25	2	680	5	0.41	0.5	2	140	60	0.43	Blocking occurred in L-box. Cube surface finish also bad
D3A	13	25	1	630	4	0.51	0.5	1.5	140	30	0.21	Blocking occurred in L-box. Cube surface finish also bad
A4A	7.9	30	4	580	9	0.23	0.5	2	140	60	0.43	Visual assessment indicated that this was a good mixture with a good cube surface finish
G4A	6	13	2.5	680	4	0.51	1	2	100	75	0.75	Visual assessment indicated that this was a good mixture with a reasonable cube surface finish
D4A	11	13	2	720	4	0.51	0.5	1.5	140	90	0.64	Visual assessment indicated that this was a good mixture with a very good cube surface finish

Table 6.3: Workability results for the mixture design investigation 1 (continued)

Mixture Number	Tattersall Results		Slump flow		V-Funnel		L-Box					Observations and Comments
	τ_o (Pa)	μ (Pas)	T50 (sec)	Final (mm)	Flow time (sec)	Speed (m/s)	T20 (sec)	T40 (sec)	H1 (mm)	H2 (mm)	H2/H1	
D5B	7.6	26	3	630	6	0.34	1	2	105	75	0.71	Showed signs of segregation. Cube surface finish was very good
D5C	17	25	3	620	8	0.26	1	3	130	50	0.39	Mixture was very cohesive. Cube surface finish was very bad
D5D	19	36	3	645	26	0.08	1	3	180	30	0.17	Showed signs of segregation and blocking. V-Funnel test was done last, therefore bad results
D5E	10	23	1	620	7	0.29	0.5	1	110	70	0.64	Visual assessment indicated that this was a good mixture with a good cube surface finish
D5F	9.5	23	2	625	4	0.51	0.5	2	110	50	0.46	Mixture was very cohesive. Cube surface finish was very bad
D6A	15	12	1.5	625	5	0.41	0.5	1	120	75	0.6	Visual assessment indicated that this was a good mixture with a very good cube surface finish

In interpreting the results shown in Table 6.3, it is useful to refer to the EFNARC Specifications[14], which require that the results conform to the range values shown in Table 6.4[14]. The results in the shaded cells do not conform to these specifications.

Table 6.4: EFNARC Specifications for SCC workability tests[14]

Slump flow	650 – 800 mm
T_{50} slump flow	2 - 5 sec
V Funnel	6 – 12 sec
L Box	$H_2 / H_1 = 0.8 – 1.0$
J-Ring (st_j)	0 – 10 mm

Mixtures A1A, G1A and D1A were the first set of mixtures tested after the trial mixtures were done. The admixture dosage was decreased and a visible increase in yield stress was noticed. This increase in yield stress was confirmed by the blockage in the L-Box and the low slump flow values.

The extra fly ash used in mixtures A2A, G2A and D2A, showed an improvement in the yield value as well as a better plastic viscosity. Mixture G2A had an unacceptably low yield value, which was because of the segregation that occurred. This result correlates well with the slump flow and L-box values. The L-box value of 0.9 indicates that blockage was not a problem, but if all the results are considered and the visual assessment taken into account, this L-Box result is misleading. This result is misleading, because mixture G2A segregated and bled.

The high V-funnel time is because this test was executed last, workability retention was lost and segregation occurred.

Ultra fine fly ash was used in mixtures A3A, G3A and D3A, to determine the effect on the rheology of the SCC. The results show a decrease in yield stress as well as plastic viscosity for mixture A3A, which was expected. When using ultra fine fly ash the flowability and the cohesiveness should increase. The yield stress and plastic viscosity for mixtures G3A and D3A both increased, which was not expected. The reason for this must be the change in admixture dosage.

As mentioned earlier in this chapter, the binder content was increased for mixtures A4A onward. With this change as well as the change in water:cement ratio from 0.65 to 0.5, there was a significant change in the workability results. The yield stress was less than those obtained with the previous mixtures. This indicates that these mixtures were much more flowable and had better SCC characteristics. The V-Funnel and L-box results were also much more acceptable with no indication of blocking between the reinforcing steel bars.

Mixtures D4A, D5B, D5C, D5D, D5E and D5F were all the same, except for the superplasticizer type. Each of these mixtures contained a different superplasticiser type.

From the results (Table 6.3) it is clear that superplasticizer A gave the best flowability (slump flow of 720mm) and superplasticiser types C and D gave the worst workability results. The results from the other superplasticisers (B, E and F) are acceptable with a relatively low yield stress.

Mixture D6A contained condensed silica fume. The CSF made the mixture very cohesive as shown by the high yield stress value and the low plastic viscosity value. The V-funnel time is still acceptable according to the EFNARC specifications[14]. The unacceptably low slump flow values indicate that more fines are needed in the mixtures. From the trial mixtures it was obvious that more superplasticiser does not necessarily give better flow, but segregation occurs.

6.5.3 The fresh properties of SCC mortar

When using the same mixture proportions as for the concrete mixtures reported in Table 6.1, it was found that the mortar sample segregated and bled to such an extent that it was, in most cases, not possible to do the tests. At first the admixture dosage was reduced, but this minimised the opportunity for comparison with the concrete mixture. It was decided to adapt the mortar mixture by adding sand until a yield value of 1000 litres was reached. The results for the modified mixtures are given in Table 6.5. Mixture A4A gave the best results with the lowest yield stress and highest plastic viscosity values.

Table 6.5: SCC mortar, workability results.

Mixture Number	Tattersall results				V-Funnel		Slump flow			Comments
	h (Nms)	g (Nm)	τ_o (Pa)	μ (Pas)	Flow time (sec)	R_m (mm)	d_1 (mm)	d_2 (mm)	Γ_m (mm)	
A1A	0.05	0.00	-0.24	5.49	3	3.33	310	300	8.3	Showed signs of severe segregation.
G1A	0.05	0.06	4.46	5.76	11	0.91	210	230	3.83	Visual assessment indicated that this was a good mixture
D1A	0.02	0.01	0.55	2.23	3	3.33	310	290	7.99	Showed signs of segregation.
A4A	0.07	0.02	1.69	8.35	6	1.67	230	240	4.52	Visual assessment indicated that this was a good mixture
G4A	0.04	0.00	-0.35	5.43	2	5.00	320	330	9.56	Showed signs of segregation.
D4A	0.05	0.04	3.09	6.05	7	1.43	185	180	2.33	Visual assessment indicated that this was a good mixture

Table 6.6 gives a summary of the mortar results compared with the corresponding concrete results. No noticeable comparison is evident between the yield stress of the mortar and the concrete. Figure 6.1 shows the relation between the mortar yield stress and the concrete yield stress. From the scatter of these results, there is no noticeable relation between the yield stress of a concrete mixture and the yield stress of an equivalent mortar mixture. There is also no clear relation between the plastic viscosity of the mortar mixtures and concrete mixtures (Figure 6.2). This could either mean that no relation exists or that the Tattersall measurement for the mortar is not accurate.

Table 6.6: Mortar and concrete Tattersall rheology results.

Mixture Number	Mortar		Concrete	
	τ_o (Pa)	μ (Pas)	τ_o (Pa)	μ (Pas)
A1A	-0.24	5.49	15	31
G1A	4.46	5.76	8.4	15
D1A	0.55	2.23	11	24
A4A	1.69	8.35	7.9	30
G4A	-0.35	5.43	6	13
D4A	3.09	6.05	11	13

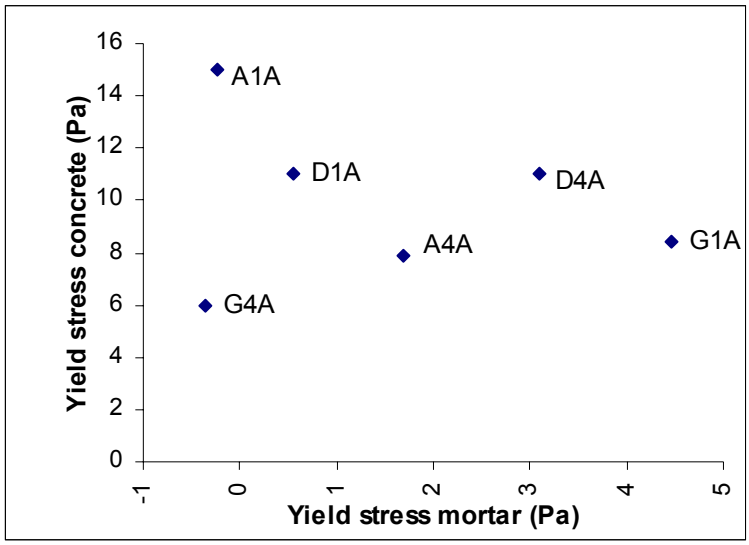


Figure 6.1: Relation between yield stress for concrete and mortar mixtures.

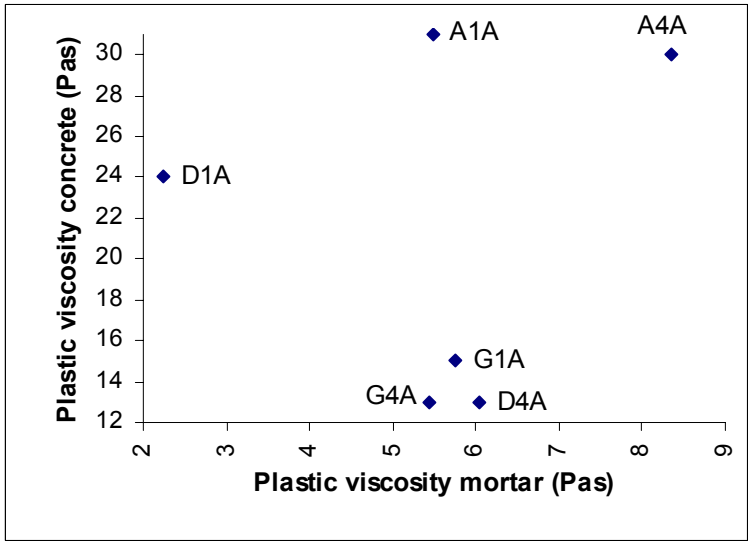


Figure 6.2: Relation between plastic viscosity for concrete and mortar mixtures.

6.5.4 Workability retention of the mortar mixtures

The workability retention results are given in Table 6.7. These results show the different workability retentions of the five different superplasticisers used in this investigation. Superplasticizer A gave the best results with a workability retention of about two hours.

Table 6.7: Workability retention results**.**

Mixture Number	Slump retention					Comments
	1 Min (mm)	30 Min (mm)	60 Min (mm)	90 Min (mm)	120 Min (mm)	
D4A	185	170	170	165	155	Good
D5B	230	190				Little Retention
D5C	270	270	290			Segregated & Bled
D5D	300	300	295	240		Segregated & Bled
D5E	315	285				Little Segregation
D5F	200	160				Very Cohesive

6.5.5 Comparison between workability and rheological parameters

According to Billberg[1], Utsi[9] and Nielsson and Wallevik[50] the final diameter of the slump flow describes the yield stress and the T50 value describes the plastic viscosity of the SCC mixture. These comparisons are shown in Figure 6.3 and Figure 6.4 respectively. As a rule, the slump flow diameter should increase if the yield value decreases. Similarly the T50 value increases if the plastic viscosity is higher. The large scatter of the results shows the inaccuracy of the slump flow test. This is partly due to the difficulty in setting the correct start and stop times. The slump flow test has to be done by two persons. One person lifts the slump cone while the second person starts the stopwatch. This operations needs to be

done simultaneously for accurate results. As with the slump test, the slump flow test is not very accurate but gives a good indication of the flowability and stability of the mixture and is therefore still used extensively to judge the workability of SCC mixtures.

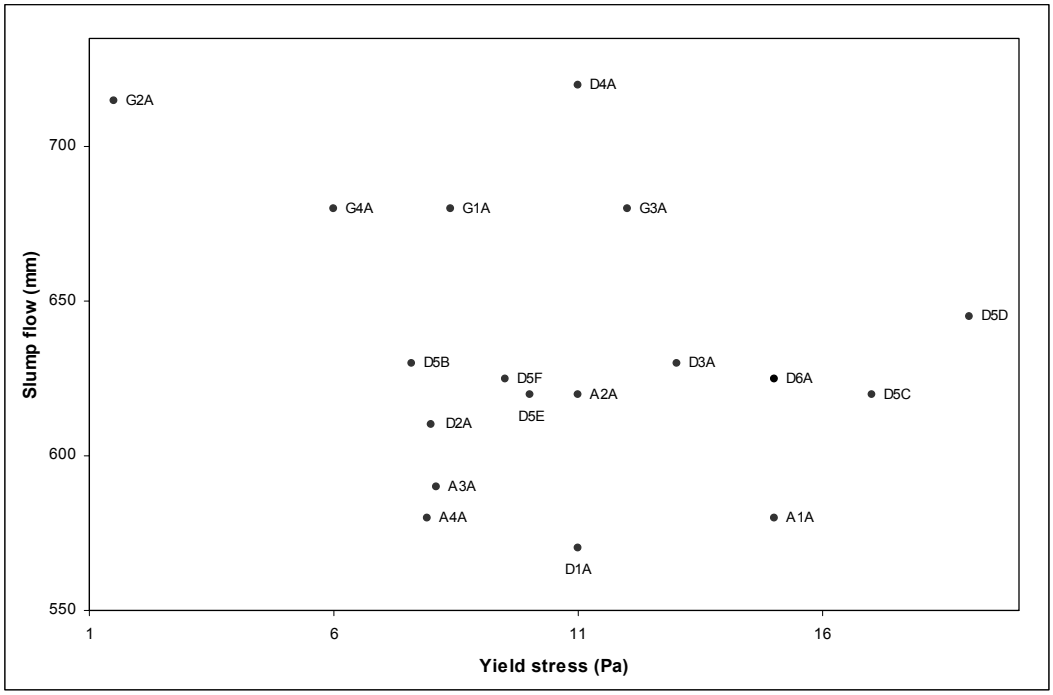


Figure 6.3: Comparison between the slump flow and yield stress for the SCC mixtures tested

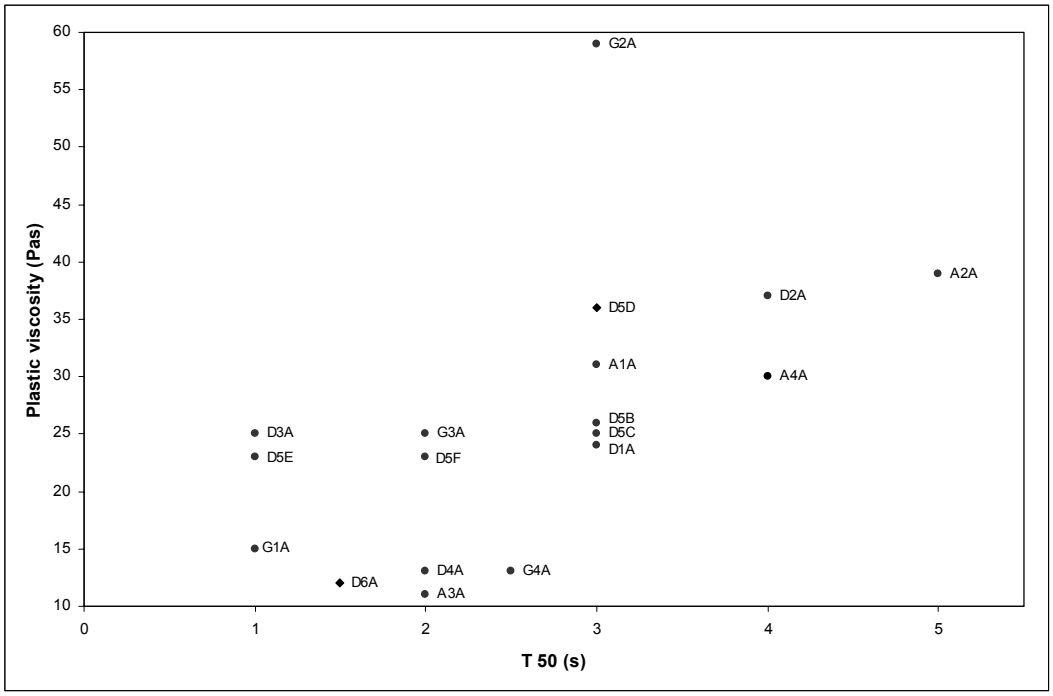


Figure 6.4: Comparison between the T 50 times and plastic viscosities for the SCC mixtures tested.

The comparison between the V-funnel time and the plastic viscosity is shown in Figure 6.5. This graph shows a good trend between V-Funnel times and plastic viscosity. The scatter of some points is due to the operator sensitivity as well as the adhesion to the walls of the apparatus. A comparison between the V-funnel and T50 results is shown in Figure 6.6. In this comparison there is also not a noticeable relation. This could also be because of operator inaccuracies or the lack of comparison between the test methods. The empirical single-point tests measure either different properties or try to measure the same properties differently. The same influencing factors have different relative importance across the tests[(2)]. Because of these differences, there is a large degree of scatter between the results. This shows that the empirical single-point tests not only have limitations, but can also be misleading.

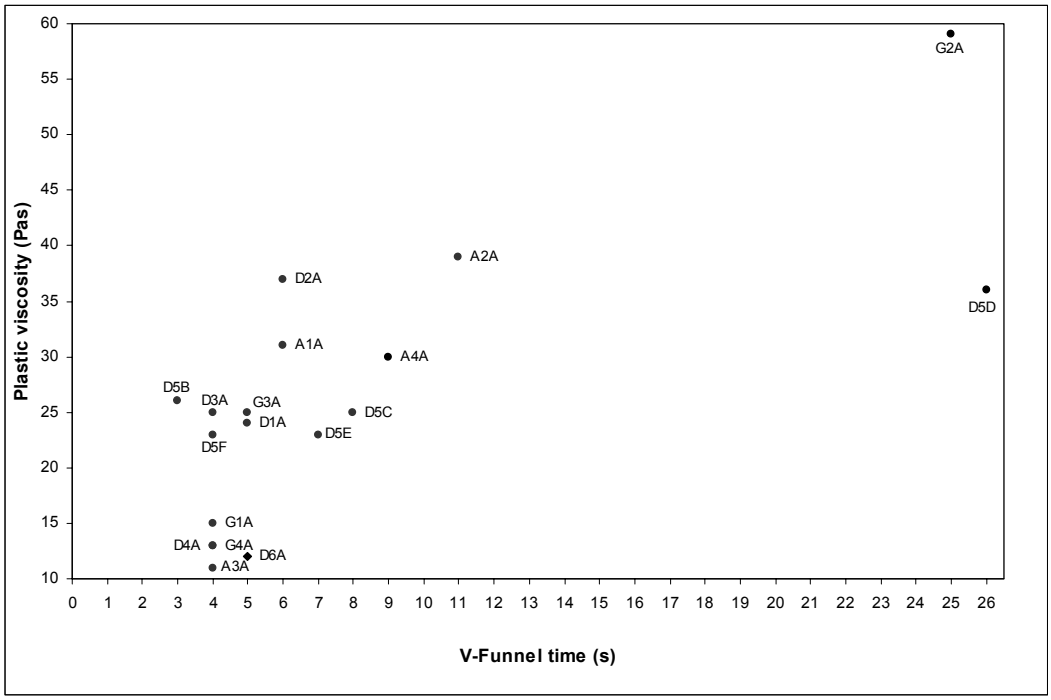


Figure 6.5: Comparison between the V-Funnel times and plastic viscosities for the SCC mixtures tested.

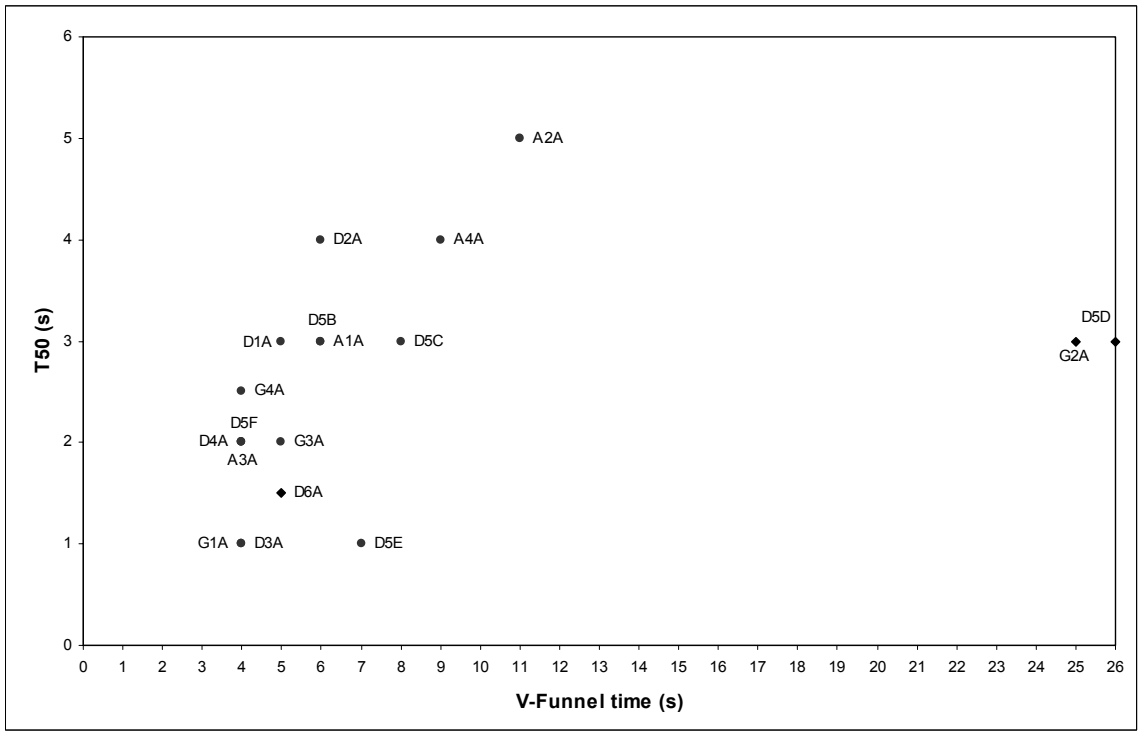


Figure 6.6: Comparison between the V-Funnel times and T 50 times for the SCC mixtures tested.

Figure 6.7 shows the relation between the V-Funnel times and the slump flow. In Figure 6.8 the relation between the slump flow and T 50 times is shown. In both there is not a noticeable comparison. A recommendation would be to do the tests simultaneously for accurate results.

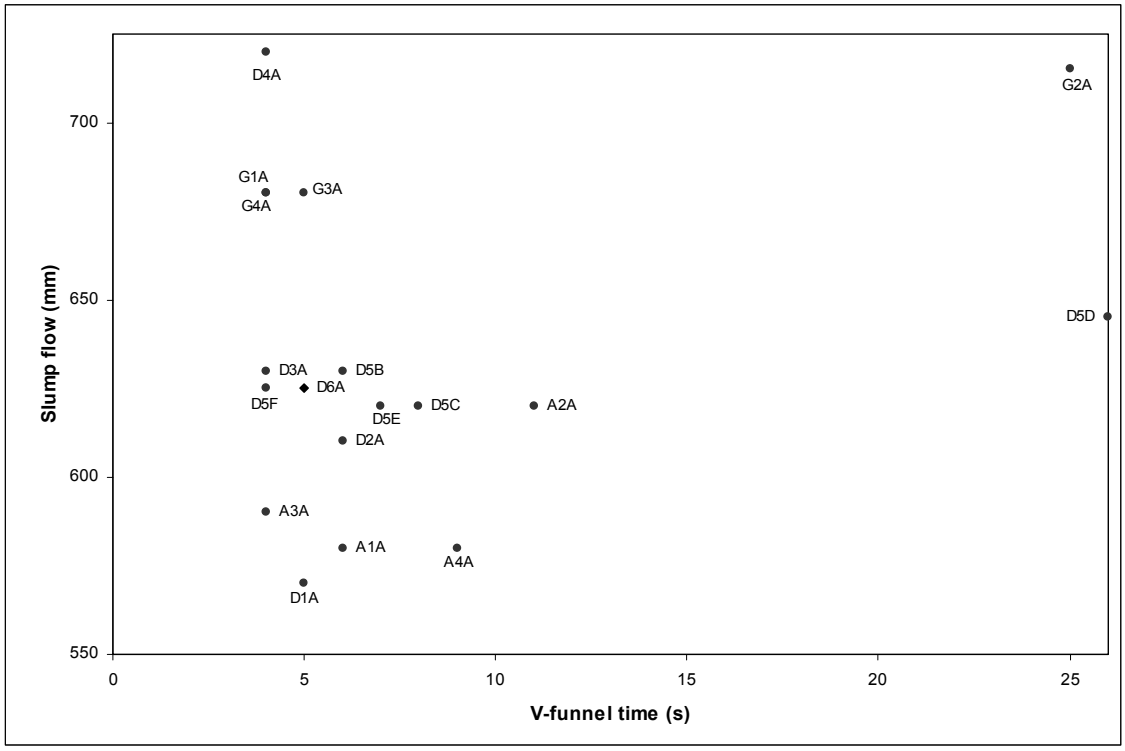


Figure 6.7: Comparison between the V-Funnel times and slump flow for the SCC mixtures tested.

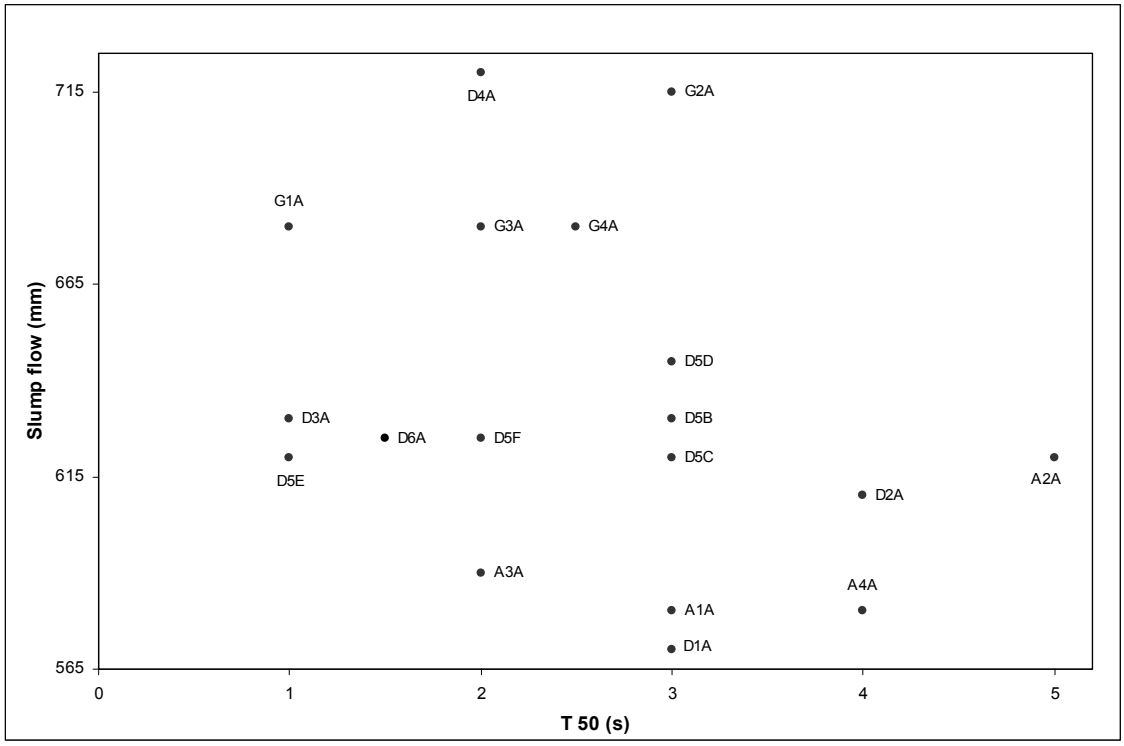


Figure 6.8: Comparison between the T 50 times and slump flow for the SCC mixtures tested.

A comparison between the plastic viscosity and the flow time of the L-box was not done. In a comparison like this, the time from when the gate is opened until the concrete reaches the end of the L-box is required. This was not measured in these tests and according to Nielsson and Wallevik[50] the restriction of flow by the steel reinforcement bars influences the results too much for a comparison. This test was also done last which influenced the results to such an extent that the results were unacceptable. The L-box was mainly used to assess the passing and filling ability of the SCC.

The time required to do all the tests mentioned, after mixing had stopped, was not sufficient and accurate results could not be obtained from the last test done. A

time period of about ten minutes was available. It is therefore recommended to use the J-ring test instead of the L-box test in future investigations. The J-ring test is done with the slump flow test to assess the blocking and stability of the SCC. By doing the J-ring test with the slump flow test, the time for testing is used more effectively.

6.6. Conclusion

The test results indicate that SCC can potentially be made with the materials used in this investigation, but this mixture design method is not very reliable. This trial and error method is too random and is therefore not recommended. Since this method can not be used as a reliable SCC mixture design, the results are used to compare the different test methods used to describe the workability of SCC. The next chapter proposes a mixture design model that can be used with any aggregate type.

CHAPTER 7

ALTERNATIVE MIXTURE DESIGN MODEL AND RESULTS.

7.1 Introduction

The method of mixture design for SCC proposed and used in this chapter is based on a method developed in Taiwan by Su, et al[51]. The main objective of this method is to determine the amount of paste required to fill the openings between loosely piled aggregate. The reason for proposing this particular model is its simplicity and adaptability. Because of limited design procedures and testing this method is more acceptable to SCC producers who do not have special facilities and testing equipment. This model could also be used for other aggregate types and any required designed strength.

7.2 Mixture design procedure

Step 1: Aggregate content

From the slump flow and visual assessment results of a number of trial mixtures it was found that the volume of the total amount of aggregate should be between 60% and 63%. Because of the shape of the crushed stone used in this investigation, the optimum amount of fine aggregate used was found to be between 52% and 60% of the total amount of aggregate. The amount of coarse and fine aggregate was determined using the packing factor (PF), which is the ratio of tightly packed aggregate mass, to that of the loosely packed mass of the coarse aggregate. This tightly packed mass was determined using the procedure

described in SABS 845:1994[52]. It was found by experimenting with different PF's that the most suitable value for crushed aggregates in South Africa is 1,05. The following equations are used to calculate the content of coarse and fine aggregate:

$$C_g = PF * C_{gL}\left(1 - \frac{S}{a}\right) \tag{7.1}$$

$$C_S = PF * C_{SL}\left(\frac{S}{a}\right) \tag{7.2}$$

Where C_g = content of coarse aggregate in kg/m^3

C_S = content of fine aggregate in kg/m^3

C_{gL} = loose bulk density of loosely piled saturated surface-dry coarse aggregate in air (kg/m^3)

C_{SL} = loose bulk density of loosely piled saturated surface-dry fine aggregate in air (kg/m^3)

PF = Packing factor, ratio of mass of coarse aggregates in a tightly packed state in SCC to that of a loosely packed state in air

$\frac{S}{a}$ = volume ratio of fine aggregate to total aggregate, ranging between 52 % and 60 % which was pre-determined using trial mixtures and slump flow results.

The loose and compacted bulk densities were determined in accordance to SABS 845:1994[52].

Step 2: Cement content

As a rough first estimate, the compressive strength was used to determine the cement content. According to Su, et al[51] the compressive strength of SCC used in Taiwan is 0.138 MPa for each kilogram of Portland cement. This relationship was used in this investigation.

The cement content is therefore calculated using the following equation:

$$C_C = \frac{f_{cu}}{0.138} \tag{7.3}$$

Where C_C = cement content in kg/m^3

f_{cu} = designed compressive strength in MPa

Step 3: Water content

Since the relationship between compressive strength and water:cement ratio for SCC is similar to that of conventional concrete, the same principle as for conventional concrete is applied in this design model. The water:cement ratio is obtained from curves in ACI Standard 211.1-91[53], or from actual performance results. A water:cement ratio of 0.55 was used in this part of the investigation.

Step 4: Extender content

This design model provides for the use of two different extender types to make the model more adaptable and flexible. If only one extender is used, the option for

the other is taken as zero. To make up the paste content required to ensure flowability, fly ash (FA) and ground granulated blast-furnace slag (GGBS) were used as filler materials. The inclusion of FA and GGBS reduces the cement content, heat of hydration as well as reducing the cost. FA also assists in making the mixture more flowable and cohesive while GGBS increases the durability of the mixture[49]. While the cement content and water:cement ratio determines the compressive strength, the FA and GGBS makes up the paste volume required for segregation resistance, flowability and self-compactability.

To calculate the water:FA ratio (*W/F*) and the water:GGBS ratio (*W/B*), the mortar flow test was carried out to ensure flow values of FA and GGBS pastes equal to that of the cement paste. The procedure for the mortar flow test used to determine the flow values is described in Chapter 4. Silica sand, specially graded to conform to the ViscoCorder sand grading was used and the superplasticiser content was kept at 1.8 % of the binder content for all the mixtures. The sand:binder ratio was 3:1 and the spread (determined with the mortar flow test as described in Chapter 4) for the cement mortar was 250 mm. After various trial mixtures, it was found that $W/F = 0.3$ and $W/B = 0.54$ gave the required spread of 250 mm.

The volume of FA paste (V_{Pf}) and GGBS paste (V_{PB}) is then calculated using Equation 7.4:

$$V_{Pf} + V_{PB} = 1 - \frac{C_g}{1000 * G_g} - \frac{C_S}{1000 * G_S} - \frac{C_C}{1000 * G_C} - \frac{C_{WC}}{1000 * G_W} - V_a \qquad (7.4)$$

Where G_g = relative density of coarse aggregate

G_S = relative density of fine aggregate

G_C = relative density of cement

G_W = relative density of water

V_a = air content in SCC (%), taken as 1% for this investigation.

The total amount of extender, C_{pm} (kg/m^3), is made up of *A%* FA and *B%* GGBS by weight and calculated using Equation 7.5, which is then substituted into Equation 7.4:

The volume of FA paste $= \frac{mass \cdot FA \cdot mixing \cdot water}{relative \cdot density \cdot water} + \frac{mass \cdot FA \cdot as \cdot \% \cdot of \cdot total}{\cdot relative \cdot density \cdot FA}$,

$V_{Pf} = \frac{A\% * C_{pm} * (W/F)}{1000 * G_W} + \frac{A\% * C_{pm}}{1000 * G_f}$ and. the volume of GGBS paste =

$\frac{mass \cdot GGBS \cdot mixing \cdot water}{relative \cdot density \cdot water} + \frac{mass \cdot GGBS \cdot as \cdot \% \cdot of \cdot total}{\cdot relative \cdot density \cdot GGBS}$,

$V_{PB} = \frac{B\% * C_{pm} * (W/B)}{1000 * G_W} + \frac{B\% * C_{pm}}{1000 * G_B}$ and then

$$V_{Pf} + V_{PB} = A\% \cdot C_{pm}\left(\frac{W/F}{1000 * G_W} + \frac{1}{1000 * G_f}\right) + B\% \cdot C_{pm}\left(\frac{W/B}{1000 * G_W} + \frac{1}{1000 * G_B}\right) \qquad (7.5)$$

Where G_f = relative density of FA

G_B= relative density of GGBS

G_W= relative density of water

Since fly ash improves the workability of a concrete mixture, FA is taken as 80 % and GGBS as 20 % of the total amount of extender used[48].

The FA content, C_f (kg/m^3), and the GGBS content, C_B (kg/m^3), are then calculated using Equations 7.6 and 7.7 respectively:

$$C_f = A\ \% * C_{pm} \tag{7.6}$$

$$C_B = B\ \% * C_{pm} \tag{7.7}$$

The water content required by the FA is calculated using Equation 7.8:

$$W_{wf} = \left(\frac{W}{F}\right) C_f \tag{7.8}$$

The water content required by the GGBS is calculated using Equation 7.9:

$$W_{wB} = \left(\frac{W}{B}\right) C_B \tag{7.9}$$

Step 5: Total water content

The total amount of water required for the mixture is determined by adding the water required for the extenders to the water required for the cement.

$$W_W = W_{WC} + W_{Wf} + W_{WB} \tag{7.10}$$

Step 6: Superplasticiser dosage

The superplasticizer dosage is calculated as a percentage of total binder content. As a starting point this percentage is based on the range advised by the supplier.

The dosage is then adjusted until the mixture appears satisfactory (good flowability without signs of segregation) and a slump flow of at least 600 mm.

Step 7: Trial mixtures and workability tests

Trial mixtures were done to assess and adjust the mixture design. Various quality control tests (the slump flow, the L-box, the V-funnel, the U-test, or the J-Ring), can then be done to ensure that the SCC mixture meets the following requirements:

- Fresh concrete properties are according to the standards set out by the EFNARC Specifications[14].
- The mixture does not bleed or segregate.
- Cube strength results satisfy the design strength.

Step 8: Mixture adjustments

From the quality control test results, the mixture proportions can then be adjusted if necessary. If the mixture shows signs of bleeding, segregation or poor flow and passing ability, the fines content is increased by reducing the PF value[51].

Sample calculation:

Step 1: Aggregate content.

Use a PF = 1.05

Fine aggregate: C_S = 1.05 * 1491 * 58% = 1003 kg/m^3

Coarse aggregate: C_g = 1.05 * 1365 * (1-0.58) = 602 kg/m^3

Step 2: Cement content.

C_C = 30/0.138 = 218 kg/m^3

Step 3: Water content.

C_{WC} = 0.55 * 218 = 120 kg/m^3

Step 4: Extender content.

$$V_{Pf} + V_{PB} = 1 - \frac{602}{1000 * 2.7} - \frac{1003}{1000 * 2.7} - \frac{218}{1000 * 3.1} - \frac{120}{1000 * 1} - 0.01$$

$$= 0.205 \text{ kg/m}^3$$

$$\frac{0.8 * C_{pm} * 0.3}{1000 * 1} + \frac{0.8 * C_{pm}}{1000 * 2.2} + \frac{0.2 * C_{pm} * 0.54}{1000 * 1} + \frac{0.2 * C_{pm}}{1000 * 2.9} = 0.205 \text{ kg/m}^3$$

C_{pm} = 261 kg/m^3

FA content = C_f = 0.8 *261 = 209 kg/m^3

GGBS content = C_B = 0.2 *261 = 52 kg/m^3

Step 5: Total water content.

Water content for FA = W_{wf} = 0.3 *209 = 63 kg/m^3

Water content for GGBS = W_{WB} = 0.54 *52 = 28 kg/m^3

Total water = 120 + 63 + 28 - 2 = 209 kg/m^3

Table 7.1 shows an example of the mixture design sheet used to calculate the proportions.

Table 7.1: Example of mixture design sheet.

Material	RD	L/m^3	kg/m^3
Cem I 42.5	3.1	70.32	218
Fly ash(C_f)	2.2	96.35	209
GGBS(C_B)	2.9	18.02	52
ViscoCorder sand(C_S)	2.7	371.5	1003
13 mm Granite(C_g)	2.7	223	602
Water(Total)	1	208.5	209
Super plasticizer 0.7%	1.2	2.796	3.4
Total Binder		166.7	479
(V_{pf}+V_{pb}) Extender volume			0.205
Total extender amount (C_{pm})			261
Water(W_{wc})	1	119.9	120
Water(W_{wf})	1	62.72	63
Water(W_{ws})	1	28.23	28
Water(W_{sp})	1	2.315	2
Yield		990.5	3250
W:C			0.55

7.3 Laboratory Procedures

7.3.1 Mixture proportions

Table 7.2 shows the mixture proportions of the different mixtures used in this investigation. The mixtures are identified as follows, the first letter indicates the aggregate type (Andesite (A), Granite (G) and Dolomite (D)), the first number indicates the mixture series and the last two numbers the superplasticizer dosage. Mixtures G734 to A733 were designed for the three different aggregate types using crusher sand as fine aggregate to assess the suitability of the design model for different aggregate types. Mixtures G831 to A831 were done with the same

three aggregate types but with ViscoCorder sand used as fine aggregate in all three mixtures to compare the performance of the three types of aggregate.

Table 7.2: Concrete mixture proportions for alternative mixture design model.

MIXTURE G734		**MIXTURE D732**	
Material	**kg/m³**	**Material**	**kg/m³**
Cem I 42.5	218	Cem I 42.5	218
Fly ash(Cf)	209	Fly ash(Cf)	192
GGBS(C_B)	52	GGBS(C_B)	48
ViscoCorder sand(Cs)	1003	ViscoCorder sand(Cs)	1003
13 mm Granite(Cg)	602	13 mm Dolomite(Cg)	694
Water(Total)	209	Water(Total)	201
Super plasticizer A	3.4	Super plasticizer A	3.2
W:C	0.55	W:C	0.55
MIXTURE A733		**MIXTURE G831**	
Material	**kg/m³**	**Material**	**kg/m³**
Cem I 42.5	218	Cem I 42.5	218
Fly ash(Cf)	208	Fly ash(Cf)	179
GGBS(C_B)	52	GGBS(C_B)	45
ViscoCorder sand(Cs)	986	Granite Crusher(Cs)	1022
13 mm Andesite(Cg)	666	13 mm Granite(Cg)	659
Water(Total)	208	Water(Total)	196
Super plasticizer A	3.3	Super plasticizer A	3.1
W:C	0.55	W:C	0.55
MIXTURE D820		**MIXTURE A831**	
Material	**kg/m³**	**Material**	**kg/m³**
Cem I 42.5	218	Cem I 42.5	218
Fly ash(Cf)	205	Fly ash(Cf)	182
GGBS(C_B)	51	GGBS(C_B)	46
Dolomite crusher(Cs)	917	Andesite crusher(Cs)	1129
13 mm Dolomite (Cg)	814	13 mm Andesite (Cg)	666
Water(Total)	208	Water(Total)	197
Super plasticizer A	2.0	Super plasticizer A	3.1
W:C	0.55	W:C	0.55

7.3.2 Mixing procedure

Twenty liter mixtures were prepared and mixed in an 80 liter pan mixer. The dry ingredients were mixed before the water was added. After mixing for approximately one minute the superplasticizer was added and mixed for another minute. The mixer was stopped and the mixture assessed visually. The workability tests were then carried out, starting with the slump flow test. After the slump flow test the concrete was returned to the mixer and mixed for a minute before the J-Ring test was performed. The concrete was returned to the mixer again and mixed for another minute before the rheology test was done in the Tattersall Two Point Tester.

7.4 Results

7.4.1 Compressive strength

To ensure that the compressive strength of each mixture was according to the design strength, the cube test was performed for each mixture. Six cubes were tested according to SABS 860: 1994[40] for each mixture, cured and then crushed at 7 and 28 days. The 7 and 28 day cube strength results are given in Table 7.3.

The lower densities of the first three mixtures show that the poorly graded VicoCorder sand prevented these mixtures to be fully self compacting. This emphasise the need for well grade sand to be used in the mixture design of self-compacting concrete.

Table 7.3: Compressive strength results for the alternative mixture design mixtures.

Mixture Number	Date	Compressive Strength Results						28 Day Strength 1kg binder (MPa/kg)
		7 Days			28 Days			
		Density (kg/m^3)	Single (MPa)	Ave (MPa)	Density (kg/m^3)	Single (MPa)	Ave (MPa)	
G734	21 Jun 2005	2335	32.4	32.5	2314	53.7	53.5	0.25
		2345	33.3		2286	52.7		
		2323	31.9		2343	54		
D732	29 Jun 2005	2304	21.1	21.0	2376	37.1	37.0	0.17
		2289	21		2342	36.4		
		2312	20.9		2310	37.5		
A733	27 Jun 2005	2354	21.7	22.4	2349	44.5	41.8	0.19
		2329	22.8		2338	41.3		
		2311	22.7		2364	39.6		
G831	27 Jun 2005	2239	27	26.9	2259	48.5	48.4	0.22
		2246	27.6		2243	46.8		
		2248	26		2255	50		
D820	26 Jul 2005	2465	22.6	21.7	2471	51.8	50.6	0.23
		2452	21.6		2476	49		
		2471	20.9		2495	50.9		
A831	27 Jun 2005	2434	28.4	27.7	2461	56.9	55.1	0.25
		2446	26.6		2478	53.1		
		2460	28		2458	55.2		

7.4.2 The fresh properties of the mixtures

Table 7.4 presents the test results obtained from the Tattersall Two Point Tester, the slump flow test and the J-ring test. In interpreting the slump flow and J-Ring results, it is useful to refer to the EFNARC Specifications, which require that the materials conform to the range values shown in Table 6.4[(14)]. The shaded results did not conform to these values.

Table 7.4: Workability results for alternative mixture design model.

Mixture Number	Tattersall Results				Slump Flow		J-Ring Results				
	h (Nms)	g (Nm)	τ_o (Pa)	μ (Pas)	T50 (sec)	Final flow (mm)	Final spread (mm)	h_m (mm)	h_r (mm)	st_j (mm)	ß
G734	0.13	0.04	2.6	15.77	6	635	730	2.0	5.5	7.0	0.09
D732	0.16	0.05	3.5	19.63	5	615	620	3.5	14.0	21.0	0.27
A733	0.14	0.03	2.4	17.45	5	620	650	4.5	10.0	11.0	0.14
G831	0.17	0.03	2.3	20.84	5	600	660	8.0	10.0	4.0	0.12
D820	0.17	0.11	7.9	20.29	4	670	640	6.0	19.0	26.0	0.33
A831	0.12	0.20	14.8	14.48	5	615	635	3.5	15.5	24.0	0.31

In the observation of the trial mixtures (not included in this investigation), it was found that there was severe segregation, bleeding and blocking. This problem was rectified with a change in the PF value (from 1.18 to 1,05) and increasing the fines content using more FA and GGBS (Mixtures in Table 7.2). The increase in the fines content made the mixtures more cohesive and segregation was minimized. Even though the test results did not always meet the requirements set by EFNARC[14], most of these mixtures preformed well when assessed visually. Visual assessment was done as soon as mixing stopped by assessing the flow and resistance to segregation of each mixture. The Tattersall results, low yield stress and high plastic viscosity, complements these observations. The results obtained from mixture G831 gave the best overall workability results and mixture A831 the worst. It was again realised that Granite gave the better workability results, but did not compact well under self weight only. Andesite gave the worst workability

results and Dolomite requires less superplasticizer than the previous two aggregates for similar flowabilities.

7.4.3 Comparison between workability and rheological parameters

According to Billberg[1], Utsi[9] and Nielsson and Wallevik[50] the final diameter of the slump flow describes the yield stress and the T50 value describes the plastic viscosity of the SCC mixture. These comparisons are shown in Figure 7.1 and Figure 7.2 respectively. As a rule, the slump flow diameter should increase if the yield value decreases. Similarly the T50 value increases if the plastic viscosity is higher. The large scatter of these results shows that there is no significant relationship between rheology results and empirical results. This proves, as with the comparison done in Chapter 6, that empirical measurements are not accurate and rheology is required to describe the workability of SCC. The slump flow test is not very accurate but gives a good indication of the flowability and stability of the mixture and is therefore still used extensively to judge the workability of SCC mixtures.

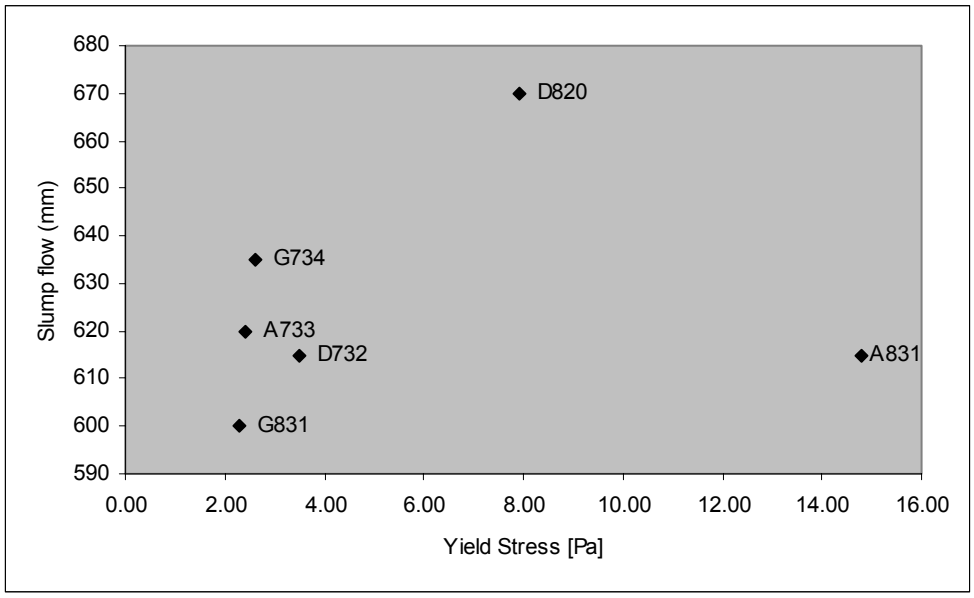


Figure 7.1: Comparison between the slump flow and yield stress for the SCC mixtures tested

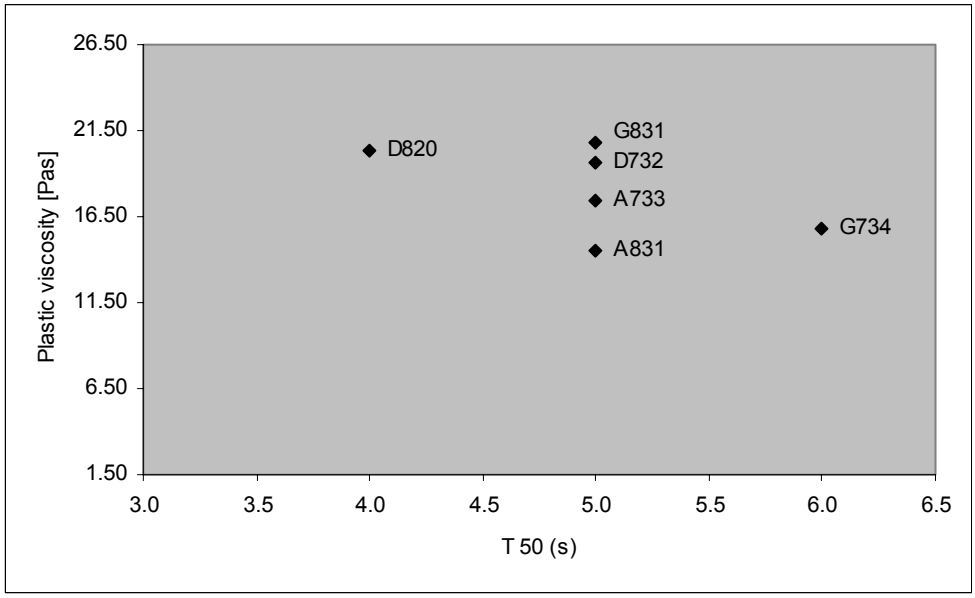


Figure 7.2: Comparison between the T 50 times and plastic viscosities for the SCC mixtures tested.

7.5 Conclusion

From the test results it is apparent that the proposed mixture design model can be used for the design of SCC in South Africa. The model shows better results than the previous model, when used with the selected aggregate, indicating the adaptability of the method. The results show that this method can be used with local aggregate to produce acceptable SCC mixtures.

The test results also indicate that when using sand with a high fines content, like the ViscoCorder sand grading, the rheology of the SCC mixture improves but the density of the hardened concrete is low. This indicates that poorly graded sand prevents the mixture to be fully self-compacting. Between the three different aggregate types used with this sand, the granite from the Jukskei quarry gave the best results. When the same aggregate was used with crusher sand, the result was very different with a higher yield stress reading. The granite from the Jukskei quarry gave the better workability result and the andesite used with andesite crusher sand gave the worst result.

The J-ring test was done with the slump flow test to assess the blocking and stability of the SCC. By doing the J-ring test with the slump flow test, the time for testing was used more effectively. It was also found that the J-ring test was very operator sensitive and that the measurements need to be taken accurately.

Since most of the 'step of blocking (St_j)' results indicate blocking, these mixtures did not seem to block when assessed visually.

The large percentage FA used in the mixtures reduced the superplasticizer dosage from the recommended 1,2 % to 0,7 % of the total cementitious content. The mixtures containing dolomite required only 0,42 % superplasticizer. This reduces the cost of the SCC significantly.

To end this investigation the next chapter summarises the conclusions and gives recommendations for further research on SCC.

CHAPTER 8

CONCLUSION AND RECOMMENDATIONS

8.1 Conclusions

In the comparisons between the rheologies of paste, mortar and concrete the results were not positive. Neither the comparison between the yield stress, and the plastic viscosity showed a noticeable relationship. However, it can intuitively be accepted that some relationship should exist between the rheological properties of these three phases. It may be that such a relationship will become evident if all phases are tested with the same equipment and under the same conditions. This is, however, very difficult since, even if it exists; such equipment is not available in South Africa.

Rheology is necessary to evaluate the flow properties of SCC as well as for describing and verifying the important qualities needed for it to be self-compacting, low yield stress and sufficiently high plastic viscosity[1]. The rheological data is therefore needed in the mixture design of SCC. The two values, g (yield stress) and h (plastic viscosity) characterise the total physical effort required to place and compact fresh concrete. The yield value (g) quantifies the effort to start movement and plastic viscosity (h) the extra effort to sustain the movement at a reasonable speed[17]. The two point test can therefore be used to investigate and improve SCC mixture designs. If the yield stress is too high it indicates that more superplasticizer is required and the mixture needs to be adjusted. The plastic viscosity results will depend on the application that the

mixture is intended for. SCC designed for vertical members, like columns, requires a cohesive mixture and therefore a lower plastic viscosity than for horizontal members (floors) where a very flowable mixture with a high plastic viscosity is suitable. An increase in the fines content (including cement and extenders) or the addition of a viscosity modifier increases the plastic viscosity which ensures sufficient stability[53].

Additional benefits in using rheology to describe the workability of concrete are that the results are based on fundamental properties, have numerically similar values and are reproducible. Unlike the commonly used terms, like "wet" or "plastic", rheology can be used to describe concrete flow more accurately.

Two mixture design models were used in this investigation. Both methods gave good results indicating suitability for use with South African materials. The first method is based on personal experience and is therefore not easily defined or quantified and not recommended for the design of SCC mixtures. The second method, on the other hand, is more suitable for commercial use. Further investigation regarding the use of filler sand as part of this mixture design method is recommended for a more economical mixture. Both methods need to be tested on a bigger scale to determine the reliability and repeatability.

From the test results it can be concluded that SCC can be made with the materials used in this investigation. It is also possible to make SCC with a lower binder content. Using a lower binder content not only reduces the cost but can also have a positive effect on shrinkage.

The test results showed that the granite from the Jukskei quarry gave the best workability results but the densities of the concrete test cubes indicate that the mixtures containing this aggregate did not show good self-compactibility. The dolomite from the Olifantsfontein quarry, on the other hand required less cement and admixture making it a more economical mixture. From the densities of the concrete test cubes these mixtures show better self-compactibility. Because of the high flakiness of the Eikenhof Andesite these mixtures was susceptible to blocking and needed higher admixture dosages and increased fines content for good flowability. Because of the higher paste content the densities of the cubes were better. The workability and flowability increased when more fly ash was used in the mixture but segregation occurred when fly ash was omitted.

The use of ultra fine fly ash did not improve the workability of the mixture, but made the mixture more cohesive without the need for a viscosity modifier. It could be beneficial to change the proportion of ultra fine fly ash or to use it in combination with other grades of fly ash and ground granulated blast furnace slag.

SCC is very sensitive to the admixture dosage. This creates a fine line between a mixture with the required properties and a mixture that segregates. A viscosity modifier can be used to assist with this problem but then the cost is increased and workability retention is shorter. If condensed silica fume or ultra fine fly ash is used in the mixture it has a similar effect as a viscosity modifier, but with less material cost and workability loss.

8.2 Recommendations

- Further research is required on SCC in South Africa.
- Full scale trials are necessary to determine the cost implications involved when using SCC.
- The Civil Engineering industry needs to be made aware of the benefits of SCC and the opportunities for increasing its usage.
- Better control of the aggregate size and shape is required for consistent SCC.

The Tattersall Two Point Tester used in this investigation is one of the very first models produced and needs to be upgraded if accurate results are required. For future research on rheology and workability it is recommended that the J-ring test method be utilized. The J-ring is a combination of the slump flow and L-box tests. This test will make workability testing quicker and easier, since the L-box test is very cumbersome and sensitive to the time lapse between mixing and testing.

8.3 Future research

- Mixture design to create the most economical SCC mixture.
- The effect of different extenders and extender combinations on the workability of SCC.
- Shrinkage behavior of SCC.
- Creep prediction of SCC.
- Rebar bond analysis in SCC.
- Fiber reinforced SCC.
- Usage of byproducts from the mineral and metallurgical industries as fillers.
- Use of artificial or recycled aggregate in SCC.
- Optimizing SCC usage in the precast industry.
- Concrete rheology measurements using alternative equipment.
- Durability of SCC.

Finally, Billberg[1] has stated: "As long as there is one stone left unturned in the work there is also a need to investigate what is underneath this stone, where every possible aspect of SCC must be investigated as in the case of conventional concrete."

REFERENCES

1. Billberg, P. **Self-compacting concrete for civil engineering structures – The Swedish experience**. CBI Report 2:99, Swedish Cement and Concrete Research Institute, SE-100 44 Stockholm.
2. Ballim, Y. Private communication, The University of the Witwatersrand, October 2002.
3. Domone P.L. Chai H-W., Design and testing of self-compacting concrete, proc. **International RILEM Conference**, Paisley, Scotland, 1996, pp 223 – 225.
4. Okamura, H. and Outchi, M. Applications of Self-compacting concrete in Japan, **Self-compacting concrete, third international RILEM symposium**, Reykjavik, Iceland, Aug. 2003, p3.
5. Skarendahl, A. The present – The future, **Self-compacting concrete, third international RILEM symposium**, Reykjavik, Iceland, Aug. 2003, p6.
6. Gazendam, M. **Durability of Self-compacting concrete,** BIng thesis, Cape Town: University of Stellenbosch, 2003
7. Walraven, J. Structural aspects of Self-compacting concrete, **Self-compacting concrete, third international RILEM symposium**, Reykjavik, Iceland, Aug. 2003, p15-22.
8. Corradi, M. Innovative Technology to improve precast processes, **Zero energy system workshop**, Treviso, Italy, Oct. 2001.

9. Utsi, S. Self-compacting concrete: Properties of fresh and hardening concrete for civil engineering applications, **Licentiate thesis**, Lulea, Sweden: Lulea University of Technology, 2003.
10. Hurd, M.K. Self-compacting concrete. Can you fill your forms without vibrating?, **Concrete Construction**, Jan 2002, pp.44-50.
11. Parrock, A and Jerling, W. The Nelson Mandela Bridge: The use of concrete on a predominantly steel structure. **Developing concrete to serve practical needs Conference**. 14 Oct. 2004. Midrand, South Africa, pp 244 – 245.
12. Lonsdale, L. Crossing the lines on the Nelson Mandela Bridge, **Concrete Engineering International**. Autumn 2003. pp 54 – 56.
13. Concrete Beton Nr.106, May 2004, **Significant project: Bridge 2235 – N4 PlatinumToll Highway**, Midrand: The Concrete Society of Southern Africa, 2004.
14. EFNARC2002, **Specification and guidelines for self-compacting concrete**, Surrey, UK, Feb. 2002, pp 7-9.
15. Kleinhans, E. Private communication, Johannesburg: Lafarge, March 2004.
16. Naidoo, R. Private communication, Johannesburg: Holcim, July 2004.
17. Tattersall, G.H. **Workability and quality control of concrete**, 1st ed. London, E & FN SPON., 1991, pp 54-77
18. Tattersall, G.H. and Banfill, P.F.G. **The rheology of fresh concrete,** 1st ed. Boston, Pitman, 1983, p 15-115.
19. Banfill, P.F.G. The rheology of fresh mortar. **Magazine of Concrete Research, vol. 43**, No. 154, Mar. 1991, pp. 13-21.

20. Wallevik, O.H. Rheology – A scientific approach to develop Self-compacting concrete. **Self-compacting concrete, third international RILEM symposium**, Reykjavik, Iceland, Aug. 2003, p29.
21. Ferraris, C.F. and Brower, E.B. Comparison of concrete rheometers: **International tests at LCPC** (Nantes, France), 2000, NIST. Pp 33-36
22. Domone, P.L.J. and Jin, J. Properties of mortar for Self-compacting concrete, **Self-compacting concrete, first international RILEM symposium**, Stockholm, Sweden, Sept. 1999, p109-119.
23. Jin, J and Domone, P.L.J. Relationships between the fresh properties of SCC and its mortar component. **Proceedings of the First North American Conference on the Design and Use of Self- Consolidating Concrete**. Centre for Advanced Cement Based Materials, North Western University, Chicago, November 2002 pp 33-38.
24. Bartos, P. **Fresh concrete, properties and tests**. 1st. ed. Amsterdam, Elsevier, 1992, p 23.
25. Ferraris, C.F. and Gaidis, J. Connection between the rheology of concrete and the rheology of cement paste. **ACI Materials Journal**. Title no. 89-M43. July-August 1992, pp. 388-393.
26. Struble, L., Szecsy, R. and Salinas, G. Rheology of fresh concrete. **Sixth International purdue conference on concrete pavement "Design and materials for high performance"**, Indianapolis, U.S.A., Nov. 1997, pp 149-157.
27. Banfill, P.F.G. The rheology of fresh cement and concrete – A review. **11th International congress on the chemistry of cement**, 2003, pp 50

28. Petersson, O., Gibbs, J. and Bartos, P. Testing SCC: A European Project, **Self-compacting concrete, third international RILEM symposium**, Reykjavik, Iceland, Aug. 2003, pp 299-304.
29. Bartos, P.J.M., Sonebi, M. and Tamimi, A.K. **Workability and rheology of fresh concrete: Compendium of tests**. France: RILEM, 2002, p103
30. Tattersall, G.H. and Bloomer, S.J. Further development of the two-point test for workability and extension of its range, **Magazine of Concrete Research,** vol.31, no.109, Dec. 1979, pp 202-210.
31. Banfill, P.F.G. **Calibration of the 2 point workability apparatus**. The University of Liverpool. September 1978.
32. Föll, H. (2005). Arrhenius-Plot. INTERNET. www.techfak.uni-kiel.de/matwis. Cited 26 August 2005.
33. Banfill, P.F.G. Use of the ViscoCorder to study the rheology of fresh mortar. **Magazine of Concrete Research, vol. 42**, No. 153, Dec. 1990, pp. 213-221.
34. Banfill, P.F.G. Rheological methods for assessing the flow properties of mortar and related materials. **Construction and building materials, vol.8**, 1994, pp. 43-50
35. Wüstholz, T. Fresh properties of Self-Compacting Concrete (SCC). **Otto-Graf-Journal**, vol. 14, 2003, pp 179-188.
36. SABS EN 196-1: 1994 **Methods of testing cement Part 3: Determination of setting time and soundness**. Pretoria, South Africa Bureau of Standards.

37. Ouchi, M and Edamatsu, Y. A simple elevation method for interaction between coarse aggregate and mortar particles in Self-compacting concrete. **Self-compacting concrete, first international RILEM symposium**, Stockholm, Sweden, Sept. 1999, pp 121-130.
38. Skarendahl, A and Petersson, O. **Self-compacting concrete,** RILEM, 2000. (RILEM Technical Committee 174-SCC)
39. Badenhorst, S. Private communication, Johannesburg: Holcim, January 2005.
40. SABS Method 860: 1994, **Concrete tests – dimensions, tolerances and uses of cast test specimens**, Pretoria: South African Bureau of Standards, 1994.
41. SABS Method 861-3: 1994, **Concrete tests – making and curing of test specimens**, Pretoria: South African Bureau of Standards, 1994.
42. SABS Method 863: 1994, **Concrete tests – compressive strength of hardened concrete**, Pretoria: South African Bureau of Standards, 1994.
43. British Standards Institution. **Pulverised-fuel ash-cementitious component in concrete**. BS 3892: Part 1, BSI, London, 1997.
44. SABS 1491-2: 2002, **Portland cement extenders, Part 2: Fly ash (FA) and ultra-fine fly ash (UFFA)**. Pretoria: South African Bureau of Standards, 2002.
45. Kruger, J.E. **South African Fly ash: A cement extender.** The South African Coal Ash Association. South Africa. 2003. p 27.
46. Fossey, S.D., Byars, E.A. and Zhu, H.Y. Super classified PFA for Self-compacting concrete. **International congress on the chemistry of cement**, 2003, pp 769-778

47. Shadle, R and Somerville, S. The benefits of utilizing fly ash in producing Self-compacting concrete. **First North American conference on the design and use of Self-compacting concrete**, Nov. 2002, p 218.
48. Addis, B. and Owens, G. editors., **Fulton's concrete technology**, 8th ed, Midrand, Cement and Concrete Institute, South Africa, 2001, p 145.
49. Banfill, P.F.G. E-mail correspondence, September 2004.
50. Nielsson, I and Wallevik, O.H. Rheological evaluation of some empirical test methods – Preliminary results, **Self-compacting concrete, third international RILEM symposium**, Reykjavik, Iceland, Aug. 2003, pp 59-68.
51. Su, N., Hsu, K-C. and Chai, H-W. A simple mix design method for self-compacting concrete. **Cement and Concrete Research,** vol.31, 2001, pp 1799-1807.
52. SABS Method 845: 1994, **Bulk densities and voids content of aggregates**. Pretoria: South African Bureau of Standards, 1994.
53. ACI 211.1-91(1997), **Standard practice for selecting proportions for normal, heavyweight, and mass concrete**, Farmington Hills, Michigan:American Concrete Institute, 1997.

APPENDIX A

CALIBRATION CALCULATIONS

ViscoCorder calibration

The silicone di-methyl (Newtonian fluid) was tested in the MC1 Rheolab rheometer at five different temperatures as shown in Table A1. This information was then used to draw an Arrhenius plot (Figure A1) of ln η against the inverse of the absolute temperature ($1/T_a$) at which the silicone di-methyl was tested (the temperature is converted to absolute temperature by adding 273.2). An Arrhenius plot is used to show if the scatter of data points, determined experimentally, is small or large. If there is an Arrhenius relation the data points will be in a straight line[32].

Table A1: Viscosity measurements for Silicone di-methyl

Temp.(°C)	Ta (K)	1/Ta (1/K)	η (Pas)	*ln* η (Pas)
17	290.2	0.003446	21.33	3.06
26	299.2	0.003342	17.93	2.89
30	303.2	0.003298	16.62	2.81
36	309.2	0.003234	14.91	2.70
45	318.2	0.003143	12.89	2.56

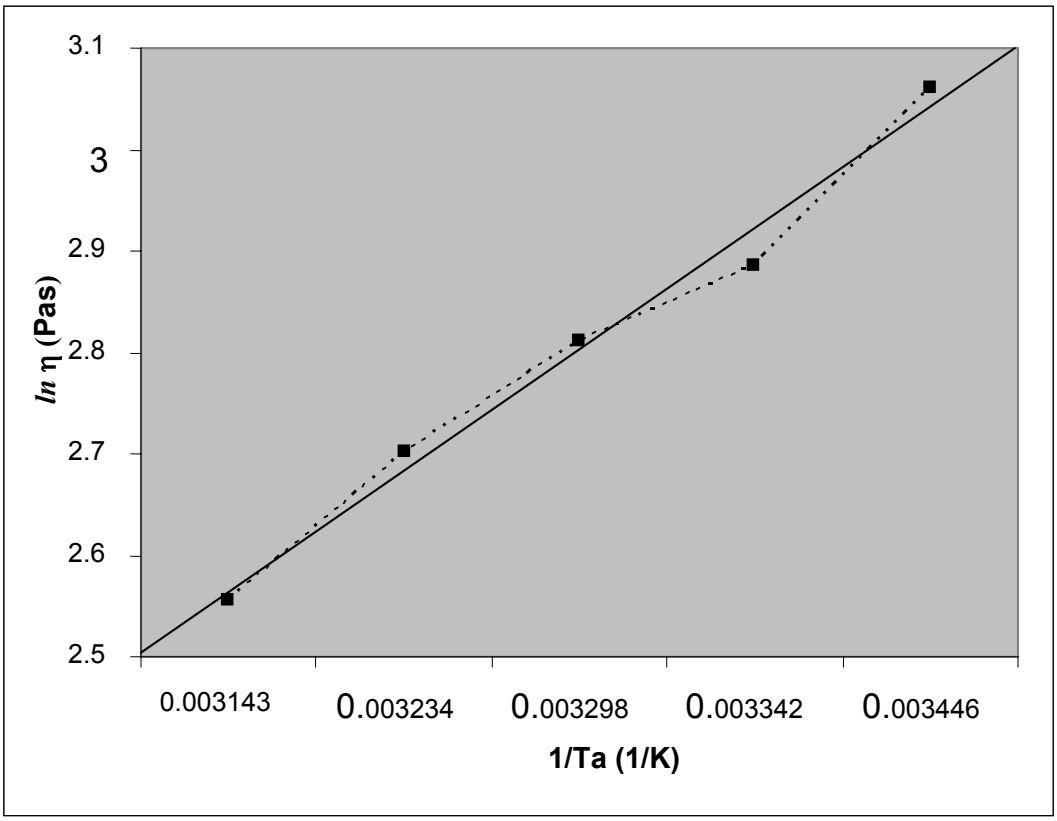


Figure A1: Arrhenius plot of *ln* η (in Pas) against the inverse of the absolute temperature (in 1/K)

The silicone di-methyl was also used in the ViscoCorder to measure the torque at five different speeds and three different temperatures. The viscosities (η) at the working temperatures used in the ViscoCorder were found by interpolating and converting the values from Figure A1. Table B1 contains the readings obtained in the ViscoCorder as well as the calculations for the slope of the T/N graph. The value for G, apparatus constant, is then calculated using equation A1.

$$\frac{T}{N} = G\eta \qquad \text{(A1)}$$

Table A2 is a summary of these results.

Table A2: Variation of viscosity with temperature for the ViscoCorder.

Temp (°C)	$1/T_a$ (1/K)	η (Pas)	Slope T/N (Nms)
30	3.3×10^{-3}	16.62	0.022
36	3.23×10^{-3}	14.91	0.02
45	3.14×10^{-3}	12.89	0.019

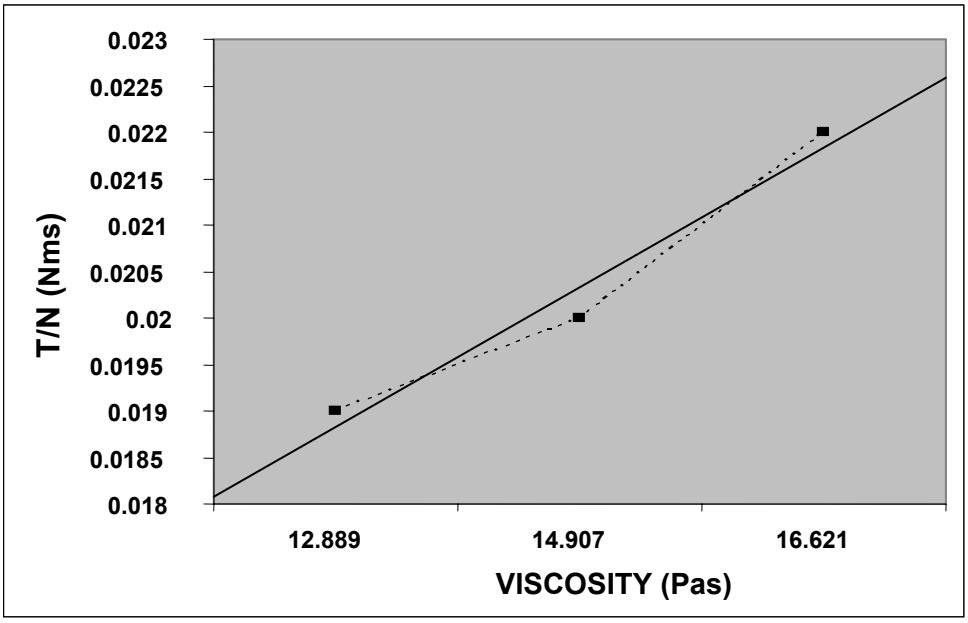


Figure A2: T/N against η for the ViscoCorder

The value G = 0.0008 m^3 is the slope of the best straight line of the T/N against η relation[31] as shown in Figure A2. This value of G will be used in all the following calculations as well as the conversion of the g and h values obtained in the ViscoCorder.

To determine the value of K, constant of proportionality, two aqueous solutions of hydroxy ethyl cellulose (1.92 % and 3.00 %) were used. These are pseudo plastic fluids that obey the power law relation given in Equation A2.

$$\tau = k\dot{\gamma}^{n} \tag{A2}$$

The torque values at five different speeds were measured using these solutions in the ViscoCorder. The results, as shown in Table B2, were used to determine the relationship between *ln* Speed (*ln* N) and *ln* Torque (*ln* T). The slope of this line is equal to q (constant used in Equation A3) and from the intercept on the y-axis (*ln* p) the value of p is obtained in Equation A3:

$$ln\ T = ln\ p + q\ ln\ N \tag{A3}$$

The same aqueous solutions of hydroxy ethyl cellulose were used in a MC1 Rheolab rheometer to determine the relation between $ln\,\dot{\gamma}$ and *ln* τ at twenty different speeds (Table B3 and B4, Appendix B). Shear stress values is taken up to a speed of 0.69, readings at faster speeds show too much turbulence (the flow curve bends towards the speed axis). From these values, linear regression is done to determine the relation between $ln\,\dot{\gamma}$ and *ln* τ. The slopes of these lines (linear), shown in figure A3, are equal to s and from the intercept *ln* r the value of r is obtained in Equation A4.

$$ln\ \tau = ln\ r + s\ ln\,\dot{\gamma} \tag{A4}$$

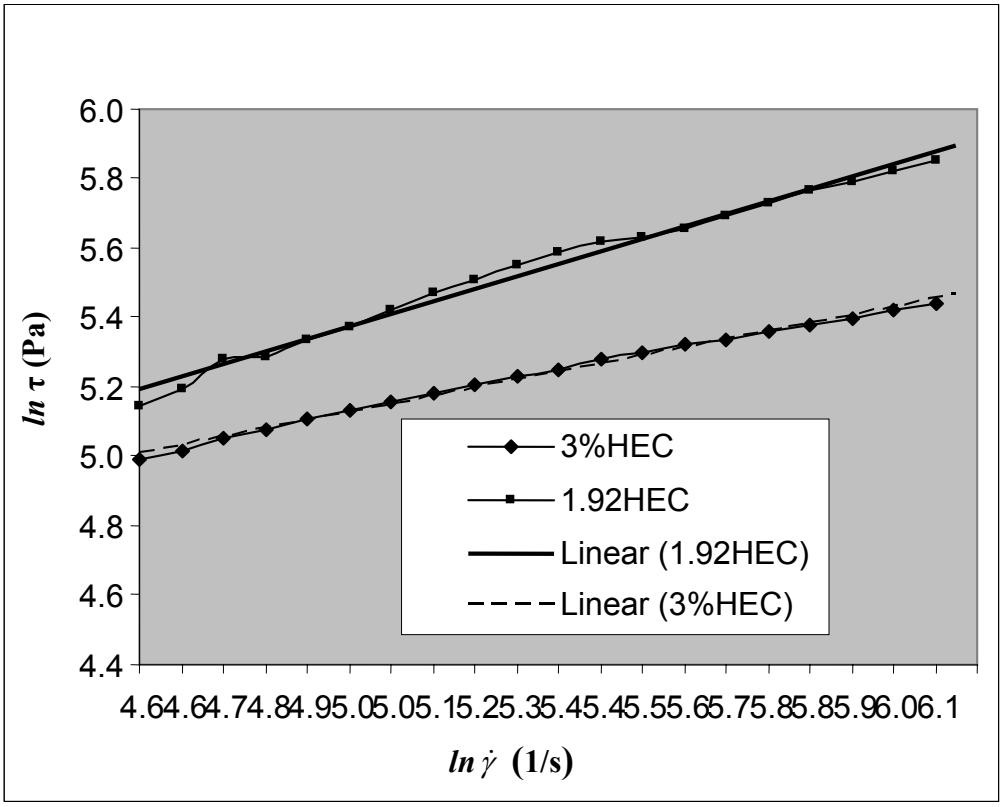


Figure A3: Relation between $ln\,\dot{\gamma}$ and $ln\,\tau$ for the ViscoCorder

Table A3 is a summary of the calibration results for the ViscoCorder.

Table A3: Power law parameters for hydroxy ethyl cellulose for the calibration of the ViscoCorder.

	***ln* p**	**p**	**q**	***ln* r**	**r**	**s**
1.92 %	-4.344	0.013	0.404	3.69	39.96	0.384
3 %	-3.402	0.033	0.214	3.66	38.79	0.296

The degree of approximation was calculated for each solution using Equation A5.

$$\frac{q-1}{s-1} \qquad \text{(A5)}$$

For the 1.92% hydroxy ethyl cellulose solution, $\frac{q-1}{s-1} = 0.97$, which is close to one, indicating that the relationship between shear rate and speed is independent of the speed and is one of simple proportionality. Equation A6 was then used to calculate the proportionality constant, $K = 4.3$.

$$K = \left(\frac{p}{rG}\right)^{\frac{1}{s-1}} \quad (31) \qquad \text{(A6)}$$

For the 3.00 % hydroxy ethyl cellulose solution the answer for $\frac{q-1}{s-1}$ is 1.117 and $K = 0.9$

According to Banfill[33] the discrepancies are due to a shortcoming of the theory, but the value for K using the 1.92 % hydroxy ethyl cellulose solution compares well with calibration constants derived using other ViscoCorders. A value of $K = 4.3$ will therefore be used in this investigation.

The values of $G = 0.0008$ and $K = 4.3$ can be used to express the g and h values obtained from the ViscoCorder in terms of τ_o and μ using Equations A7 and A8 respectively.

Therefore:

$$\tau_o = 5.375 * g \qquad \text{(A7)}$$

$$\mu = 1.25 * h \qquad \text{(A8)}$$

Where g and h are in Nmm and Nmm.s respectively.

APPENDIX B

CALIBRATION MEASUREMENTS

Table B1: ViscoCorder measurements and slope calculations for Silicone di-methyl

Temp.	Speed N	Torque T	$(Speed)^2$ $(N)^2$	N x T	Viscosity η	Slope T/N
(ºC)	(1/s)	(Nm)	$(1/s)^2$	(Nm/s)	(Pas)	(Nms)
30	0.833	0.024	0.694	0.020	**16.62**	**0.022**
	1.666	0.046	2.776	0.077		
	2.5	0.065	6.250	0.163		
	3.333	0.083	11.109	0.277		
	4.167	0.099	17.364	0.413		
36	0.833	0.022	0.694	0.018	**14.907**	**0.020**
	1.666	0.040	2.776	0.067		
	2.5	0.057	6.250	0.143		
	3.333	0.073	11.109	0.243		
	4.167	0.088	17.364	0.367		
45	0.833	0.020	0.694	0.017	**12.889**	**0.019**
	1.666	0.037	2.776	0.062		
	2.5	0.052	6.250	0.130		
	3.333	0.068	11.109	0.227		
	4.167	0.082	17.364	0.342		

Table B2: ViscoCorder measurements and slope calculations for two aqueous solutions of hydroxy ethyl cellulose

Number	Speed	Torque	*ln* Speed	*ln* Torque	(*ln* N)^2	*ln* N x *ln* T	Slope (q)	ln p	p
	(1/s)	(Nm)	(1/s)	(Nm)	(1/s)^2	(Nm/s)	Nms	Nm	Nm
3.00 %	0.833	0.032	-0.183	-3.442	0.033	0.629	**0.214**	**-3.402**	**0.033**
25 ºC	1.666	0.037	0.510	-3.297	0.261	-1.683			
HEC	2.5	0.041	0.916	-3.194	0.840	-2.927			
	3.333	0.043	1.204	-3.147	1.449	-3.788			
	4.167	0.045	1.427	-3.101	2.037	-4.426			
1.92 %	0.833	0.012	-0.183	-4.423	0.033	0.808	**0.404**	**-4.344**	**0.013**
25 ºC	1.666	0.016	0.510	-4.135	0.261	-2.111			
HEC	2.5	0.019	0.916	-3.963	0.840	-3.632			
	3.333	0.021	1.204	-3.863	1.449	-4.651			
	4.167	0.023	1.427	-3.772	2.037	-5.384			

Table B3: MC1 Rheolab rheometer measurements and slope calculations for 1.92 % aqueous solutions of hydroxy ethyl cellulose for the calibration of the ViscoCorder.

Number	τ	$ln\ \tau$	$\dot{\gamma}$	$ln\ \dot{\gamma}$	$(ln\ \dot{\gamma})^2$	$ln\ \dot{\gamma}$ x $ln\ \tau$	Slope s	ln r	r
	(Pa)	(Pa)	(1/s)	(1/s)	$(1/s)^2$	(Pa/s)	(1/Pas)	(1/s)	(1/s)
	172	5.15	50	3.91	15.30	20.14	**0.384**	**3.69**	**39.96**
	180	5.19	54.9	4.01	16.04	20.80			
19 ºC	196	5.28	60.4	4.10	16.82	21.65			
HEC	197	5.28	66.4	4.20	17.60	22.17			
1.92 %	207	5.33	72.9	4.29	18.40	22.87			
	216	5.38	80.1	4.38	19.21	23.56			
	226	5.42	88	4.48	20.05	24.27			
	237	5.47	96.8	4.57	20.91	25.00			
	246	5.51	106	4.66	21.75	25.67			
	258	5.55	117	4.76	22.68	26.44			
	267	5.59	128	4.85	23.54	27.11			
	276	5.62	141	4.95	24.49	27.81			
	279	5.63	155	5.04	25.44	28.40			
	285	5.65	170	5.14	26.38	29.03			
	297	5.69	187	5.23	27.36	29.78			
	308	5.73	206	5.33	28.39	30.53			
	320	5.77	226	5.42	29.38	31.27			
	328	5.79	248	5.51	30.40	31.94			
	337	5.82	273	5.61	31.47	32.65			
	349	5.86	300	5.70	32.53	33.40			

Table B4: MC1 Rheolab rheometer measurements and slope calculations for 3.00 % aqueous solutions of hydroxy ethyl cellulose for the calibration of the ViscoCorder.

Number	τ	$ln\ \tau$	$\dot{\gamma}$	$ln\ \dot{\gamma}$	$(ln\ \dot{\gamma})^2$	$ln\ \dot{\gamma}$ x $ln\ \tau$	Slope s	ln r	r
	(Pa)	(Pa)	(1/s)	(1/s)	$(1/s)^2$	(Pa/s)	(1/Pas)	(1/s)	(1/s)
	147	4.99	96.3	4.57	20.86	22.79	**0.296**	**3.66**	**38.79**
	151	5.02	104	4.64	21.57	23.30			
19 ºC	156	5.05	113	4.73	22.35	23.87			
HEC	160	5.08	122	4.80	23.08	24.38			
3.00 %	165	5.11	132	4.88	23.84	24.93			
	169	5.13	143	4.96	24.63	25.46			
	174	5.16	155	5.04	25.44	26.02			
	178	5.18	166	5.11	26.13	26.49			
	182	5.20	182	5.20	27.08	27.08			
	187	5.23	197	5.28	27.91	27.64			
	191	5.25	213	5.36	28.74	28.16			
	196	5.28	231	5.44	29.62	28.73			
	200	5.30	250	5.52	30.49	29.25			
	205	5.32	270	5.60	31.34	29.80			
	208	5.34	293	5.68	32.26	30.32			
	213	5.36	317	5.76	33.16	30.88			
	217	5.38	343	5.84	34.08	31.41			
	221	5.40	371	5.92	35.00	31.94			
	226	5.42	402	6.00	35.96	32.50			
	230	5.44	430	6.06	36.77	32.98			

APPENDIX C

EXAMPLE TO CALCULATE YIELD STRESS AND PLASTIC VISCOSITY

To calculate the values of *g*, intercept on the torque axis, and *h,* the reciprocal slope of the line, the following linear least squares solution was used. The solution for the measured values of speed and torque has the form:

$$y = ax + b \tag{C1}$$

$$a = \frac{m\left(\sum_{i=1}^{m} x_i y_i\right) - \left(\sum_{i=1}^{m} x_i\right)\left(\sum_{i=1}^{m} y_i\right)}{m\left(\sum_{i=1}^{m} x_i^2\right) - \left(\sum_{i=1}^{m} x_i\right)^2} \tag{C2}$$

$$b = \frac{\left(\sum_{i=1}^{m} x_i^2\right)\left(\sum_{i=1}^{m} y_i\right) - \left(\sum_{i=1}^{m} x_i y_i\right)\left(\sum_{i=1}^{m} x_i\right)}{m\left(\sum_{i=1}^{m} x_i^2\right) - \left(\sum_{i=1}^{m} x_i\right)^2} \tag{C3}$$

Speed is put into the equation as x and torque as y and 'a' will be the slope and not the reciprocal slope.

Table C1 gives an example of calculations for *g, h,* τ_o and μ from experimental data obtained from the Tattersall Two Point Tester.

Table C1: Example of the calculation for *g, h,* τ_o and μ from experimental data obtained from the Tattersall Two Point Tester.

TATTERSALL READINGS Calibration constant: 0.28 Nm/MPa							**RESULTS**					
N	**Pressure (MPa)**			**T**	**N^2**	**N x T**	**h**	**g**	**G**	**K**	**τ_o**	**μ**
(1/s)	**Total**	**Idling**	**Net**	**(Nm)**	**$(1/s)^2$**	**(Nm/s)**	**(Nms)**	**(Nm)**	**(m^3)**	**(no unit)**	**(Pa)**	**(Pas)**
1.45	2.40	1.30	1.1	0.31	2.10	0.45	**0.11**	**0.145**	**0.0082**	**0.6**	**11**	**13**
1.25	2.25	1.25	1	0.28	1.56	0.35						
1.05	2.10	1.21	0.89	0.25	1.10	0.26						
0.85	2.00	1.15	0.85	0.24	0.72	0.20						
0.65	1.85	1.10	0.75	0.21	0.42	0.14						
0.45	1.75	1.05	0.7	0.20	0.20	0.09						
0.25	1.65	1.02	0.63	0.18	0.06	0.04						